uOttawa

L'Université canadienne
Canada's university

FACULTÉ DES ÉTUDES SUPÉRIEURES ET POSTOCTORALES

uOttawa

L'Université canadienne
Canada's university

FACULTY OF GRADUATE AND POSDOCTORAL STUDIES

Philip Harold Links
AUTEUR DE LA THÈSE / AUTHOR OF THESIS

Ph.D. (Biochemistry)
GRADE / DEGREE

Department of Biochemistry, Microbiology and Immunology
FACULTÉ, ÉCOLE, DÉPARTEMENT / FACULTY, SCHOOL, DEPARTMENT

Protein Factors Involved in the Assembly of Very Low Density Lipoproteins

TITRE DE LA THÈSE / TITLE OF THESIS

Zemin Yao
DIRECTEUR (DIRECTRICE) DE LA THÈSE / THESIS SUPERVISOR

CO-DIRECTEUR (CO-DIRECTRICE) DE LA THÈSE / THESIS CO-SUPERVISOR

EXAMINATEURS (EXAMINATRICES) DE LA THÈSE / THESIS EXAMINERS

Khosrow Adeli

Illimar Altosaar

Chris Kennedy

James Van Huysse

Gary W. Slater
LE DOYEN DE LA FACULTÉ DES ÉTUDES SUPÉRIEURES ET POSTDOCTORALES /
DEAN OF THE FACULTY OF GRADUATE AND POSTDOCORAL STUDIES

Protein Factors Involved in the Assembly of Very Low Density Lipoproteins

Philip Harold Links B.Sc. M.Sc.

A Thesis Submitted to the School of Graduate Studies and Research in Partial Fulfillment of the Requirements for the Degree of Doctor of Philosophy in Biochemistry

Supervisor: Dr. Zemin Yao

Department of Biochemistry, Microbiology and Immunology
Ottawa Heart Institute
Faculty of Medicine
University of Ottawa

Your file Votre référence
ISBN: 0-494-10985-8
Our file Notre référence
ISBN: 0-494-10985-8

Abstract

Genetic data have suggested a correlation between apolipoprotein C-III (apoC-III) and familial combined hyperlipidemia (FCHL). This observation has been confirmed by clinical data that show an elevation of circulating apoC-III in FCHL patients. Yet the underlying mechanism for the hyperlipidemic effect of apoC-III remains unclear. We postulate that an elevation of apoC-III expression might be associated with enhanced hepatic very low density lipoprotein (VLDL) secretion. To test this hypothesis, human apoC-III cDNA was transfected into McA-RH7777 rat hepatoma cells, that lacked endogenous apoC-III protein; triacylglycerol (TG) apolipoprotein B and VLDL secretion was determined. In transient ($p<.0005$) and stable transfectants ($p<.0008$), expression of recombinant apoC-III led to a two-fold increase in ^{3}H-TG secretion only in the presence of 0.4 mM exogenous oleate (OA). This increased ^{3}H-TG secretion was specifically associated with the $VLDL_1$ sub fraction (S_f) > 100. ApoB-100 in the $VLDL_1$ sub fraction also increased with apoC-III expression. I postulated that structural determinants shared by the other apoC proteins, apoC-I and apoC-II may also lead to an increase in $VLDL_1$. Stable cell lines expressing apoC-I and apoC-II also stimulated ^{3}H-TG secretion as well as apoB100 in the $VLDL_1$ fraction. Thus, hepatic apoC levels increase $VLDL_1$ secretion particularly in the presence of OA. Finally I attempted to identify a novel TG synthetic enzyme, phosphatidate phosphohydrolase (PAP-1). This enzyme activity hydrolyzes the phosphate group of phosphatidic acid to produce diacylglycerol (DG) for TG production. Since limiting TG levels lead to apolipoprotein B-100 degradation and aborted lipoprotein synthesis I postulate that PAP-1 may be involved in lipoprotein assembly and secretion. This research addresses two accessory protein factors apoC-III and PAP-1, involved in lipid mobilization for TG rich lipoprotein assembly and secretion.

Acknowledgements

I would like to thank my supervisor Dr. Zemin Yao who has always engaged this field with a vision and energy that I have not yet seen surpassed. I would also like to thank a number of post doctoral fellows who have been instrumental in my training namely Dr. Roger McCleod, Dr. Khai Tran, Dr. Jim Burgess and Dr. Xiaohui Zha. It has been my pleasure to work with and collaborate with a number of very skilled people throughout this work including Dr. Hongyu Zhang, Dr. Fengcheng Sun, Mr. Robert Brown and Mr. Donald Kerr. I would like to especially recognize Mrs. Jing Shan and Miss Jennifer Raven for their help in purifying hepatocytes and preparation of differential display-PCR fragments respectively, both of which were of great help in the PAP-1 work. Finally I would like to thank all those who came before me, namely Dr. Jay Wang, Shermin Rahimkhani and Dawn Sun. These people developed pioneering data which set the foundations for this work. I would also like to thank my thesis committee members Dr. Ross Milne and Dr. Heidi McBride as well as my comprehensive examiners, Dr. Dr. James Van Huysse, Dr. Illimar Altosaar, and Dr. Steffany Bennett. These professors have spent many hours reviewing this data and evaluating my approach; for this I am truly grateful.

Dedications

This work on cardiovascular disease was sparked by my paternal grandfather's battle with cardiovascular disease (CVD) and heart failure. His brave fight with this disease has resulted in several bypasses, angioplasty and a cornucopia of drug interventions. Through it all he has been an exemplar of courage and diligence in personal exercise and health which sets a high example for us all. It is with great hope that the summation of all these works will lead to new and better therapies for people suffering with CVD and their families. I would like to thank my wife who has been a steadfast companion and confidant throughout this difficult time. She has made my life immeasurably better and for that she has my love and adoration. For my parents and in-laws I am grateful for the love and support that you have provided as I have made this long journey. I hope that with the completion of this project I will be able to spend more time with family. To my brother Matthew I wish all of life's successes, especially all those which work can not provide. To all my friends who have been there for me, thank you.

Table of Contents

List of Figures

List of Tables

Abbreviations

Apo	apolipoprotein
ARF	ADP ribosylation factor
A.U.	arbitrary units
BFA	brefeldin A
BSA	bovine serum albumin
CE	cholesteryl ester
CHAPS	3-[(3-cholamidopropyl)dimethylammonio]-1-propane-sulfonate
CHD	coronary heart disease
COP	coat protein
CVD	cardiovascular disease
ddH_2O	double distilled water
DD-PCR	differential display polymerase chain reaction
DTT	dithiothreitol
DG	diacylglycerol
DMEM	Dulbecco's modified Eagle's medium
ER	endoplasmic reticulum
FBS	fetal bovine serum
FC	free cholesterol
FCHL	familial combined hyperlipidemia
FFA	free fatty acid
FH	familial hyperlipidemia
HEPES	4-(2-hydroxy-ethyl)-1-piperazine-ethanesulfonic acid

HDL	high density lipoprotein
HL	hepatic lipase
HSPG	heparan sulfate proteoglycans
IEF	isoelectric focusing
IDL	intermediate density lipoprotein
IPG	immobilized pH gradient
iPLA$_2$	Ca^{2+} independent phospholipase A2
kb	kilobases
LCAT	lecithin cholesterol acyl transferase
LDL	low density lipoprotein
LDL-R	LDL receptor
LOD	log of odds score
LpB	apoB containing lipoprotein
LPL	lipoprotein lipase
LPP	lipid phosphate phosphatase
LRP	LDL receptor related protein
NEM	*N*-ethylmaleimide
MALDI TOF	matrix assisted laser desorption ionization time of flight
MTP	microsomal triglyceride transfer protein
OA	oleic acid
PA	phophatidic acid
PAGE	polyacrylamide gel electrophoresis
PAP	phosphatidic acid phosphohydrolase

PBS	phosphate buffered saline
PC	phosphatidylcholine
PDI	protein disulfide isomerase
PE	phosphatidylethanolamine
PEMT	phosphatidylethanolamine methyltransferase
PI	phosphatidylinositol
PL	phospholipid
PLD	phospholipase D
PPAR	peroxisome proliferator-activated receptor
PS	phosphatidylserine
RCT	reverse cholesterol transport
RXR	retinoid X receptor
SDS	sodium dodecly sulfate
S_f	sedimentation fraction
TG	triacylglycerol
TLC	thin layer chromatography
TRIS	tris(hydroxymethyl)aminomethane
TRL	triglyceride rich lipoprotein
VLDL	very low density lipoprotein

Chapter 1 Introduction

Familial Combined Hyperlipidemia (FCHL)

Cardiovascular disease (CVD) is the leading cause of death in North America. This fact is attributable both to lifestyle and genetic factors that predispose individuals to premature atherosclerotic vascular disease. There are several putative causes under active investigation, including hypertension, obesity, insulin resistance, diabetes and hyperlipidemia. Hyperlipidemias are classified into four subgroups, of which type IV or Familial Combined Hyperlipidemia (FCHL) leads to coronary artery disease in > 2% of all Canadians [1]. This syndrome is characterized by variable hypercholesterolemia and/or hypertriglyceridemia, which is diagnosed by the presence of a similar dislipidemia in at least one first-degree relative. This disorder was originally identified in a group of Seattle families that possessed both hyperlipidemia and a family member who survived a myocardial infarction. The terms hypercholesterolemic and hypertriglyceridemic were assigned to families where elevated circulating levels of cholesterol and triglyceride (TG) were detected. Pedigrees where both conditions were detected were termed FCHL. Today the classification of FCHL patients includes people with cholesterol levels > 210 mg/dl and/or triglyceride levels > 200 mg/dl. Fasting normal humans cholesterol levels are < 185 mg/dl and TG levels of 80 < mg/dl [2].

In humans circulating levels of TG and cholesterol are determined by both exogenous and endogenous lipid pathways. Dietary lipids of exogenous origin are absorbed in the intestine and secreted from the lymph into the circulation via the thoracic duct, in the form of chylomicrons (Fig. 1*Ai*). Chylomicrons are a class of macromolecules termed lipoproteins, which consist of a microemulsion, where a

Fig. 1. Exogenous and endogenous pathways of lipid metabolism.

A*i*, diagram illustrating exogenous dietary lipid trafficking which is absorbed within the gut and packaged into chylomicrons for transport to peripheral cells. Free fatty acid is released by the lipolytic activity of LPL before clearance of the remnant particle by the liver. A*ii*, the endogenous pathway involves the synthesis and secretion of triglycerides and cholesterol together with apoB-100 from the liver as VLDL particles. These particles are also catabolized by LPL and HL before being cleared from the circulation via the LDL-R. B, diagram of a lipoprotein particle, where large apolipoproteins are shown on the surface of the particle. The surface phospholipids are represented by grey circles, blue circles represent core triglyceride and yellow circles represent cholesterol.

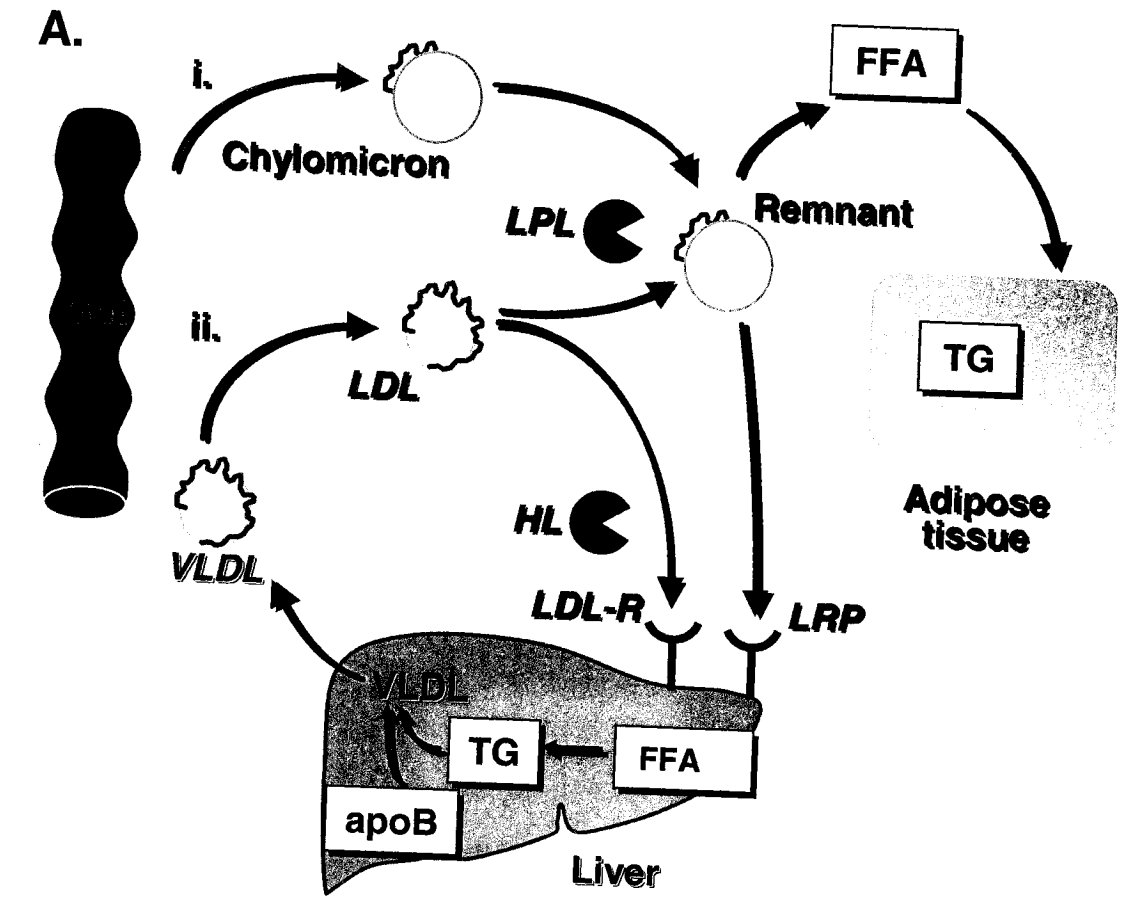
A.
i.
Chylomicron
FFA
LPL
Remnant
ii.
LDL
TG
Adipose tissue
HL
VLDL
LDL-R
LRP
VLDL
TG
FFA
apoB
Liver

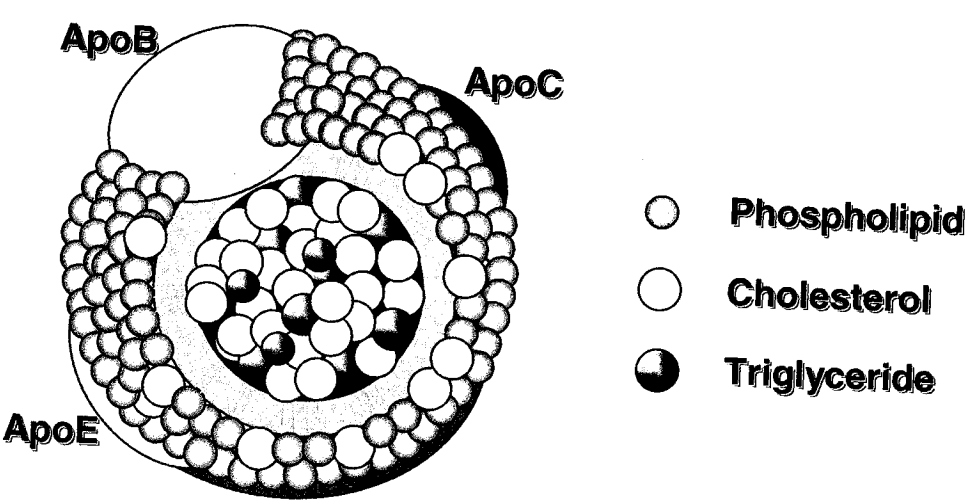
B.
ApoB
ApoC
ApoE
Phospholipid
Cholesterol
Triglyceride

phospholipid monolayer envelops a neutral lipid core (Fig. 1B).

The surface of a chylomicron is decorated with proteins termed apolipoproteins that determine the metabolic fate of the lipoprotein. In this way dietary lipid is transported from the intestine to peripheral cells (i.e. adipose tissue and skeletal muscle), where particles are acted upon by numerous lipases and transfer proteins. The release of free fatty acid (FFA) from the hydrolysis of TG occurs primarily in the circulation through the action of lipoprotein lipase (LPL) (Fig. 1A). The remnant chylomicron particles are eventually cleared from the circulation by the liver via the LDL receptor related protein (LRP). In contrast endogenous TG and cholesterol are synthesized in the liver from the catabolism of dietary carbohydrate and the re-esterification of hepatic FFA (Fig. 1A*ii*). These neutral lipids are assembled into the core of very low density lipoproteins (VLDL) and are secreted into the circulation. These particles are also acted upon by LPL and other enzymes (such as hepatic lipase HL) decreasing the particles to low density lipoproteins (LDL) before returning to the liver for clearance by the LDL receptor (LDL-R). This uptake is mediated either by apoB or apolipoprotein E (apoE) binding to the LDL-R. In addition to these endogenous and exogenous lipid pathways there is an alternative pathway whereby peripheral cholesterol can be returned to the liver for elimination in the bile. This process termed reverse cholesterol transport (RCT) allows for the efflux of cholesterol from cells in atheromous plaques to a small class of lipoprotein termed high density lipoproteins (HDL).

Lipoproteins

Lipoproteins serve as a transport system for both neutral lipids and fat soluble vitamins within the aqueous environment of the blood stream. These particles are

comprised of a phospholipid monolayer that envelops a neutral lipid core composed primarily of cholesteryl esters (CE) and TG. The surface lipids are stabilized by two classes of apolipoproteins, namely exchangeable and non-exchangeable apolipoproteins. Exchangeable apolipoproteins are generally small (<40 kDa) and often composed of regions of amphipathic alpha helices. These proteins remain loosely associated with the particle surface and are capable of interchange between lipoproteins or release into solution. This is in contrast with the non-exchangeable apolipoproteins such as apolipoprotein B (apoB) which remains irreversibly bound to a single lipoprotein particle due to regions of extended beta sheet, that grip the phospholipid surface. Lipoproteins are classified, by their buoyant density, into sub-fractions from the densest particles to particles of the lowest density (Table 1). Each class of lipoproteins can be sub-categorized based on their lipid composition and apolipoprotein content. The general protein composition and densities are detailed in the table below.

Table 1. Human lipoprotein classification

Density	Lipoprotein	Constituent Apolipoproteins
d < 0.098 g/ml	Chylomicron	ApoB-48, ApoA-I, A-II, A-IV, ApoC-I, C-II, C-III
0.098 < d < 1.006 g/ml	VLDL	ApoB-100, ApoC-I, C-II, C-III, ApoE
1.006 < d < 1.019 g/ml	IDL	ApoB-100, ApoC-I, C-II, C-III, ApoE
1.019 < d < 1.063 g/ml	LDL	ApoB-100
1.063 < d < 1.210 g/ml	HDL	ApoA-I, A-II, A-IV, ApoC-I, C-II, C-III, ApoE

Triglyceride transport is achieved primarily through VLDL sized particles which in addition to apoB-100 are decorated with several different exchangeable apolipoproteins that affect the fate of the circulating particle and apoB-100. The circulating levels of lipoproteins and their constituent lipid cargo are determined by their rates of production and clearance. In FCHL, elevated levels of VLDL, small dense LDL particles, and reduced levels of HDL are commonly detected. Patients with this disorder sometimes also display overproduction of apoB [3]. Apolipoprotein B is a key structural, non-exchangeable apolipoprotein, which remains irreversibly bound to the surface of a serum lipoprotein particle during its assembly, circulation and clearance [4]. The elevated lipid levels of both cholesterol and TG seen in patients may reflect an increase in apoB-containing lipoprotein (LpB) secretion, a decrease in lipoprotein catabolism, or both. To date, FCHL is not associated with defects in LDL-R mediated clearance of lipoproteins [5]. Several candidate genes such as apolipoprotein (apoC-III), hepatic lipase (HL), peroxisome proliferators-activated receptor gamma (PPARγ), lecithin cholesterol acyl transferase (LCAT) and lipoprotein lipase (LPL) have been proposed to cause FCHL [6;7]. Animal models of FCHL have also been produced such as the St. Thomas mixed hyperlipidemic rabbit and HcB19 mice [8]. In the case of the St. Thomas rabbit, elevated plasma cholesterol and TG levels were attributed to an overproduction of apoB containing VLDL particles [9]. In HcB19 mice, there is an elevation in plasma apoB as well as hypertriglyceridemia and hypercholesterolemia [10]. A novel gene *Hyplip1*, found in a region of the mouse chromosome analogous to human chromosome 1q21-23 is proposed to be involved in this phenotype. Several human genome wide scans have also been performed in FCHL patients yielding loci with high (>2.5) log of odds (LOD)

scores in regions of chromosome 16q22-24 (LOD 2.7), chromosome 1p31 (LOD 3.4), and chromosome 1q21-23 (LOD 5.9) [11].

Several linkage studies have also found a direct association between the AI/CIII/AIV gene cluster on human chromosome 11q23 and elevated circulating TG levels (Fig. 2B) [12;13]. One study of 86 young Swedish patients who survived a myocardial infarction showed an association between TG levels and a C-T polymorphism in *APOC-3* (nt 1100) [14]. This polymorphism was also studied in an Icelandic population and was shown to associate with an increase in circulating TG levels [15]. In a larger study performed on samples collected in the Atherosclerosis Risk in Communities Study trial (ARIC), a polymorphism generating an SstI site in the 3' UTR of *APOC-3* was shown to be significantly associated with hypertriglyceridemia [16]. Patients from the European Atherosclerosis Research Study II (EARSII) also showed linkage between the apoC-III SstI and a G-T polymorphic site (nt -2854) and elevated post prandial TG levels in response to oral glucose tests (Fig. 2C) [17]. Other researchers have proposed caution in interpreting these small data sets. In fact Wijsman and colleagues [18] have presented an analysis that suggests that the AI/CIII/AIV gene cluster is not linked with FCHL. At present it seems that this complex disorder may not be amenable to conclusive linkage analysis due to heterogeneity in the genotypes of the families studied and the possibility of more than one dislipidemic disease gene in these large pedigrees.

The role of apoC-III in the production of TG rich VLDL has also been supported by human studies using fenofibrates. This class of drugs is used clinically to decrease circulating TG in patients [19]. Further human studies have shown that the treatment of

Fig. 2. Structure of the human apolipoprotein AI/CIII/AIV gene locus.

A, putative mechanism of action of fenofibrate class of drugs, which are thought to interact with heterodimeric RXR nuclear receptors within the nucleus, preventing transcriptional activation. B, organization of the AI/CIII/AIV gene locus on human chromosome 11q23. All distances indicated in kilobases (kb) and arrow heads denote gene orientation. The putative RXR nuclear receptor binding site, and the *APOA-V* gene located 39 kb 3' of the locus are indicated. C, intron-exon structure of neighboring genes to *APOC-3*, and an intestinal response element (IRE) i indicated with a hatched box. ApoC-III/apoA-IV enhancer element is indicated with a dotted box. Several common polymorphisms are denoted by the number of nucleotides from the initiation of *APOC-III* transcription.

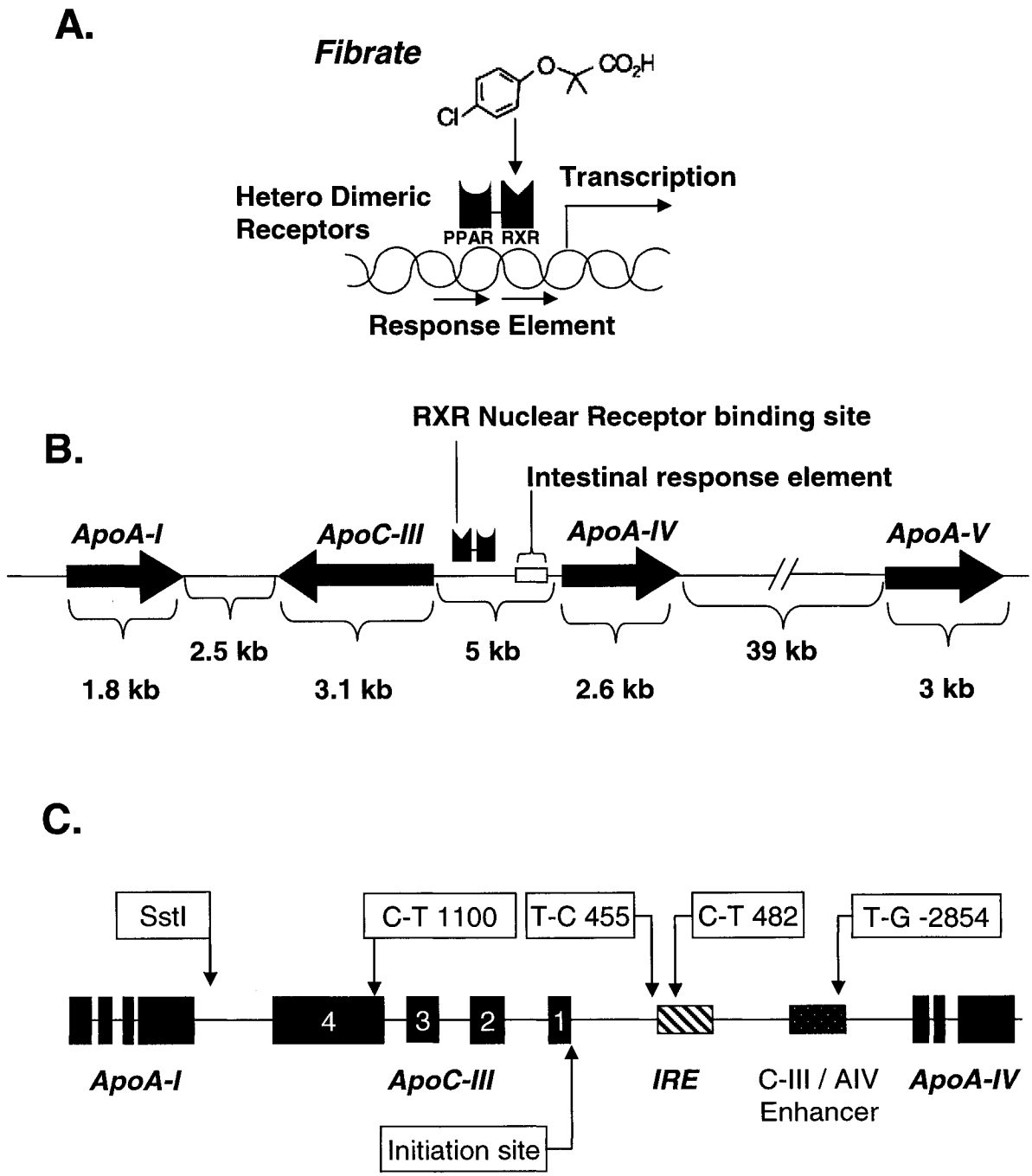
A.
Fibrate
Cl
O
CO2H
Hetero Dimeric
Receptors
PPAR RXR
Transcription
Response Element
B.
RXR Nuclear Receptor binding site
Intestinal response element
ApoA-I
ApoC-III
ApoA-IV
ApoA-V
2.5 kb
5 kb
39 kb
1.8 kb
3.1 kb
2.6 kb
3 kb
C.
SstI
C-T 1100
T-C 455
C-T 482
T-G -2854
4
3
2
1
ApoA-I
ApoC-III
IRE
C-III / AIV
Enhancer
ApoA-IV
Initiation site

patients with fenofibrates has decreased the synthetic rate of apoC-III. Treatment of hamsters with fenofibrates led to an increase in LPL mRNA and a decrease in apoC-III expression in the liver [20]. This work has been confirmed in primary rat hepatocytes where treatment with fenofibrates reduced the levels of apoC-III mRNA. The mechanism of this reduction appears to be through the disruption of a heterodimeric nuclear receptor complex that is necessary for *APOC-3* gene transcription (Fig. 2A) [19]. The correlation between elevated levels of TG rich lipoproteins (TRL) and circulating apoC-III protein has been known for some time [21], but to date a mechanistic explanation for this correlation has hinged on the inhibitory function of apoC-III on lipoprotein lipase [22].

Apolipoprotein C-III (apoC-III)

Apolipoprotein C-III is one of the most ubiquitous apolipoproteins in human plasma at a circulating concentration of 12 mg/dl [23]. It is a small (79 amino acid residue) protein that is distributed on HDL particles, but can also be found on apoB containing VLDL and LDL particles. ApoC-III was shown to inhibit [24;25] one of the first described functions of the apolipoproteins, namely the activation of LPL by apoC-II [26]. This early observation was extended to explain the association between elevated plasma apoC-III levels and hypertriglyceridemia [22]. It was postulated that the primary function of apoC-III was to act as a competitive inhibitor of apoC-II thus leading to a balanced regulation of LPL activity. Recent studies have also suggested that apoC-III is capable of disrupting hepatic lipase (HL) function [27].

Apolipoprotein C-III is comprised of two domains which were initially characterized by thrombin cleavage (Fig. 3A). A central β turn within the protein is

Fig. 3. Alpha helical structure of apolipoprotein C-III.

A, schematic diagram of apoC-III protein, cylinders represent alpha helical domains within the protein. The numeric values denote the calculated hydrophobic moment for each domain. Thrombin cleavage site is represented by **T**. Hexagons represent an O-linked glycosylation site at Thr-74. B, illustration indicating the interaction of an amphipathic alpha helix, with a plane of polar lipids. Charges represent the distribution of polar amino acids around the cylinder of the helix. C, cross sectional view of an alpha helix. The hydrophobic moment represents the avidity of the helix for the hydrophobic surface of the phospholipid monolayer (indicated by blue downward arrow). Helices are categorized by the angle that subtends the cylinder end (red curved arrow), and the avidity of the hydrophobic moment is generated by composite amino acids; G* and A_2 helical classes are illustrated.

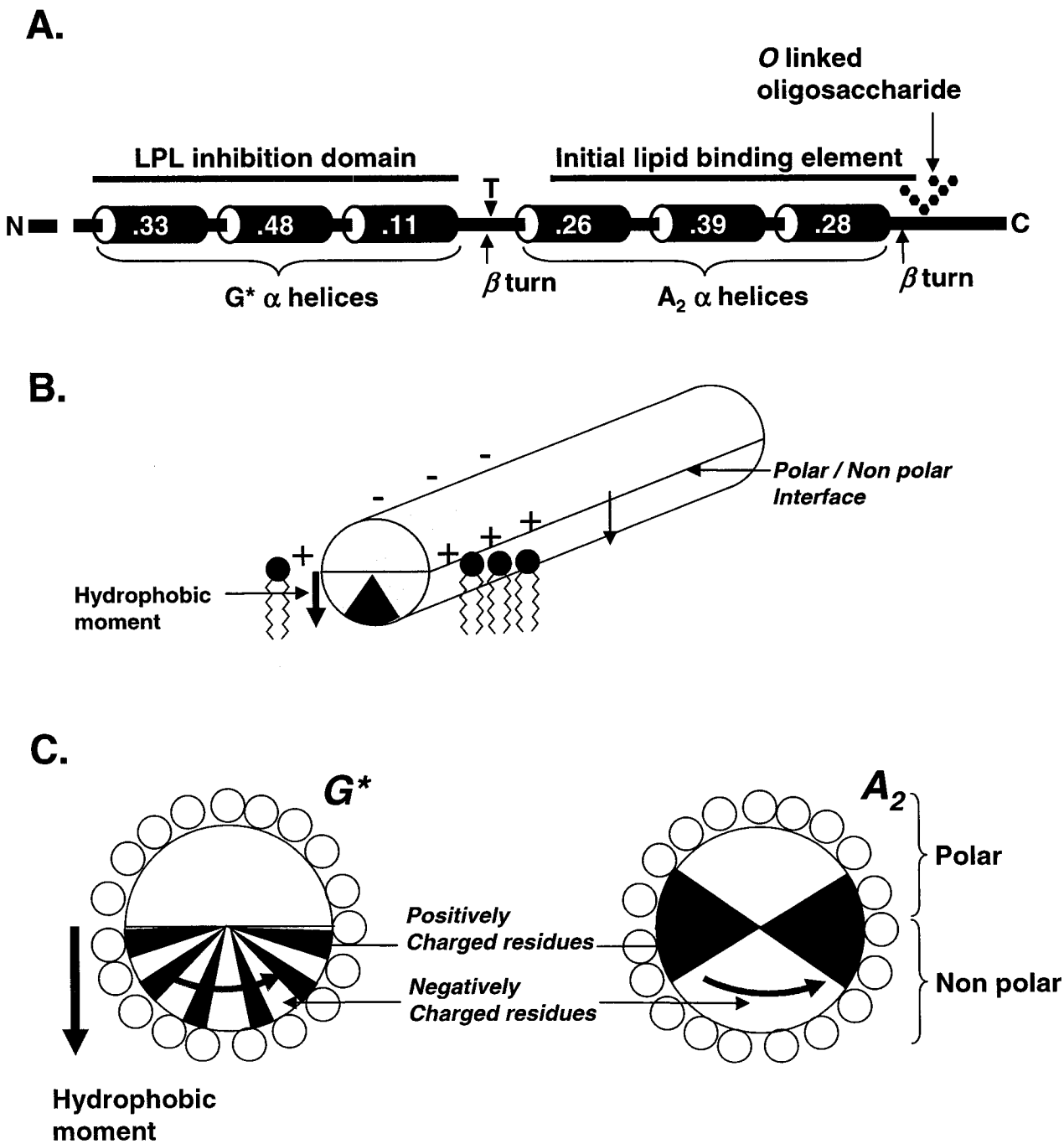
A.
O linked
oligosaccharide
LPL inhibition domain
Initial lipid binding element
T
N
.33
.48
.11
.26
.39
.28
C
G* α helices
β turn
A2 α helices
β turn
B.
Polar / Non polar
Interface
Hydrophobic
moment
C.
G*
A2
Polar
Positively
Charged residues
Negatively
Charged residues
Non polar
Hydrophobic
moment

susceptible to proteolysis yielding N and C terminal domains that have been shown in vitro to possess LPL inhibitory and lipid binding functions respectively [28]. ApoC-III contains a single *O*-linked carbohydrate at Thr-74, which can contain 0(CIII), 1($CIII_{s1}$), or 2($CIII_{s2}$) sialic acid residues [29]. Deletion of this site did not alter secretion or intracellular transport of apoC-III, nor was the distribution of apoC-III between VLDL and HDL disrupted [30]. There is also a small signal peptide that targets apoC-III to the lumen of the ER that is cleaved before the peptide is secreted.

The C apolipoproteins, like most of the exchangeable apolipoproteins, are composed mainly of amphipathic alpha helices. The structure of an alpha helix is formed by amino acid residues rotating 100° while rising 1.5 Å in a complete turn [28]. In exchangeable apolipoproteins, these structures are often found in units of 22 amino acid residues or 6 complete turns. Amphipathic helices are defined as i) possessing a large non polar face that associates with the acyl chains of the phospholipids, ii) possessing a polar face in which Asp(-), Glu(-), Lys(+) and/or Arg(+) residues are distributed with negatively charged residues at the center and positively charged residues at the periphery (Fig. 3B) [31]. The non-polar residues can be described by an angle that subtends the long axis of the helix (Fig. 3C red arrow). This angle is one of the features that classify the type of helix and influence its avidity and affinity for lipid membranes. The negatively charged polar residues which tend to be axial are thought to interact with the polar head groups of the lipid membrane while the non-polar face of the helix penetrates into the membrane and interacts with the acyl chains of the phospholipids. ApoC-III consists of high affinity helices (G* and A_2) that bind reversibly lipid membranes. The class A_2 helix which is a major structural motif for the exchangeable apolipoproteins, is characterized

by the proximity of hydrophobic residues near the interface (Fig 3C). Whereas the G* helix is characterized by its near random, radial distribution of charged residues on the non-polar face [32].

By over expressing human apoC-III in a mouse model researchers generated a hypertriglyceridemic animal [33;34]. While this animal possessed many copies of the *APOC-3* gene, the hyperlipidemic phenotype was profound [35]. The fasting plasma of transgenic animals had a milky appearance as seen in patients with severe hypertriglyceridemia. This model established a correlation between circulating plasma TG levels and plasma apoC-III. Also Breslow and colleagues [35] showed a marked increase in VLDL even in the fasting plasma of these animals. These VLDL particles were later found to have an altered apolipoprotein composition, and since apoC-III is a known inhibitor of LPL, elevated VLDL levels were thought to be due to decreased particle lipolysis and catabolism. In support of this, radio-labeled VLDL was reintroduced into mice, and apoC-III enriched VLDL was cleared seven times more slowly. When apoC-III enriched VLDL were incubated with hepatoma cells, the particles showed decreased uptake. However when apoC-III enriched VLDL was isolated and compared to VLDL from wild type animals, the VLDL from transgenic animals was found to be an equally good substrate for LPL [36].

This finding suggested that LPL may not be the only factor mediating the hyperlipidemic phenotype in these animals [37]. Recently the hypertriglyceridemia seen in apoC-III over-expressing mice has been attributed to displacement of apoE from the surface of circulating lipoproteins. In hyperlipidemic apoE expressing transgenic animals, the phenotype is ablated by crossing the mice with apoC-III transgenic mice [38]. It has also

been proposed that apoC-III disrupts the interaction between heparan sulfate proteoglycans (HSPG) and circulating lipoproteins [39]. Thus, the mechanism of apoC-III in the catabolic regulation of TG-rich lipoproteins remains in dispute.

Using gene-targeting researchers have also generated apoC-III knockout animals[40]. In this system, the plasma TG levels decrease by 33%. The LpB from these animals demonstrated an electrophoretic shift in migration from a preβ to β migration, suggesting particles are TG depleted. Also in knockout animals, the postprandial[1] response to fat loading was almost completely abolished. This postprandial response to fat feeding normally leads to a dramatic increase in secretion of TG-rich VLDL in response to dietary lipid intake. This finding suggests that the absorption or re-secretion of dietary lipids (exogenous) is grossly affected in these knockout animals. To ensure that the gene knockout had not affected the absorption of dietary lipid in the gut, researchers measured and found no change in uptake and retention of [^{3}H]triolein. Heterozygous animals also showed an intermediate TG phenotype, suggesting a gene-dose effect. These findings suggest that apoC-III also may play a role in TG-rich postprandial particle secretion.

In summary apoC-III has been implicated in three distinct mechanisms of lipoprotein metabolism. ApoC-III has been shown to antagonize the lipolytic function of LPL by competition with its obligate co-factor apoC-II in vitro[41;42]. It has been widely speculated that this inhibitory mechanism leads to the hyperlipidemic phenotype seen in apoC-III over expressing transgenic mice. In support of this, the murine over-expression model of apoC-III demonstrates that VLDL lipolysis and clearance is indeed impaired. A

[1] *Prandial from Latin* ***prandium*** *meaning morning meal, breakfast or lunch. Postprandial, is associated with a metabolic state that occurs shortly after feeding.*

second distinct mechanism proposed for apoC-III is the alteration of VLDL metabolism by disrupting particle uptake through the displacement of apoE from the lipoprotein surface. Since apoE serves as a ligand for the LDL-R some researchers suggest that this displacement of apoE will prevent lipoprotein clearance. However, increasing clinical data suggest that models in which only these two mechanisms are considered are not sufficient to explain the profound effect of this small apolipoprotein on VLDL metabolism [43]. Finally tracer studies in humans have indicated that another function is required to explain the profound correlation between circulating apoC-III levels and VLDL [44]. Since apoC-III is associated with not only circulating levels of apoB, but also independently with elevated circulating levels of TG [45], it is possible that apoC-III may increase the production of VLDL by the liver in addition to its effects on LPL in the circulation.

Assembly of Very Low Density Lipoproteins (VLDL)

The assembly of VLDL is dependent on constituent lipids and the large hydrophobic apoB protein. The apoB protein remains irreversibly bound to the surface of the particle which is comprised chiefly of phosphatidylcholine (PC) and phosphatidylethanolamine (PE) while the core of the particle contains neutral lipids TG and CE. In humans this protein is constitutively expressed from a mammoth gene located on the short arm of chromosome two [46]. The apoB mRNA can be post-transcriptionally modified by the editing enzyme APOBEC-1 (apoB mRNA editing catalytic subunit 1) after polyadenlyation but before the RNA transcript reaches the cytoplasmic compartment [47]. This 15kb apoB-100 mRNA transcript can be deaminated at nucleotide 6666, leading to the generation of a stop codon, thus encoding only the N terminal 48%

of the apoB protein [48]. This "B48" mRNA product is subsequently translated and assembled into mature lipoproteins which are secreted by the intestine as chylomicrons. The physiological importance of apoB mRNA processing remains to be elucidated, but apoB-48 lacks a region near residue 3500 that is responsible for apoB-100 binding to the LDL receptor [49]. Mutations in this region of apoB (R-Q 3500) have been shown to generate a disorder phenotypically indistinguishable from LDL-R deficiency [50]. In humans, the expression of APOBEC-1 is very high in the intestine, which means that dietary lipid (exogenous) is transported from the gut to the liver by apoB48-containing lipoproteins that will not directly bind the LDL-R. This truncation may allow for differential targeting of hepatic and intestinal lipoproteins to different tissues, through different cell surface receptor interactions. However in some animals such as rats and mice, there is significant APOBEC-1 editing activity present in the liver which leads to the production of both apoB-48 and full length apoB-100.

ApoB-100 has been modeled in a pentapartite domain structure based on computer predictions derived from primary amino acid sequence (Fig. 4A) [51]. The four C terminal domains consist of alternating regions of amphipathic α strands and β helical domains. One distinctive domain within the N terminal region of apoB-100 shares sequence homology with a lamprey protein, lipovitellin and microsomal triglyceride transfer protein (MTP) [52]. It is this structural domain that is thought to form a lipid pocket, initiating the co-translational lipidation of apoB. This co-translational lipidation is termed "first step assembly" where nascent particles of LDL density are generated (Fig. 4B). Completion of VLDL assembly and secretion requires a multi step process,

Fig. 4. Apolipoprotein B structure and very low density lipoprotein assembly

A, schematic diagram of pentapartite domain structure of apoB-100, rectangles represent individual domains [53], thin vertical lines represent the eight disulfide bonds [54], and hexagons represent 16 N-linked glycosylation sites [55]. The location of the N terminal lipovitellin homology domain and LDL-R binding domain are indicated [56]. B, First step assembly involves apoB translocation and co-translational lipidation influenced by luminal MTP. If translocation becomes arrested, the nascent apoB polypeptide (black line) becomes exposed to the cytosol where HSP 90 and HSP 70 assist in the ubiquitination and proteosomal degradation of apoB. C, second step assembly occurs in a post ER compartment which requires COP coated vesicles to bud from the ER. The action of ARF, is required before nascent lipoproteins are carried to the Golgi or post ER compartment. I postulate that PAP-1 may generate a pool of TG that is stabilized by apoC-III before particle fusion that leads to the formation of VLDL particles.

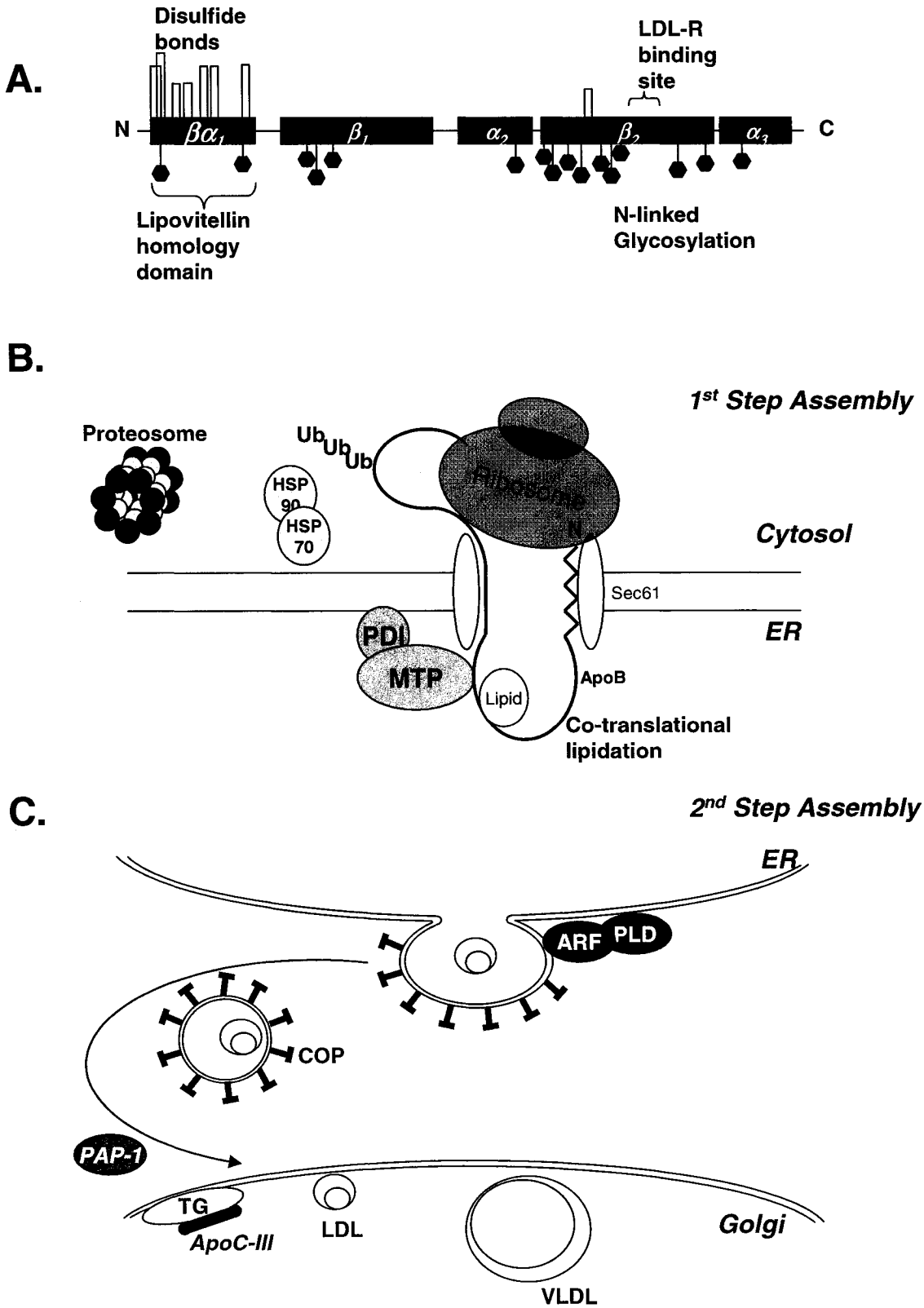
A.
Disulfide bonds
LDL-R binding site
N
C
Lipovitellin homology domain
N-linked Glycosylation
B.
1st Step Assembly
Proteosome
Ub Ub Ub
HSP 90
HSP 70
Ribosome
Cytosol
Sec61
ER
PDI
MTP
Lipid
ApoB
Co-translational lipidation
C.
2nd Step Assembly
ER
ARF
PLD
COP
PAP-1
TG
ApoC-III
LDL
Golgi
VLDL

which can be broadly divided, into first and second step assembly [57]. The first step of LpB assembly is primarily driven by the interaction of proteins at the translocon, while the second step likely occurs in a post ER compartment and is very sensitive to lipid components (Fig. 4C).

While the first step of LpB assembly occurs primarily at the translocon and is mediated primarily by protein factors, second step lipidation and maturation is acutely sensitive to lipid constituents or lipid transport proteins that act as assembly co-factors. MTP is an obligate co-factor for apoB secretion. The absence of this protein leads to abetalipoproteinemia, an autosomal recessive disease where no circulating LpB are detected [58]. The reintroduction of this protein into heterologous cell systems in the presence of apoB is sufficient to mediate the secretion of partially lipidated particles [59]. MTP is composed of two non-covalently bound subunits, a large 97 kDa lipid transfer subunit ("M") and a small 55 kDa protein disulfide isomerase subunit (PDI). It is the large M subunit that through an amino-terminal beta barrel domain binds directly to apoB during tanslocation (Fig. 4B). In this way MTP acts as a chaperone to ensure correct translocation and initial lipidation of the nascent apoB polypeptide during first step of LpB synthesis. MTP also appears to play a role in later stages of VLDL assembly through its ability to provide neutral lipids for second step assembly. This lipid transfer activity has been shown to be independent from the binding of MTP to the N-terminus of apoB [60].

Apolipoprotein B-100 secretion is regulated at the co- or post-translational levels. This is to say that alterations of the apoB100 mRNA are not responsible for altered levels of circulating apoB protein. Circulating levels of LpB are thus determined largely by the

degradation or aborted assembly of nascent particles. ApoB protein degradation has been detected in both hepatoma cell lines and primary hepatocytes, and occurs through both proteosomal and non proteosomal pathways [61]. The proteosomal degradation of apoB occurs during aborted first step assembly. In early in vitro translocation experiments, apoB appeared to adopt a bitopic orientation during translation (Fig. 4B), exposed to both the cytosol and the lumen of the ER [62]. Protease protection assays showed that nascent apoB was accessible to the cytosol and also possessed domains fully translocated into the lumen and therefore protected from proteolysis [63]. Co-translational degradation of apoB during first step of assembly requires the ubiquitination and interaction of apoB with cytosolic proteins HSP 70 and HSP 90 [64]. It remains debated how apoB becomes accessible to the cytoplasmic proteosome and several mechanisms have been proposed. In the retrotranslocation model it is proposed that apoB is extruded back through the translocon into the cytosol (Fig. 4B) [65], or alternatively apoB may be extruded by a second translocon that directs the N terminus back into the cytosol for degradation [66]. Structural domains within the N terminus of apoB are proposed to possess pause translocation motifs (LKK-T----N---A or LKK---SE) [67] that are capable of arresting translocation but not translation of the nascent peptide [68]. Recent data have suggested the structural importance of β sheets within the second domain of apoB that may also arrest in the translocon [69]. When chimera proteins with these β sheet regions of apoB were expressed, their translocation was improved by the addition of OA [70]. In addition, mutations within the signal peptide of apoB which occur in >20% of the population, can lead to increased co-translational proteosomal degradation during aborted first step assembly [71]. This degradation results from a deletion (Leu Ala Leu) that shortens the

signal peptide from 27 to 24 residues, and disrupts proper interaction and translocation of apoB through the translocon [72].

Lipidation of Very Low Density Lipoprotein Particles

In hepatocytes neutral lipid availability for "second step assembly" appears to comprise both spatial and temporal elements [73]. The appearance of TG-rich LpB occurs with a temporal delay of approximately 15 minutes between translation and assembly,. Also recent electron microscopy studies have suggested that VLDL sized particles exist in the Golgi apparatus [74] and not the ER as was previously reported [75]. The location of VLDL particle formation remains a subject of debate, and not all researchers concur with an assembly model requiring post ER lipidation [76]. It is known that the availability of TG for VLDL secretion can be enhanced by treating cells with OA particularly rat hepatocytes [77]. The TG available for LpB secretion has been grouped into three categories, 1) a cytosolic pool which maintains a long half life, 2) an ER pool that has a very short half life, and 3) a microsomal luminal pool which may be comprised of both lipoprotein and non lipoprotein lipid also possessing a short half life [5]. MTP is thought to play a critical role in not only first step assembly but also the mobilization of TG for LpB in the lumen of the microsome [78]. This second step of VLDL assembly is acutely sensitive to lipid co-factors as demonstrated by n-3 polyunsaturated fatty acids (Personal communication Dr. Khai Tran). The supplementation of these FFA in humans leads to a specific decrease in VLDL but not LDL secretion [79]. The mechanism for this aborted second step assembly has been termed post-ER pre-secretory proteolysis (PERPP) and is thought to occur in a post ER compartment [80].

Recent reports with apoB-48 have suggested that the second step of LpB assembly occurs in a compartment separate from the rough ER [81]. In mice, VLDL assembly has also been reported to occur in the Golgi [82]. This issue remains under active debate since other researchers believe that VLDL assembly is achieved in the ER [76]. It has been reported that this VLDL assembly can be inhibited with low doses of brefeldin A (BFA) [83]. Some have interpreted this as a general disruption of the secretion pathway [84] but recent evidence has shown that BFA can inhibit ADF Ribosylation Factor (ARF-1) directly [85]. This small guanine nucleotide exchange factor is involved in the recruitment of the cotomer protein 1 (COP-1) complex which is required for transport of the maturing lipoprotein particle within the ER. [86]. The over expression of an ARF-1 mutant was sufficient to inhibit the production of VLDL but not LDL particles in hepatoma cells [87]. It is also noteworthy that ARF is capable of binding and activating phospholipase D (PLD) which hydrolyses PC to PA [88]. The TG pool for VLDL assembly is derived in part from PC [89], through the conversion of PC to PA by PLD which may provide substrate for TG production (Fig. 14). Thus to date the effect of ARF-1 on VLDL production may be either through regulation of COP-1 vesicle transport of nascent lipoprotein particles or it may directly activate PLD providing substrate for TG production. Inhibition of the calcium independent phospholipase A_2 ($iPLA_2$) has also been shown to specifically interrupt VLDL but not LDL secretion in a post ER compartment [90]. This effect is likely mitigated by the necessity of active phospholipid remodeling for LpB assembly since phospholipids are requisite constituents of lipoproteins [91]. It is also possible that the turnover of phospholipid by $iPLA_2$ which provides FFA for TG re-acylation is the mechanism by which $iPLA_2$ participates in VLDL assembly. The literature suggests that

the inhibition of VLDL assembly that occurs with $iPLA_2$ inhibition is independent of TG synthesis[2].

Phosphatidate Phosphohydrolase (PAP)

Treatment of rat hepatocytes with the glucocorticoid analog dexamethasone leads to increased TG synthesis [92] and activation of phosphatidic acid phosphohydrolase (PAP)[93]. Since this enzyme converts phosphatidic acid (PA) to diacylglycerol (DG) for triglyceride (TG) production, it may mobilize TG for VLDL assembly. In fact in primary rat hepatocytes dexamethasone treatment induces a four-fold increase in VLDL secretion [94]. PAP-1 has also been shown to translocate to the microsomal membranes and become active in response to OA treatment, thus in addition to its activity the sub-cellular distribution of this enzyme may be important for VLDL assembly [95]. While this enzyme activity may play a key role in TG production for VLDL assembly, to date it has eluded purification. Previous work has shown that treatment of primary rat hepatocytes with dexamethasone leads to increased secretion of TG rich lipoproteins [96]. Identical treatment conditions have been shown to increase PAP-1 activity. Induction of this enzyme by dexamethasone may lead to increased intracellular TG production and result in the overproduction of VLDL. Thus PAP-1 may act as a novel protein regulator of lipid availability for the second step assembly of TG rich VLDL lipoproteins.

---

[2] *In some cell lines PAP-1 activity has been shown to decrease by BEL treatment which is commonly used as a specific $iPLA_2$ inhibitor in Murine cells [176] and U937 THP-1, MonoMac phagocytes, Raw264 macrophage, Jurkat cells and GH3 Human Pituitary cells [177;177], but not in McA-RH7777 cells [90].*

Once TG has been generated and appears within the lumen, it remains only transiently in the absence of apoB [5]. The exchangeable apolipoproteins such as apoC-III may serve to stabilize this primordial lipid droplet until fusion with LpB occurs (Fig. 4C). It is at this post translational or second step that nascent LpB is thought to incorporate bulk lipid and form VLDL (Fig. 4C). Data from our lab have suggested that this is both temporally and spatially distinct from nascent apoB translation [83]. Recent work in our lab has suggested that this final lipid assembly step occurs immediately before secretion [74;83]. Thus candidate proteins such as apoC-III or PAP-1 may play a role in the Golgi or late in the secretory pathway. I propose that unidentified protein factors remain, that are necessary for the second step addition of lipid which will lead to the production and stabilization of nascent VLDL and propose that two of these proteins are PAP-1 and apoC-III respectively.

Hypothesis and Specific Aims

To date the investigation of an intracellular role for apoC-III has been hampered by a lack of biochemical tools, such as high quality antibodies. Researchers also believe that since apoC-III can be acquired by a lipoprotein particle after secretion, that the apoC proteins do not play an intracellular role in LpB formation. Finally most human lipoprotein samples are obtained in the fasted and not fed state (*postprandial*), leading researchers to detect apoC-III replete VLDL, which may not be the case postprandially where high circulating FFA levels are present. I hypothesize that apoC-III expression in McA-RH7777 rat hepatoma cells will play an intracellular role in increasing VLDL secretion by increasing intracellular TG but not apoB. Since VLDL secretion largely occurs postprandially, I will evaluate apoC-III in McA-RH7777 cells with oleate (OA)

supplementation. In this way I will determine if the effect of apoC-III is constitutive or dependent on OA supplementation. Also by examining different cell lines I will determine if apoC-III expression levels influence TG secretion in a dose dependant manner. I will evaluate apoB synthesis and secretion, by metabolic labeling, and its secreted density by rate floatation ultracentrifugation. I suspect that apoC-III expression will lead to an increase in TG-rich $VLDL_1$ secretion. Finally I will compare expression of apoC-I and apoC-II to determine if a similar metabolic effect is evident in cells expressing these proteins, and whether this is due to common structural elements.

I further propose to investigate purification methods for the isolation of the PAP-1 enzyme. I will examine the utility of mechanical isolation techniques such as ammonium sulfate precipitation, liposome absorption and hydroxyapatite chromatography. I hypothesize that the use of metabolically labeled cell lysates (or sub-cellular fractions) from primary cell cultures will significantly enhance the sensitivity of chromatographic or other purification techniques. These methods will be coupled to 2D purification and chromatographic purification approaches to determine a practicable approach to clone PAP-1. In concert I will evaluate the utility of a differential display PCR (DD-PCR) cloning approach to isolate PAP-1 by exploiting dexamethasone induced increases in activity, reported in primary rat hepatocytes.

Chapter 2 Materials and Methods

Materials - Medium and reagents used for cell culture studies were obtained from Life Technologies Inc. DNA restriction and modification enzymes, Pfu DNA polymerase, T4 DNA ligase, and MMLV reverse transcriptase were obtained from New England Biolabs. Antibodies against apoC-I, C-II or C-III were purchased from Academy Biomedical, Houston TX. [^{35}S]methionine/cysteine (1000 Ci/mmol), protein A-Sepharose™ CL-4B beads, and horseradish peroxidase-linked anti-mouse and anti-rabbit IgG antibodies were obtained from Amersham Corp. [2-^{3}H]glycerol (9.6 Ci/mmol), [^{14}C]oleate (80 mCi/ mmol), and horseradish peroxidase-linked anti-goat antibody was obtained from Sigma Chemical Company. Protease inhibitor mixture and chemiluminescent substrate were purchased from Roche Diagnostics. Oleic acid, TG, and phospholipid standards were procured from Avanti Polar Lipids, Alabaster, AL. Polyclonal antiserum against rat VLDL was produced in our laboratory. Purified human apoC apoproteins were a gift of Dr. Karl Weisgraber (Gladstone Institute of Cardiovascular Disease, San Francisco). ApoC-III antibody was received from Karmin O (University of Hong Kong). The [^{3}H]PA was a generous gift of Dr. David Brindley (University of Alberta, Edmonton).

Construction of Human ApoC Expression Plasmids - Total RNA was isolated from HepG2 cells using the Triazol™ method, reverse transcription was performed using MMLV reverse transcriptase and an oligo-dT primer. The HepG2 cDNA was used to amplify the coding sequences of apoC-I, C-II and C-III by polymerase chain reaction (PCR). The sequences of the PCR primers are shown in Table II. Restriction sites BamHI

and HindIII were included in the forward and reverse primers, respectively. The amplified apoC cDNA fragments were ligated into the pCMV5 expression vector that was digested with BglII and HindIII. The cDNA was confirmed using bi-directional sequencing analysis.

Cell Culture and Transfection - McA-RH7777 cells obtained from American Type Culture Collection were cultured in Dulbecco's modified Eagle's medium (DMEM) containing 20% fetal bovine serum (FBS). Co-transfection of the apoC expression plasmids with pSV2neo was performed by calcium phosphate co-precipitation and glycerol shock to generate stable transformants [97]. Two days after initial transfection, the neomycin analog, G418 (200 μg/ml) was added to the culture medium and resistant colonies were selected. Secretion of recombinant protein was detected by immunoblotting of conditioned medium using appropriate antibodies. Stable cell lines expressing varying levels of apoC protein were selected for further studies.

[^{3}H]Glycerol Labeling of Cellular Lipids – Cells were seeded at 1.2 x 10^5 cells/well on six well Falcon dishes and cultured overnight in the presence of DMEM containing 20% FBS, and G418. Each well was incubated with 2 ml of labeling medium containing [^{3}H]glycerol (7 μCi/ml) in the presence or absence of 0.4 mM oleate (OA) and 20% FBS for 2 h. Medium and cellular samples were extracted with chloroform/methanol/acetic acid/NaCl saturated H_2O/H_2O (4:2:0.01:1:2, by volume). The chloroform layer was removed and samples were dried completely under N_2 in sialized tubes, samples were re-solubilized in 25 μl chloroform containing egg yolk carrier and spotted onto HPTLC

Silica Gel 60 plates. The plates were run half way in a chloroform/methanol/acetic acid/formic acid/H_2O solvent system (70:30:12:4:2, by volume) to separate the phospholipid samples, plates were dried and transferred to a second hexane/diethyl ether/acetic acid solvent system (70:30:1, by volume) to resolve neutral lipids [98;99]. Lipid species were identified by I_2 staining and the radioactivity associated with individual lipid samples was scraped and collected for quantification by liquid scintillation counting (Wallac 1409 counter). Cellular protein levels were quantified by the Bradford method [100].

[^{14}C]Oleate Pulse Chase of Lipids - Cells were seeded at 1.2 x 10^5 cells/well onto six well Falcon dishes and cultured overnight in the presence of DMEM containing 20% FBS and G418. Each well was labeled with 2 ml of medium containing [^{14}C]oleate (5 μCi/ml) 0.4 mM OA and 20% FBS for 2 h. After this pulse labeling period, medium was removed and cells were placed in medium containing 20% FBS and 0.4 mM OA. The chase medium and cellular samples were collected over a period up to 4 h and lipids were extracted and separated as above. Lipid samples were quantified by liquid scintillation counting and expressed as a ratio of cpm/mg cellular protein.

^{35}S Labeling of ApoB-100 – Cells were cultured to 80% confluency on 60 mm Primaria Falcon dishes in the presence 20% FBS and G418. Cells were labeled for 2h with [^{35}S]methionine/cysteine (200 μCi/ml) in 2 ml of methionine/cysteine free DMEM (-met/cys) containing 20% FBS and 0.4 mM OA. ^{35}S-labeled apoB protein was recovered by immunoprecipitation in RIPA buffer. Proteins were resolved by reducing SDS-PAGE,

gels were dried and subjected to autoradiography. Individual bands were excised and counted in a Wallac 1409 liquid scintillation counter [97].

MTP Activity Assay – Cellular samples were prepared by sonication as described previously [83] and the TG transfer activity was assayed using [^{14}C]triolein as described previously [101].

Subcellular Fractionation - Two 10-cm dishes of cells were grown to 80% confluency in 20% FBS in the presence of G418. Cells were labeled for 2 h with medium containing either [^{14}C]oleate (5 μCi/ml for lipids) or [^{35}S]methionine/cysteine (7 μCi/ml for proteins) in the presence of 20% FBS and 0.4 mM OA. After 2 h cells were rinsed with ice-cold PBS and scraped into 2 ml of ice-cold Tris buffered sucrose (TBS) (1mM Tris-HCL, pH 7.4, 250 mM sucrose, 5 mM EDTA, and serine/cysteine protease inhibitor mixture). Cells were then washed twice with TBS and centrifuged at low speed (900 rpm) to remove any residual medium. Cells were homogenized by passing the suspension through a ball bearing homogenizer twenty times. Post nuclear supernatants were obtained by centrifugation in glass Corex tubes (9,500 rpm, 10 min, 4 °C, Sorval SS-34 rotor). The supernatant was loaded into polypropylene tubes and separated into microsomal and cytosolic fractions by ultracentrifugation (100,000 rpm, 16 min 15 °C, TLA 100.4 rotor). The cytosolic supernatant was decanted and the microsomal pellet was washed twice before resuspending in 2 ml of TBS by passing the sample through a 28-gauge needle. Then luminal contents were released by treating the microsomal samples with 0.1 mM sodium carbonate, pH 11.3 (final concentration), and nutating the

samples for 30 min at room temperature. To separate the luminal contents from the microsomal membranes, membranes were pelleted by ultracentrifugation (100,000 rpm, 15 °C 16 min, TLA 100.4 rotor) [90]. Proteins were then isolated by immunoprecipitation or lipids were extracted from the microsomal lumen and membrane as described above.

Ultracentrifugation of Secreted Lipoproteins – Cells were grown to 80% confluence in the presence of 20% FBS and G418 in 10 cm Falcon dishes. Cells were labeled for 2 h with medium containing either [^{14}C]oleate (5 μCi/ml for lipids) or [^{35}S]methionine/cysteine (7 μCi/ml for proteins) in the presence of 20% FBS and 0.4 mM OA. After 2 h medium was collected and separated by cumulative rate floatation ultracentrifugation. Four ml of medium was adjusted to d = 1.10 g/ml with dry KBr. This sample was underlayed below 3 ml of d = 1.065 g/ml NaBr, 3 ml d = 1.02 g/ml NaBr, and 3 ml of d = 1.006 g/ml NaCl. Samples were centrifuged (40,000 rpm 20 °C 148 min) and the $VLDL_1$ sub fraction (S_f) > 100 was removed, placed at 4 °C and the remaining sample was centrifuged again (37,000 rpm, 15 °C for 18 h). Samples were removed from the top of the tube to obtain 12 fractions [83], and were processed for lipid extraction and quantification or protein immunoprecipitation and quantification as described above.

Isolation of Primary Rat Hepatocytes for PAP-1 Detection - Hepatocyte cultures were prepared from 75 g male Sprauge Dawley rats. Rats were lightly anesthetized with 3% isoflourane and injected with 0.2 ml Somnitol (50 nmol/g). The abdominal cavity of the animal was exposed and the liver was perfused with HEPES buffered saline solution (140

mM NaCl, 4 mM KCl, 5.5 mM glucose, 10 mM HEPES, 10 mM EGTA pH 7.4) at a rate of 10 ml/min via the portal vein. Once the liver was clear of blood, ligatures tied around the superior and inferior vena cava were tightened and the liver was perfused with HEPES buffered saline (140 mM NaCl, 4 mM KCl, 5.5 mM glucose, 10 mM HEPES, 1.5 mM $CaCl_2$-$2H_2O$, 1 mM MgCl-$6H_2O$ pH 7.4) containing 0.5 mg/ml of collagenase. The liver was excised and hepatocytes were collected from the minced liver after filtration and low speed centrifugation, 4 °C. Cells were plated on 10 cm Falcon culture dishes coated with fibronectin and were allowed to attach for 4 h. The medium was replaced with DMEM containing antibiotic and antimycotic and 1 mg/ml BSA. Cells were grown overnight in serum-depleted medium for 16 h. After overnight serum depletion cells were treated with dexamethasone (0.1 to 20 μM) for a period of 4 h and the activity of PAP-1 was assessed.

PAP-1 substrate preparation – [^{3}H]PA (1 mCi/ml) was combined, 130 μl [^{3}H]PA: 835 μl egg PA (36 mM): 302 μl egg PC (66 mM). This mixture was dried under N_2 and solubilized in 5.56 mM EDTA/EGTA. The lipid emulsion was sonicated twice for 30 sec at maximum power in a Bronson sonicator until the emulsion became an off white color. One ml of 1 g/ml fatty acid free BSA was added and the sample was frozen and thawed 3 times to clarify.

PAP-1 Assay – Samples (20 μl) were prepared in Eppendorff tubes containing 10 μl of reaction buffer (2 M Tris maleate, 1 M DTT, 1 M Mg pH 6.5). To distinguish PAP-2 activity duplicate samples were prepared with 4 mM N-ethylmaleimide (NEM) and

incubated on ice for 30 min to inactivate PAP-1 enzyme activity. 10 µl of [^{3}H]PA (0.1 mCi/ml) was added and samples were transferred to a 37 °C heat block for 20 min. The reaction was stopped by adding 1 ml chloroform:methanol:olive oil (95:5:0.8), and unreacted substrate was precipitated by adding 200 µl of alumina oxide. Samples were vortexed briefly, centrifuged (2500 rpm, 10 min at room temperature) and the chloroform layer was removed and dried before scintillation counting.

Cytosolic PAP-1 Sample Preparation and Chromatography – Cell lysates were prepared from dexamethasone treated primary rat hepatocytes. Briefly, samples were solubilized in sucrose buffer (250 mM sucrose, 10 mM Tris-HCl, pH 7.4) and homogenized with ten strokes of a ball bearing homogenizer. The samples were subjected to a low speed centrifugation (9,500 rpm, 10 min, 4 °C), Sorval SS-34 rotor to precipitate the nuclear and mitochondrial membranes, and the supernatant was removed. The supernatant was subjected to ultracentrifugation (100,000 rpm, 16 min 15 °C, TLA 100.4 rotor) to separate the microsomal membranes from the cytosol. This cytosol was loaded onto a 3 ml column of hydroxyapatite resin that had been equilibrated with 10 mM DTT and 0.05% Tween 20. The column was washed with 10 ml of 70 mM potassium phosphate buffer (pH 7.4) and 1 ml fractions were collected. The column was treated with 10 ml of 300 mM potassium phosphate buffer (pH 7.4) to elute proteins that strongly bound to the resin. Fractions (1 ml) were then assayed for PAP-1 activity and protein concentration. The majority of the PAP-1 activity eluted in the fourth fraction of the 300 mM potassium phosphate buffer wash. Samples were also run on denaturing SDS-PAGE gels and silver stained to determine where the bulk of the proteins were eluting.

Ammonium Sulfate Precipitation – Total rat liver (5 g) was homogenized in 5 ml of 0.25 mM sucrose buffer pH 7.4 containing 2 mM DTT in a glass Dounce homogenizer and brought to a final volume of 50 ml. Forty ml was transferred to a glass beaker and stirred at 4 °C while $(NH_4)_2SO_4$ was slowly added. Samples were transferred to a glass Corex tube and centrifuged (9,500 rpm, 10 min, 4 °C, Sorval SS-34 rotor) to pellet proteins, supernatant was decanted and further $(NH_4)_2SO_4$ was added (2.24g:10% 2.28g:20% 2.36g:30% 1.2g:35% 1.24g:40% 1.24g:45% 1.28g:50% 2.64g:60% 2.76g:70%). Precipitated protein samples were dialyzed twice in 4 l of PBS before PAP-1 activity and protein concentrations were determined.

2D-PAGE Separation of Rat Liver Cytosol - Two Sprague Dawley Rats were fed by stomach tube 8 ml of 25% ethanol. Rats were left overnight to recover. The next morning livers were perfused with 0.9% NaCl and 0.25 mM sucrose (2 mM DTT, 1 mM benzamidine, 10 µg/ml aprotinin, 10 µg/ml lupeptin, 2 mM PMSF). Fifteen g of liver was homogenized in 150 ml sucrose buffer, and spun at 10,000 rpm for 10 min. Pellets were washed with 100 ml sucrose and the supernatants were pooled. Samples were spun at 35,000 rpm for 70 min, the supernatant was stored at -80 °C until use. 200 µl of rat liver cytosol (0.34 mg) was solubilized 1:1 in fresh IPG buffer (7 M Urea, 2 M thiourea, 0.4% CHAPS, 0.1% DTT in ddH_20), this was applied to a well in a Pharmacia IPG rehydration apparatus, and a BioRad pH 3-10 IPG strip was overlaid. The sample was overlaid with mineral oil, the chamber was closed and samples were allowed to absorb overnight. Strips were transferred to a BioRad IPG apparatus and electrophoresed (step

1: 250V linear current 30 min, step 2: 10000V linear current 2.5h, step 3: 10000 V rapid convex current to 40,000 Vhrs). After IEF strips were removed and equilibrated (1% DTT, 2% SDS, then 4% iodoacetamide, 2% SDS) before being added to the top of 10% SDS-PAGE gels. IPG strips were over laid with 1% agarose and the gels were run overnight at 7 Mah per gel. Proteins were revealed by silver staining in fastidiously cleaned glassware.

DD-PCR of Dexamethasone Induced Hepatocytes - Primary rat hepatocyte cultures were treated with 1 μM dexamethasone, 1 μM dexamethasone and 100 nM insulin or untreated for 4 h. Total mRNA was extracted with Triazol and reverse transcription reactions were performed as per GeneHunter® manufacturer instructions. mRNA was PCR amplified with 2 μM of degenerate and oligo dT primer (Table 3) in the presence of 0.2 mCi of α-[^{32}P]dATP (2000 Ci/mmol). PCR samples were resolved on 6% denaturing acrylamide gels and bands were revealed by fluorography. Candidate bands were cut from the dried gel and PCR amplified. Fragments were inserted into pGEM-T easy using TA cloning. DNA from transformed colonies was isolated and insertion was confirmed by EcoRI digestion and bidirectional sequencing using T7 and SP6 primers. Sequences were submitted to BLAST searching at the NCBI website.

Table 2. Nucleotide sequences of the apolipoprotein C PCR primers

ApoC-I forward	CGGGATCCTCGCCATGAGGCTCTTCCTGTCG
ApoC-I reverse	CCCCAAGCTTCAGGTCCTCATGAGTCAATC
ApoC-II forward	CGGGATCCACACTATGGGCACACGACTCCTCC
ApoC-II reverse	CCCCAAGCTTCTGGCTGTTACTCCTCTCC
ApoC-III forward	CAGTGGATCCTAGAGGCAGC
ApoC-III reverse	CCCTGAAGCTTGCAGGACCCA

All sequences are 5' to 3' direction. The BamHI and HindIII restriction sites included in the forward and reverse PCR primers are indicated (underlined).

Table 3. Nucleotide sequences for differential display PCR primers

Primer	*Sequence*	*Primer*	*Sequence*
H AP 1	AAG CTT GAT TGC C	H AP 41	AAG CTT ACG GGG T
H AP 2	AAG CTT CGA CTG T	H AP 42	AAG CTT TGC ACC G
H AP 3	AAG CTT TGG TCA G	H AP 43	AAG CTT GAA GCG G
H AP 4	AAG CTT CTC AAC G	H AP 44	AAG CTT CTC CGG A
H AP 5	AAG CTT AGT AGG C	H AP 45	AAG CTT GGC TGA C
H AP 6	AAG CTT GCA CCA T	H AP 46	AAG CTT CGG TCC T
H AP 7	AAG CTT AAC GAG G	H AP 47	AAG CTT ATG CCC G
H AP 8	AAG CTT TTA CCG C	H AP 48	AAG CTT GCG GTG A
H AP 9	AAG CTT CAT TCC G	H AP 49	AAG CTT TAG TCC A
H AP 10	AAG CTT CCA CGT A	H AP 50	AAG CTT TGA GAC T
H AP 11	AAG CTT CGG GTA A	H AP 51	AAG CTT CGA AAT G
H AP 12	AAG CTT GAG TGC T	H AP 52	AAG CTT GAC CTT T
H AP 13	AAG CTT CGG CAT A	H AP 53	AAG CTT CCT CTA T
H AP 14	AAG CTT GGA GCT T	H AP 54	AAG CTT TTG AGG T
H AP 15	AAG CTT ACG CAA C	H AP 55	AAG CTT ACG TTA G
H AP 16	AAG CTT TAG AGC G	H AP 56	AAG CTT ATG AAG G
H AP 17	AAG CTT ACC AGG T	H AP 57	AAG CTT GTT GGT A
H AP 18	AAG CTT AGA GGC A	H AP 58	AAG CTT AAC TGA G
H AP 19	AAG CTT ATC GCT C	H AP 59	AAG CTT CTA GCA T
H AP 20	AAG CTT GTT GTG C	H AP 60	AAG CTT TCG AAT C
H AP 21	AAG CTT TCT CTG G	H AP 61	AAG CTT AGT TGC T
H AP 22	AAG CTT TTG ATC C	H AP 62	AAG CTT GCA AGT T
H AP 23	AAG CTT GGC TAT G	H AP 63	AAG CTT TTA TTC G
H AP 24	AAG CTT CAC TAG C	H AP 64	AAG CTT CAT ATG C
H AP 25	AAG CTT TCC TGG A	H AP 65	AAG CTT CAA GAC C
H AP 26	AAG CTT GCC ATG G	H AP 66	AAG CTT GCC TTT A
H AP 27	AAG CTT CTG CTG G	H AP 67	AAG CTT TAT TTA T
H AP 28	AAG CTT ACG ATG C	H AP 68	AAG CTT CTT TGG T
H AP 29	AAG CTT AGC AGC A	H AP 69	AAG CTT AAT AAC G
H AP 30	AAG CTT CGT ACG T	H AP 70	AAG CTT TCA TAT G
H AP 31	AAG CTT GGT GAA C	H AP 71	AAG CTT GTA GTA A
H AP 32	AAG CTT CCT GCA A	H AP 72	AAG CTT TCA AAG A
H AP 33	AAG CTT GCT GCT C	H AP 73	AAG CTT AGT TAT C
H AP 34	AAG CTT CAG CAG C	H AP 74	AAG CTT CAA GTT T
H AP 35	AAG CTT CAG GGC A	H AP 75	AAG CTT TTA TTC G
H AP 36	AAG CTT CGA CGC T	H AP 76	AAG CTT GTT ATA G
H AP 37	AAG CTT GGG CCT A	H AP 77	AAG CTT TGA ATT C
H AP 38	AAG CTT CCA GTG C	H AP 78	AAG CTT AAA TCG A
H AP 39	AAG CTT TCC CAG C	H AP 79	AAG CTT GTC TAA A
H AP 40	AAG CTT GTC AGC C	H AP 80	AAG CTT CTA TTT C
H $T_{11}G$	AAG CTT TTT TTT TTT G		
H $T_{11}A$	AAG CTT TTT TTT TTT A		
H $T_{11}C$	AAG CTT TTT TTT TTT C		

These primers were used in a combinatorial fashion to amplify the complement of expressed mRNA in dexamethasone treated hepatocytes. All sequences are 5' to 3' direction. The EcoRI restriction sites included in all PCR primers (underlined). The 3 primers at bottom represent the 3' anchor primers that were employed in permutations with all 80 5' primers above.

Chapter 3 Apolipoprotein C-III and Very Low Density Lipoprotein Assembly

Introduction

Apolipoprotein C-III is a small (79 amino acid residues) exchangeable apolipoprotein that is known to correlate with elevated circulating levels of triglyceride (TG) in human plasma [23]. This correlation between circulating levels of apoC-III protein and elevated levels of triglyceride-rich apoB containing lipoproteins (LpB) has been known clinically for some time [21]. ApoC-III is one of a number of exchangeable apolipoprotein family members which decorate the surface of VLDL [32]. Apolipoprotein B and MTP have been shown to be indispensable to particle assembly [59] however, the role of many of these accessory molecules remains unknown. ApoC-III has been shown to inhibit the activity of lipoprotein lipase (LPL) [26] and hepatic lipase (HL) [27], I speculated that this auxiliary protein may also play a role in TG rich VLDL assembly. This is supported by recent work where a transcriptional regulator (Foxo-1) of apoC-III led to an increase in circulating TG in mice [102].

In apoC-III transgenic mouse models, this small apoprotein was sufficient to generate a profound hyperlipidemic phenotype [103]. When the apoC-III gene was disrupted by gene targeting, in mice, there was a 70% reduction of TG in homozygous mutants and an intermediate reduction in heterozygotes. This gene-dose effect implies a role for apoC-III in regulating TG-rich lipoprotein metabolism [40]. Also many genetic studies have led to debate on the role of the AI/CIII/AIV/AV gene locus in patients with Familial Combined Hyperlipidemia (FCHL) [15;16,17] This syndrome affects >2% of the western population and is associated with premature coronary artery disease [1]. At this

point the inability to determine or rule out linkage of ApoC-III with FCHL has been attributed to the multifactorial nature of this syndrome [18]. Recent clinical studies have also suggested that the steady state levels of apoC-III in patients may be due to altered secretion rather than catabolism [44]. Since apoB adopts a 1 to 1 stoichiometry on the surface of lipoprotein particles[104], these hyperlipidemic states represent either a production of a greater number of particles or larger, more lipid engorged particles [45]. Clinically this distinction is important for the treatment and outcome of patients displaying this syndrome [21;105].

I propose to test a novel intracellular mechanism of apoC-III, in the assembly and secretion of TG rich VLDL. This anabolic role can be tested directly in cell culture by over expression of human apoC-III in McA-RH7777 cells and monitoring the production of TG rich apoB containing particles, by metabolic labeling [97]. Using this well characterized system I evaluated the effect of apoC-III on LpB secretion. I also determined whether LpB was constitutively secreted or occurs only in the presence of exogenous OA, suggesting a post prandial effect. ApoC-III expression in this model allows the determination of either a hyper-TG normo-B, or hyper-TG hyper-B phenotype [105]. This determination is clinically relevant since the treatment of these two disorders, in patients is quite distinct. Small accessory molecules such as exchangeable apoproteins, may possess unknown properties that fine tune the lipoprotein profile in hypertriglyceridemic patients. I also tested whether this trait was shared by other accessory apoproteins, by expressing apoC-I and apoC-II in this system, and determining their ability to increase the secretion of TG and $VLDL_1$ apoB-100.

Transient Expression of Apolipoprotein C-III

Expression constructs of apoC were generated, by synthesizing PCR fragments from reverse transcribed mRNA produced from HepG2 cells. Fragments were inserted into the expression vector by ligating a 3'BglII restriction site within the vector to a 5' BamHI site inserted upstream of the coding sequence of the insert (Fig. 5A*i*). A convenient EcoRI site was maintained 5' of this insertion since both the BglII and BamHI sites were obliterated (Fig. 5A*ii*). The 3' end of the apoC insertion was constructed using primers that incorporated a HindIII site downstream of the stop codon. A similar strategy was employed for apoC-I, II and III and detailed primer sequences are listed in Table 2. An additional Flag epitope construct was generated to confirm the suitability of the antibodies used in this study. This strategy adopted a 3' Flag tagging strategy (Fig. 5B*i*). This construct allowed the transient expression of a protein that was used to confirm all three apoC-III antibodies employed in this study. The antiserum against human apoC-III, generously donated by Karmin O (University of Hong Kong) was compared with the monoclonal antiserum against the Flag epitope (M2 Sigma) (Fig. 5C). This confirmed that the cDNA insert encoded human apoC-III and that either antiserum was capable of detecting an immunoreactive band of correct molecular weight. I then used these reagents to confirm the immuno-reactivity of commercially available apoC antiserum from Academy Biolabs Corporation (ABC, Houston TX) (Fig. 5D). I concluded that the expression constructs were producing secreted immunoreactive apoC-III of the correct molecular weight and that the commercially available (ABC) anti-apoC-III antibody was most suitable for this study.

Fig. 5. Cloning strategy and western blotting of apolipoprotein C-III.

A*i*, diagram of cloning strategy for the expression plasmids of apoC-I, II, and III. PCR fragments were generated from reverse transcribed mRNA from HepG-2 cells. The primers incorporated a 5' BamHI site and a 3' HindIII site outside of the coding sequence. A*ii*, these were inserted into the pCMV5 eukaryotic expression vector BglII to HindIII which destroys the 5' restriction site. A convenient EcoRI site was maintained immediately upstream of the BglII / BamHI insertion. B*i*, flag tagged construct of apoC-III was also generated (Asp Tyr Lys Asp Asp Asp Asp Lys) to validate other apoC-III antibodies used in this study. B*ii*, the PCR fragment was generated from reverse transcribed HepG-2 mRNA as before, and a 5' EcoRI site was inserted upstream of the coding sequence, the 3' tail is shown as detailed. This strategy allows the addition of successive concatemers of flag epitopes by removing the coding sequence EcoRI to XbaI, and re-inserting the insert EcoRI to NheI. In this way, multiple in-frame flag epitopes can be added. Two epitopes were used in this construct. C, McA-RH7777 cells were transiently transfected with 20 μg of flag tagged CIII plasmid or mock transfected, cell lysates and medium were collected and Western blotted. The flag construct was detected only in transfected cell lysates and media by both antiserum received from Karmin O and the anti-flag (M2) antibody. D, cells were transiently transfected with constructs containing apoC-II, apoC-III, apoC-III Flag, or the pSV2neo control plasmid (neo). By Western blot anti-flag antibodies only detected flag tagged apoC-III while Western blots using antibodies from Academy Biomedical (ABC) detected either apoC-II or apoC-III and apoC-III flag respectively.

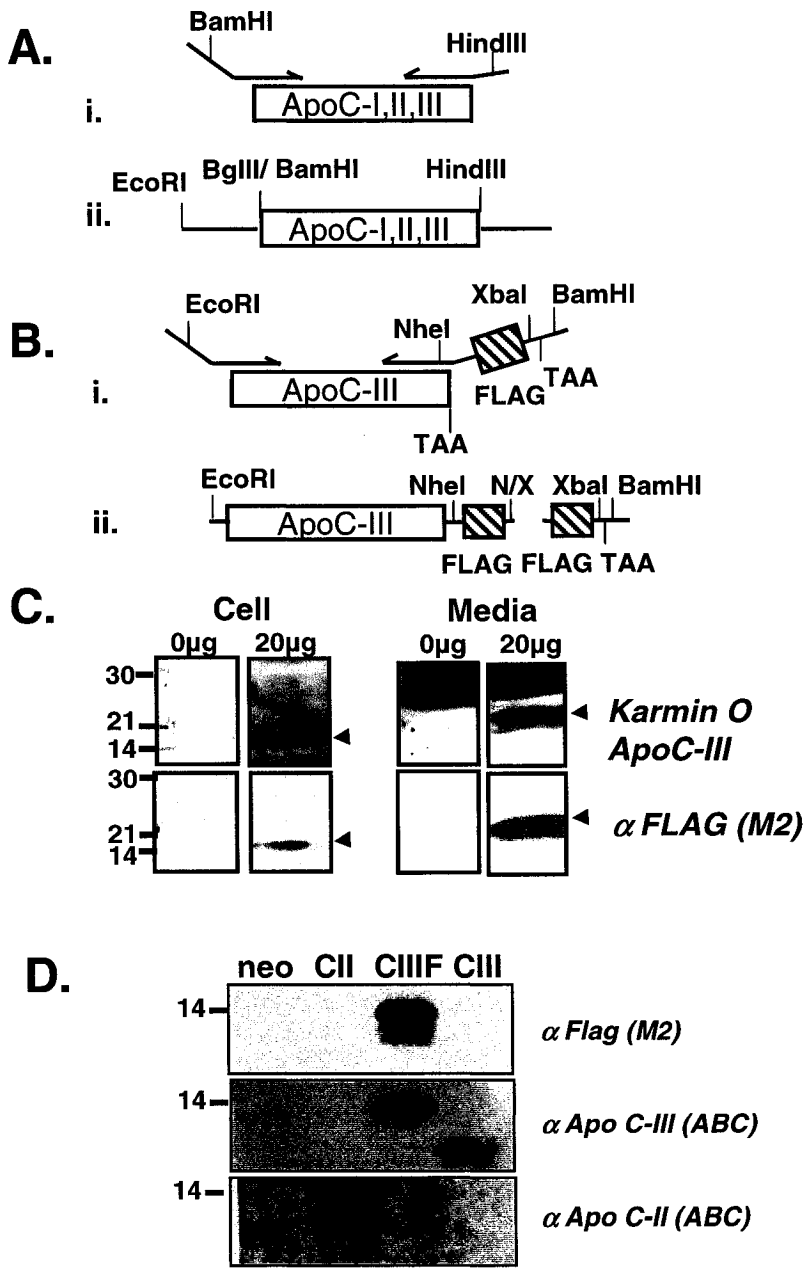
A.
BamHI
HindIII
i.
ApoC-I,II,III
EcoRI
BglII/ BamHI
HindIII
ii.
ApoC-I,II,III
B.
EcoRI
XbaI
BamHI
NheI
i.
ApoC-III
FLAG
TAA
TAA
EcoRI
NheI
N/X
XbaI
BamHI
ii.
ApoC-III
FLAG FLAG TAA
C.
Cell
Media
0µg
20µg
0µg
20µg
30
21
14
30
21
14
Karmin O
ApoC-III
α FLAG (M2)
D.
neo
CII
CIIIF
CIII
14
14
14
α Flag (M2)
α Apo C-III (ABC)
α Apo C-II (ABC)

The McA-RH7777 rat hepatoma cells did not secrete any endogenous C apolipoproteins (Fig. 6A). I transiently transfected McA-RH7777 cells, with increasing concentrations of human apoC-III plasmid. Samples were collected from conditioned medium 48 h post transfection and serum proteins were immediately concentrated using fumed silica (cab-o-sil). Proteins were eluted with Laemmli buffer at 95 °C and resolved by reducing SDS-PAGE. The immunoreactive apoC-III detected in the medium appeared in two distinct forms (8 and 10 kDa) likely corresponding to the different sialylation states of the protein, the majority is the high molecular weight form ($CIII_{S2}$). Transiently transfected cells were radiolabelled with [^{3}H]glycerol 48 h after transfection to determine the levels of ^{3}H-TG secretion. Cells were treated with or without 0.4 mM OA for 2 h in the presence of [^{3}H]glycerol to label newly synthesized glycerolipids. In the absence of OA, the cells secreted (Fig. 6C) very little ^{3}H-TG. Also in the absence of OA the incorporation of [^{3}H]glycerol into cellular ^{3}H-PC was two-fold greater than that into ^{3}H-TG (Fig. 6D). When the cells were supplemented with 0.4 mM OA, secretion of ^{3}H-TG from mock-transfected cells was increased by seven-fold (*p<.00006, Fig. 6C). When cells transfected with 15μg of apoC-III were compared to mock-transfected cells, there was a further 2 fold increase (**p <.0002) in ^{3}H-TG secretion (Fig. 6C) which was a change of 14-fold from baseline. Expression of apoC-III led to no further increase in ^{3}H-PC secretion (data not shown). There was also an increase in cellular ^{3}H-TG and ^{3}H-PC (Fig. 6D) where the magnitude of increase was greater in cellular ^{3}H-TG (7 fold, ***p<.001) than ^{3}H-PC (1.8 fold, ****p<.01). In response to 0.4 mM OA supplementation, McA-RH7777 cells increase ^{3}H-TG secretion and apoC-III expression further increases ^{3}H-TG secretion two fold (**p <.0002).

Fig. 6. Transient transfection of human apolipoprotein C-III.

A, secreted apolipoproteins collected from primary rat hepatocytes and McA-RH7777 rat hepatoma cells were resolved by SDS-PAGE. Note that the McA-RH7777 cells do not secrete high levels of apoB-48 nor the apoCs. B, McA-RH7777 cells were transiently transfected with increasing quantities of expression plasmid encoding human apoC-III. Medium samples were collected 48 h after transfection and concentrated with fumed silica, proteins were resolved by SDS-PAGE on a 15% Tris tricine gel, transferred to a nitrocellulose membrane and revealed by chemiluminescence with polyclonal anti-apoC-III antiserum (Academy Biomedical). C, 48 h after transfection cells were labeled with [^{3}H]glycerol (7 μCi/ml) and 20% FBS in the presence or absence of 0.4 mM OA for 2 h. Medium samples were collected and secreted lipids extracted as described in *Materials and Methods*. Individual lipid species were resolved by TLC and quantified by scintillation counting. Error bars represent the mean of three dishes ± S.D., findings are representative of three independent experiments (* $p<.00006$ – OA vs. + OA with 0 μg DNA, ** $p<.0002$ + OA with 0 μg vs. + OA with 15 μg DNA) D, cellular lipid samples were collected, extracted and separated as above. Cellular ^{3}H-TG or ^{3}H-PC are represented as cpm/mg cell protein. (***$p<.001$ – OA vs. + OA without C-III expression, ****$p<.01$- OA vs. + OA with CIII expression, 15μg).

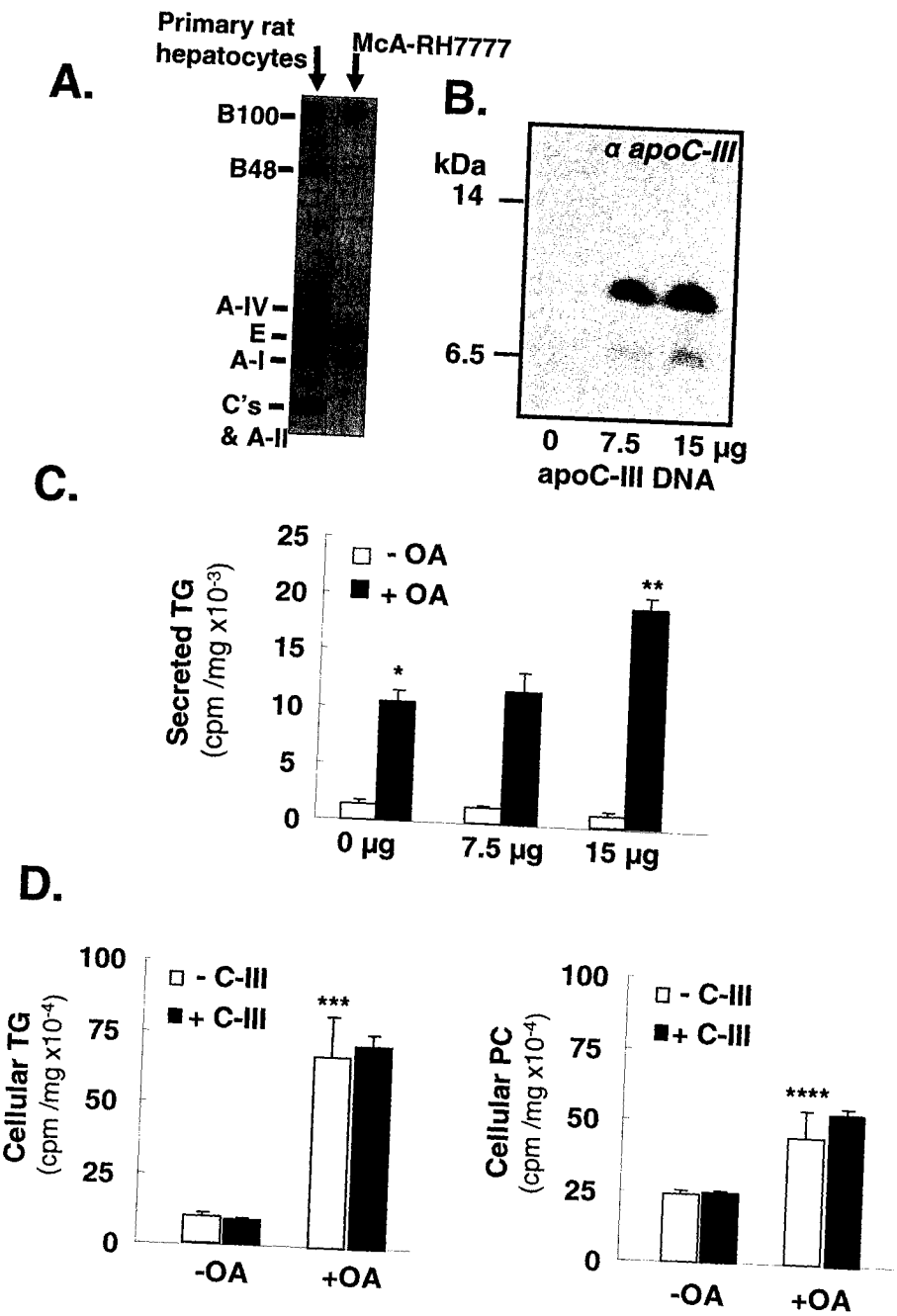
A.
Primary rat hepatocytes
McA-RH7777
B100
B48
A-IV
E
A-I
C's & A-II
B.
α apoC-III
kDa
14
6.5
0 7.5 15 µg
apoC-III DNA
C.
Secreted TG (cpm /mg x10-3)
- OA
+ OA
25
20
15
10
5
0
*
**
0 µg
7.5 µg
15 µg
D.
Cellular TG (cpm /mg x10-4)
- C-III
+ C-III
100
75
50
25
0
***
-OA
+OA
Cellular PC (cpm /mg x10-4)
- C-III
+ C-III
100
75
50
25
0
****
-OA
+OA

Generation of Stable Cell Lines Expressing Apolipoprotein C-III

Stable cell lines expressing human apoC-III were generated and medium samples from representative cell lines were collected and Western blotted (Fig. 7A inset). Densitometry revealed that relative secretion levels of apoC-III (14:8:2:0 A.U.), positively correlated with apoC-III mRNA as detected by Northern blot and quantified by densitometry (r^2 = 0.98) (Fig 7A inset). This finding suggests that apoC-III protein expression is proportional to the stable introduction of the transgene and results in a proportional secretion of immunoreactive peptide. Isoelectric focusing experiments showed apoC-III as three distinct isoforms. Of the secreted isoforms, ($CIII_{s0}$) was least abundant and ($CIII_{s2}$) the most prevalent, but ($CIII_{s1}$) was also detected, resembling the pattern found in human plasma (data not shown). The apoC-III in the medium exhibited three MW of 7, 10 and 12 kDa, representing the three sialation forms of the protein. The predominant form was the high molecular weight protein ($CIII_{s2}$) (Fig. 7B inset). Representative cell lines expressing increasing levels of apoC-III protein were metabolically labeled with [^{3}H]glycerol for 2 h in 20% FBS and 0.4 mM OA. ApoC-III cell lines showed a maximal 2-fold increase in ^{3}H-TG secretion (**p<.0008, Fig. 7B). This ^{3}H-TG secretion in response to apoC-III expression was dose dependent since intermediate cell lines showed ^{3}H-TG secretion midway between high expressing and control cells (****p<.02, Fig. 7B). To further confirm this two-fold increase in secreted ^{3}H-TG in response to 0.4 mM OA treatment I utilized stable cell lines expressing flag tagged apoC-III. When labeled with [^{3}H]glycerol in the presence of 0.4 mM OA flag tagged stable cells also showed a two-fold increase in ^{3}H-TG secretion without a concomitant rise in ^{3}H-PC secretion (Fig. 7C).

Fig. 7. Stable cell lines expressing apolipoprotein C-III.

A, RNA was isolated from stable cell lines with Triazol reagent, and resolved by agarose gel electrophoresis containing 6% formaldehyde. Samples were transferred to Hybond membrane and probed with a full length apoC-III cDNA fragment. Conditioned medium from apoC-III stable cell lines (inset) was resolved by SDS-PAGE, transferred to nitrocellulose, and apoC-III protein was detected by chemiluminescence with a polyclonal anti apoC-III antibody. Protein and RNA bands were semiquantified by densitometry and plotted as absorbance in arbitrary units (A.U.) B, conditioned medium from apoC-III stable cell lines was resolved by SDS-PAGE, transferred to nitrocellulose and Western blotted (inset). Cell lines were labeled with [^{3}H]glycerol (7 μCi/ml) in the presence of 0.4 mM OA and 20% FBS for 2 h. Medium samples were collected and secreted lipids were extracted as described in *Materials and Methods*. Individual lipid species were resolved by TLC and quantified by scintillation counting. Error bars represent the mean of three separate dishes ± S.D. and a representative experiment is illustrated (** p<.0008 apoC-III (hi) vs. control, **** p<.02 apoC-III (med) vs. control). C, flag tagged apoC-III cell lines were labeled with [^{3}H]glycerol (7 μCi/ml) in the presence of 0.4 mM OA and 20% FBS for 2 h. Medium and cellular samples were processed as described in *Materials and Methods*. Error bars represent the mean of three separate dishes ± S.D. and a representative experiment is illustrated (*.p<.0003). Inset, Western blot of conditioned medium from apoC-III flag tagged cells, medium was concentrated, resolved on SDS PAGE gels, transferred to nitrocellulose then Western blotted with anti-apoC-III (ABC) or anti-flag antisera.

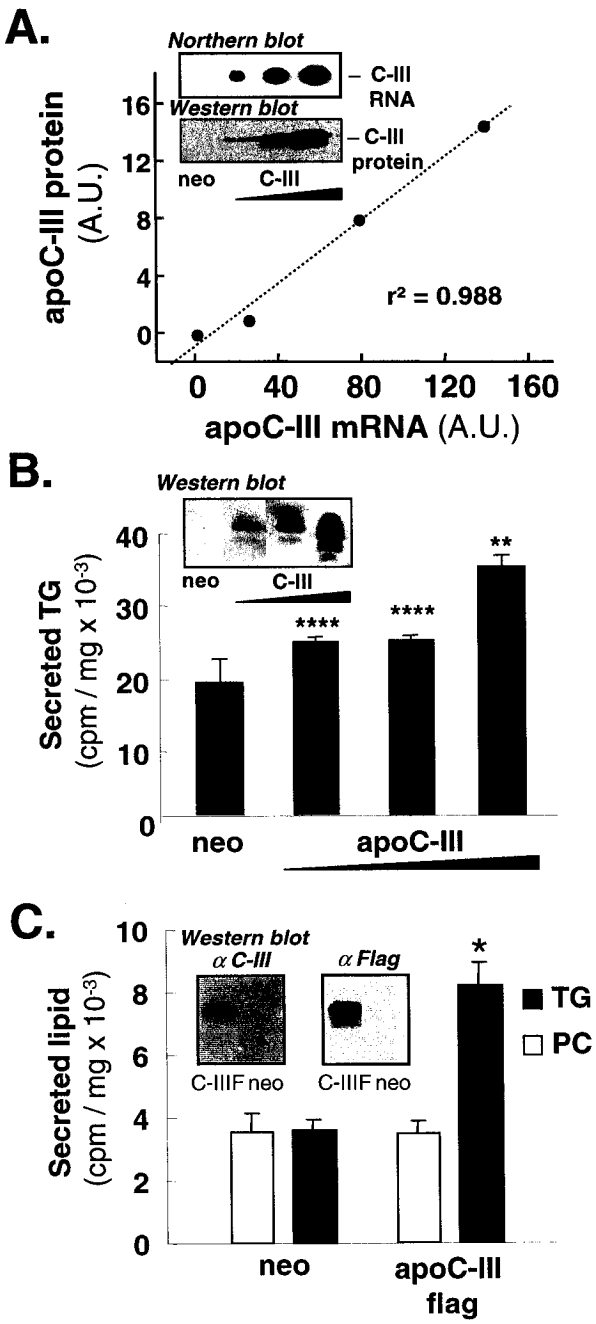
A.
Northern blot
C-III RNA
Western blot
C-III protein
neo
C-III
apoC-III protein (A.U.)
16
12
8
4
0
r² = 0.988
0
40
80
120
160
apoC-III mRNA (A.U.)
B.
Western blot
neo
C-III
Secreted TG (cpm / mg x 10⁻³)
40
30
20
10
0
****
****
**
neo
apoC-III
C.
Western blot
α C-III
α Flag
C-IIIF neo
C-IIIF neo
Secreted lipid (cpm / mg x 10⁻³)
10
8
6
4
2
0
*
TG
PC
neo
apoC-III flag

Fig. 8. Secretion kinetics of [^{3}H]glycerol labeled ^{3}H-TG and ^{3}H-PC.

A, stable cell lines expressing high, intermediate or no apoC-III were labeled for 2 h with [^{3}H]glycerol in the presence of 20% FBS and the presence or absence of 0.4 mM OA. At intervals of one or two hours the medium and cellular samples were collected and lipids were extracted as described in *Materials and Methods.* Lipids were extracted and resolved by two phase TLC, cellular ^{3}H-TG was then scraped and counted in a Wallac scintillation counter. Cellular ^{3}H-TG values were then normalized to total cellular protein. B, medium samples from A were collected and processed as above. C, cellular labeling and lipid extraction was performed as in A, and ^{3}H-PC was isolated by two phase TLC, scraped and counted. Values represent cellular ^{3}H-PC normalized to the cellular protein. D, medium samples from C were collected and processed as above. Secreted ^{3}H-PC was isolated by two phase TLC, scraped and counted, values represent cellular ^{3}H-PC normalized to the cellular protein.

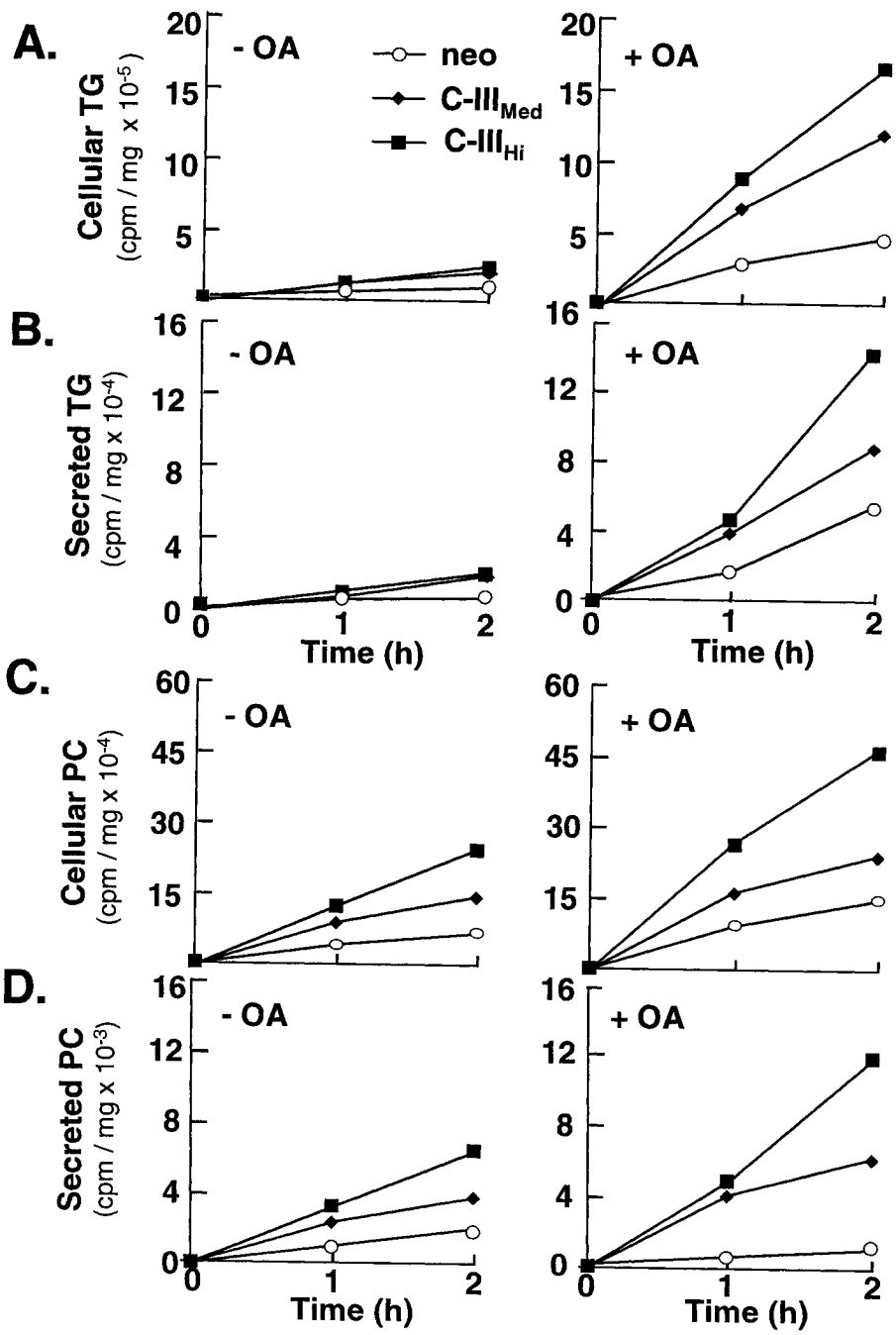
A.
B.
C.
D.
- OA
+ OA
neo
C-III$_{Med}$
C-III$_{Hi}$
Cellular TG
(cpm / mg x 10^{-5})
Secreted TG
(cpm / mg x 10^{-4})
Cellular PC
(cpm / mg x 10^{-4})
Secreted PC
(cpm / mg x 10^{-3})
Time (h)

Kinetic Analysis of [^{3}H]Glycerol Labeled Lipids

Cell lines expressing high or intermediate levels of apoC-III were labeled for periods up to 2 h in the presence or absence of 0.4 mM OA. This was done to determine the kinetics of synthesis and secretion of ^{3}H-TG and ^{3}H-PC. In the absence of OA supplementation all cell lines showed very low levels of cellular ^{3}H-TG and secretion (Fig 8A,B). This is in contrast to ^{3}H-PC which showed a basal incorporation of label into cellular PC and a concomitant secretion (Fig. 8C,D). When cells were labeled in the presence of OA the incorporation of cellular ^{3}H-TG increased proportionally to apoC-III expression level (Fig. 8A) and this was accompanied by a proportional increase in secretion of ^{3}H-TG (Fig. 8B). When the cellular ^{3}H-PC was monitored in the presence of oleate the magnitude of increase was not as great as ^{3}H-TG (Fig. 8C vs A), also the secretion of ^{3}H-PC was not increased significantly with OA supplementation (Fig. 8D vs B). This finding suggests that cellular ^{3}H-TG is more sensitive to OA supplementation than ^{3}H-PC, and this was reflected in the secretion of these lipids.

^{3}H-TG Secretion with Apolipoprotein C-III Expression

To ensure that the kinetic data on increased ^{3}H-TG secretion in response to OA was representative, stable cell lines were labeled with [^{3}H]glycerol for 2 h in the presence and absence of 0.4 mM OA so that I could determine the statistical differences contributed by OA supplementation and apoC-III expression. To determine whether OA was an obligatory factor for this effect of apoC-III expression on TG secretion, I monitored the secretion of TG in the presence or absence of 0.4 mM OA and 20% FBS. I found again a two fold increase in TG secretion mediated by apoC-III expression that

Fig. 9. Clonal and mixed culture secretion of ^{3}H-TG.

A, clonal cells stably expressing high levels of apoC-III and control cells were labeled for 2 h with [^{3}H]glycerol in 20% FBS in the presence or absence of 0.4 mM OA. After 2 h medium samples were collected and lipids extracted as described in *Materials and Methods*. Medium samples exhibited low secretion of ^{3}H-TG in the absence of OA but with OA supplementation, apoC-III expressing cells secreted 2-fold more ^{3}H-TG than control cells (*p <.0002). B, cellular lipid samples were extracted and quantified from A. Cellular ^{3}H-TG shows no difference without OA, but with OA there is a significant increase in ^{3}H-TG (**p<.006). Error bars represent the mean of three separate dishes ± S.D. a representative experiment is illustrated. C, two different mixed cultures of stably transfected or control cells were labeled for 2 h with [^{3}H]glycerol in 20% FBS in the presence or absence of 0.4 mM OA. After 2 h medium lipids were extracted, isolated and counted. Mixed cultures of apoC-III cells again demonstrated a 2-fold increase in ^{3}H-TG secretion. D, cellular ^{3}H-TG was collected from C, extracted, isolated and quantified. Cellular ^{3}H-TG showed no difference without OA, but with OA supplementation cellular ^{3}H-TG levels rise. E, secreted ^{3}H-PC showed no change with OA treatment. F, cellular ^{3}H-PC shows no difference without OA supplementation. In the presence of OA supplementation cellular ^{3}H-PC levels rise, in both apoC-III and control cells.

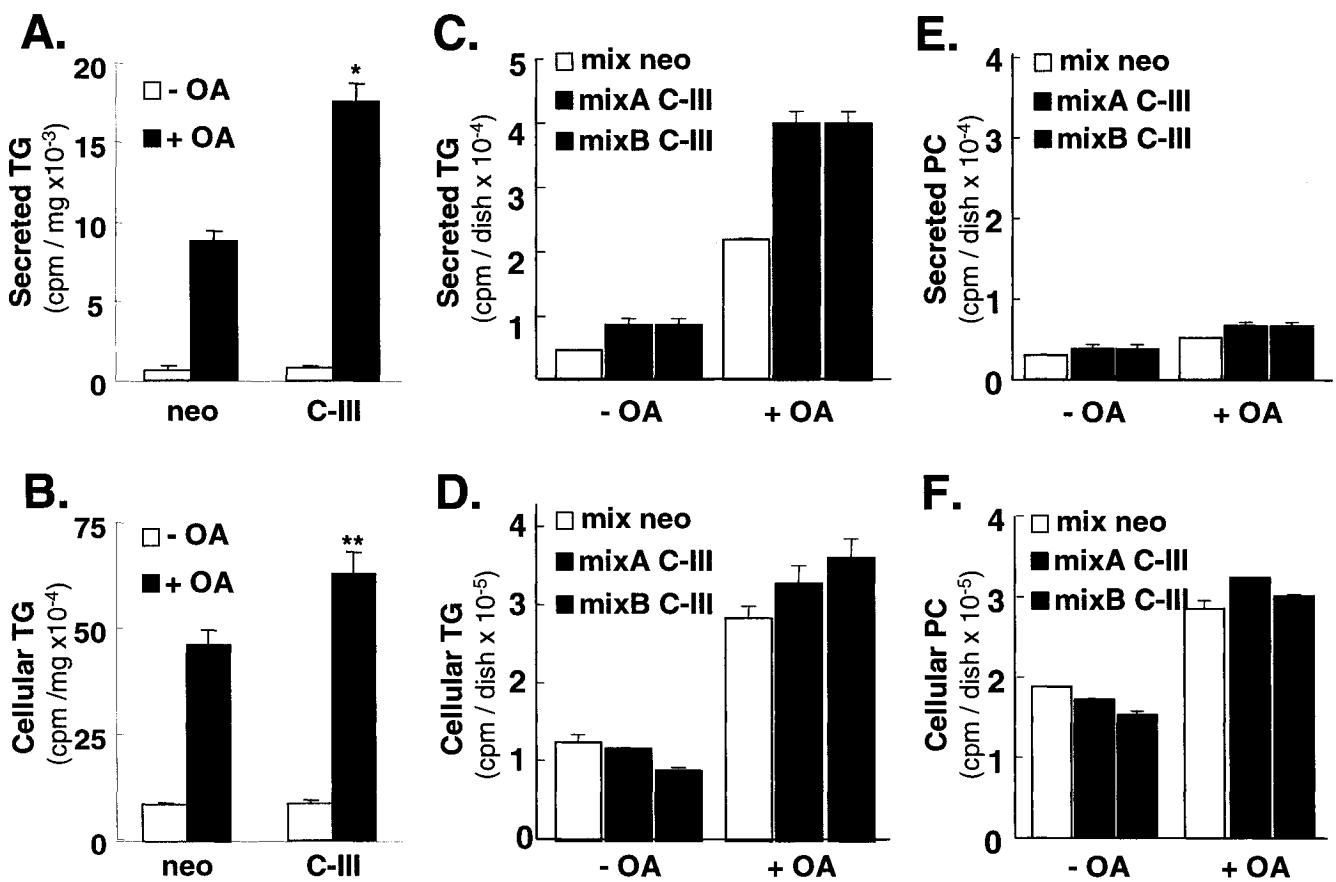
A.
Secreted TG
(cpm / mg x10-3)
20
15
10
5
0
- OA
+ OA
*
neo
C-III
B.
Cellular TG
(cpm /mg x10-4)
75
50
25
0
- OA
+ OA
**
neo
C-III
C.
Secreted TG
(cpm / dish x 10-4)
5
4
3
2
1
mix neo
mixA C-III
mixB C-III
- OA
+ OA
D.
Cellular TG
(cpm / dish x 10-5)
4
3
2
1
0
mix neo
mixA C-III
mixB C-III
- OA
+ OA
E.
Secreted PC
(cpm / dish x 10-4)
4
3
2
1
0
mix neo
mixA C-III
mixB C-III
- OA
+ OA
F.
Cellular PC
(cpm / dish x 10-5)
4
3
2
1
0
mix neo
mixA C-III
mixB C-III
- OA
+ OA

required OA supplementation (*p<.0002 Fig. 9A). While in control cells (not transfected with apoC-III) there was also an increased secretion of ^{3}H-TG in response to OA, the magnitude of the apoC-III effect was similar to the levels detected in transient transfection studies (Fig. 6C). The cellular levels of ^{3}H-TG are both markedly increased by OA treatment in apoC-III expressing and control cells. ApoC-III expressing cells showed a significant increase in cellular ^{3}H-TG only in response to OA supplementation (**p<.006 Fig. 9B). To ensure that the stable cell line experiments were valid, mixed cultures of apoC-III transfected cells were also used. This represents a population of cells which possess varied plasmid uptake and expression. For this experiment two independent apoC-III expressing mixed cultures were included. The magnitude of cellular ^{3}H-TG in response to 0.4 mM OA was very similar to stably transfected cells (Fig. 9D). Also in the mixed cultured cells there was an increase in ^{3}H-TG in control cells in response to OA (Fig. 9C). The additional ^{3}H-TG secretion in apoC-III expressing cells in response to 0.4 mM OA was again 2-fold greater than control cells (Fig. 9C). The secretion of ^{3}H-PC from mixed cultures of cells was again not dramatic (Fig. 9E), despite an increase in intracellular ^{3}H-PC in response to OA supplementation (Fig. 9F).

[^{14}C]Oleate Pulse Chase Labeling

To ensure that the increase in TG secretion mediated by apoC-III expression was *bona fide*, I employed a pulse chase methodology using [^{14}C]oleate as a tracer. This approach attempted to determine whether the incorporation of [^{14}C]oleate into TG and PC is equivalent in apoC-III expressing and control cells (Fig. 10 A vs. C). Stable cell lines expressing high levels of apoC-III and control cells were labeled for 2 h in the presence of 20% FBS and 0.4 mM OA. After the labeling period, the medium was replaced with

Fig. 10. Apolipoprotein C-III cells demonstrated increased ^{14}C-TG secretion.

A, stable cell lines expressing apoC-III (filled squares) or control cells (open circles) were labeled with [^{14}C]oleate (3 μCi/ml) in the presence of 0.4 mM OA and 20% FBS for 2 h. The labeling medium was then removed and replaced with medium containing 0.4 mM OA and 20% FBS. At time points up to 4 h, cellular samples were collected in 1:1 methanol:water and lipids were extracted as described in *Materials and Methods.* Cellular TG was resolved by TLC and quantified by scintillation counting. Values of cellular TG are expressed as cpm/mg cell protein. B, medium samples from A were collected at time intervals up to 4 h and secreted TG was extracted and quantified. C, cellular PC from A was collected in 1:1 methanol:water and was extracted as described in *Materials and Methods,* cellular PC was resolved by TLC and quantified by scintillation counting. D, secreted PC from B was collected from medium samples extracted and quantified as above.

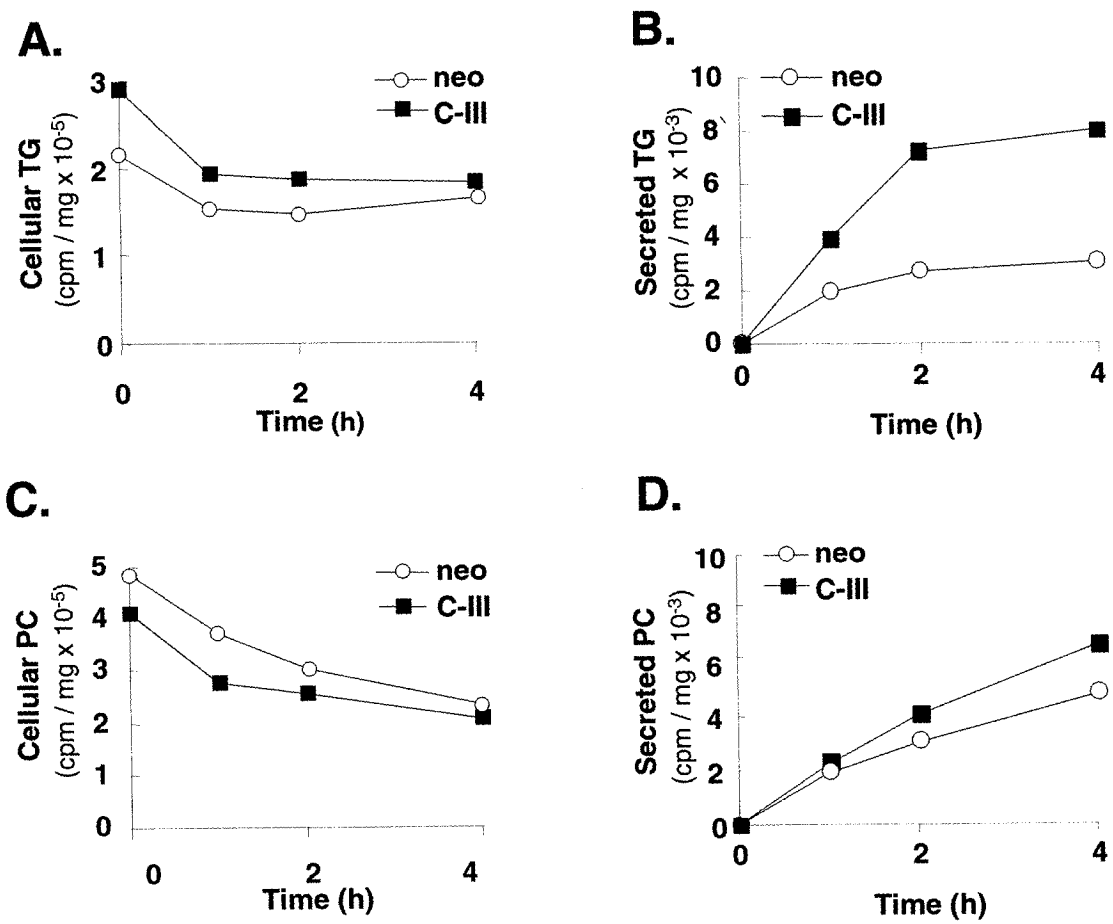
A.
Cellular TG
(cpm / mg x 10-5)
neo
C-III
3
2
1
0
0
2
4
Time (h)
B.
Secreted TG
(cpm / mg x 10-3)
neo
C-III
10
8
6
4
2
0
0
2
4
Time (h)
C.
Cellular PC
(cpm / mg x 10-5)
neo
C-III
5
4
3
2
1
0
0
2
4
Time (h)
D.
Secreted PC
(cpm / mg x 10-3)
neo
C-III
10
8
6
4
2
0
0
2
4
Time (h)

DMEM containing 20% FBS and 0.4 mM OA. Cellular and medium samples were collected at time points up to 4 h and lipid samples were extracted and separated by TLC. The apoC-III expressing cells demonstrated a small increase in cellular ^{14}C-TG after the 2 h pulse labeling period (Fig. 10A). When the cells were chased in the absence of [^{14}C]OA, cellular levels of ^{14}C-TG fell by 30% reaching the basal levels present in control cells (Fig. 10A). This decrease in ^{14}C-TG seen in the apoC-III transfected cells was accompanied by an increase in secreted ^{14}C-TG that reached maximal levels within two hours (Fig. 10B). The magnitude of the increased ^{14}C-TG secretion was again approximately 2 to 4 fold as seen with [^{3}H]glycerol labeling. It also appears the apoC-III expressing cells incorporated slightly less tracer into PC that the control cells (Fig. 10C). This small difference did not lead to any significant difference in ^{14}C-PC secretion between control and apoC-III transfected cells (Fig. 10D), but is similar to the difference seen in intracellular ^{3}H-TG using [^{3}H]glycerol labeling (Fig. 9B).

[^{35}S]Methionine/Cysteine Labeling

To determine whether apoC-III led to an increase in apoB-100 secretion I employed a metabolic labeling approach using [^{35}S]methionie/cysteine to label newly synthesized apoB-100. This continuous labeling approach would determine if apoB-100 translation was increased and would also show whether apoB-100 secretion into the media was enhanced by apoC-III expression. Stable cell lines were labeled in the presence of 0.4 mM OA and 20% FBS and at time points up to 2 h samples were collected both from the media and cell lysates and samples were subjected to immunoprecipitation for apoB. Samples were resolved by SDS-PAGE and autoradiography was performed. ApoB-100 protein was then excised from the gel and

quantified by scintillation counting. I detected no difference in the rate of apoB-100 translation when control and apoC-III cell lines were compared (Fig. 11A). I also found that in the media the amounts and rates at which apoB-100 were secreted were unchanged by apoC-III expression (Fig. 11B). These findings suggest that the increased secretion of TG in apoC-III expressing hepatoma cells was not associated with an overproduction of apoB-100 protein. This suggests that the cells are displaying a hyper-TG normo-B phenotype. There was also no significant difference in the lower level of synthesis or secretion of endogenous apoB-48.

Microsomal Fractionation of Apolipoprotein C-III Expressing Cells

Some authors have proposed that the assembly of VLDL particles occurs while apoB is associated with the inner leaflet of the ER or Golgi membranes [106]. To evaluate whether apoC-III exerts an effect on the association of the primordial particle with the microsomal membrane I evaluated the distribution of apoB between the microsomal membrane and lumen. After labeling the cells for 2 h with [^{35}S]methionine/cysteine, cells were lysed by ball bearing homogenization in sucrose buffer. Post nuclear supernatants were separated by low speed centrifugation and microsomal membranes were isolated using ultracentrifugation. The microsomal pellets were re-suspended, and the luminal contents of the microsomal membranes were released by sodium carbonate treatment (pH 11.3). Under these conditions apoC-III will not remain membrane associated, while apoB has been shown to be distributed between the membrane and the luminal fractions [81]. Proteins were isolated from the luminal or membrane fraction of

Fig. 11. Continuous labeling with [^{35}S]methionine/cysteine.

A, stably transfected cells expressing apoC-III (filled squares) or control cells (open circles) were continuously labeled with [^{35}S]methionine/cysteine (200 μCi/ml) for 2 h in the presence of 20% FBS and 0.4 mM oleate. ApoB was recovered from the cell lysates by immunoprecipitation with a polyclonal antibody against rat apoB. The precipitated proteins were resolved by electrophoresis on 5% Tris glycine SDS-PAGE gels and were visualized by fluorography (right). Radioactivity associated with apoB100 was excised from the gel quantified by scintillation counting and expressed as a ratio of cpm/mg cell protein (left). B, medium samples were immunoprecipitated with anti-rat apoB and processed as above, fluorograms (right) were quantified by excising apoB bands and scintillation counting values are reported as a ratio of cpm/mg cell protein (left).

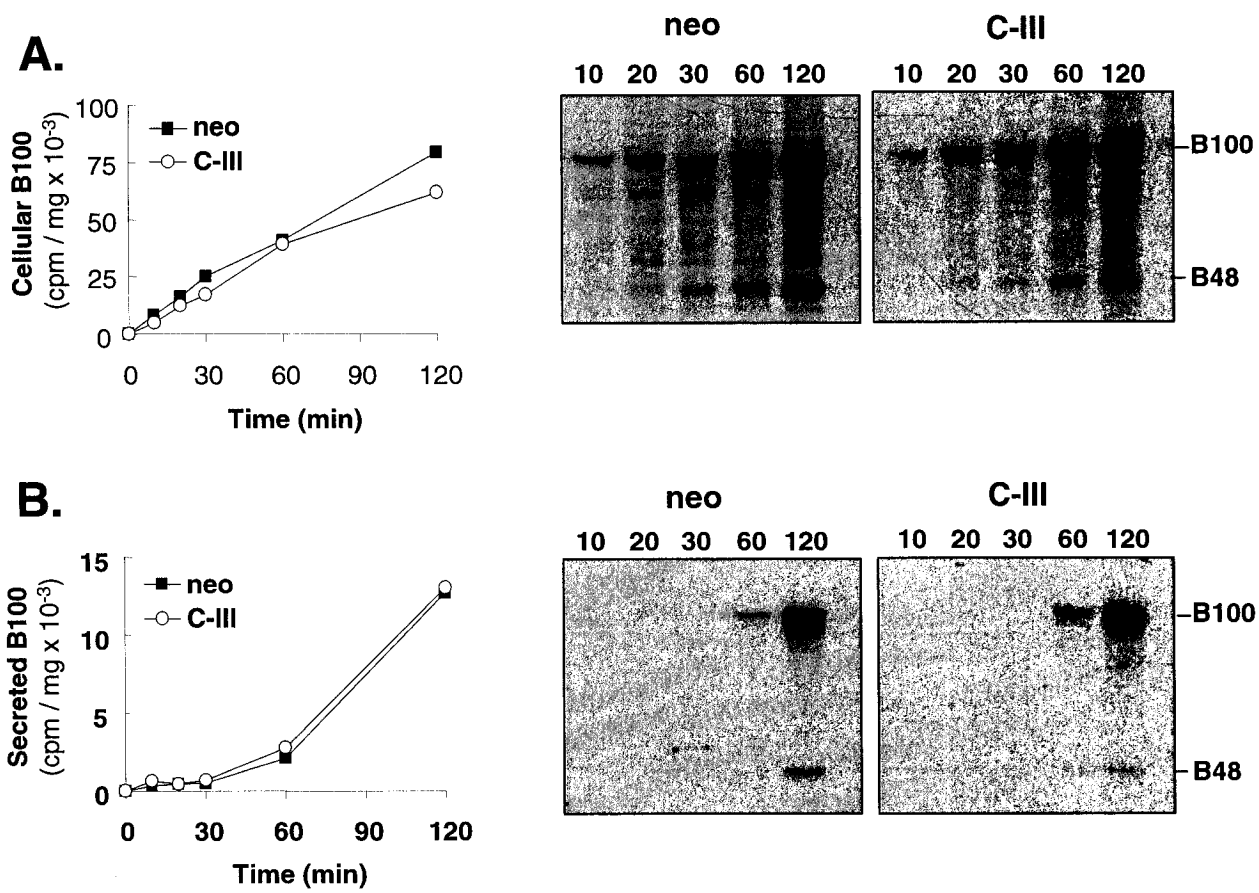
A.
Cellular B100
(cpm / mg x 10-3)
100
75
50
25
0
neo
C-III
0
30
60
90
120
Time (min)
neo
C-III
10 20 30 60 120
10 20 30 60 120
B100
B48
B.
Secreted B100
(cpm / mg x 10-3)
15
10
5
0
neo
C-III
0
30
60
90
120
Time (min)
neo
C-III
10 20 30 60 120
10 20 30 60 120
B100
B48

these preparations and immunoprecipitated. Autoradiography revealed that there was no difference in distribution of apoB-100 between the membrane and luminal fractions of cells transfected with apoC-III as compared with control cells (Fig. 12A). Since the pH is too stringent to allow apoC-III to remain associated with the membrane, apoC-III serves as a positive control to ensure complete permeabilization of the microsomal preparation. If there had been any microsomal vesicles that remained intact under these conditions apoC-III would be detected in the membrane fraction (Fig. 12A, lane M).

I then endeavored to evaluate this method for monitoring changes in the distribution of lipids within the microsomal fractions. Since the microsomal membrane fraction represents the ER and Golgi membranes, this methodology may detect changes in the lipid composition of the secretory pathway. To test this I labeled cells for 2 h in the presence of [^{14}C]oleate, 20% FBS and 0.4 mM OA. Cells were fractionated as above and lipid samples were collected for every fraction. To accurately report the proportions of radio-labeled lipids present in each cellular fraction, values were expressed as a percentage of total lipid labeled (ie. $TG_{lumen}/(\Sigma\ TG_{microsome} + TG_{cytosol} + TG_{membranes} + TG_{lumen})$). I observed that the microsomal membranes only consist of a minor portion (1 to 2%) of the total cellular TG (Fig. 12B). When the labeled lipids in the microsomal fraction of apoC-III expressing cells were compared to control cells, there was a small difference detected in the distribution of ^{14}C-TG and ^{14}C-CE (Fig. 12C). Findings are represented as a Forest plot, where the X axis represents the difference in the ratio of radiolabelled lipid in the $(M/L)_{CIII} / (M/L)_{neo}$. A value of one indicates that there is no change between the microsomal membrane (M) and lumen (L) of these two cell lines.

Fig. 12. Microsomal distribution of apolipoprotein B and ^{14}C-labeled lipids.

A, apoC-III and control cells were labeled with [^{35}S]methionine/ cysteine (200 μCi/ml) for up to 2 h in the presence of 20% FBS and 0.4 mM OA. Cells were homogenized with a ball bearing homogenizer and microsomal fractions were isolated by ultracentrifugation. The lumenal contents were released by sodium carbonate treatment at pH 11.3, and were separated by ultracentrifugation (100,000 rpm 15 °C 16 min. TLA 100.4 rotor). Proteins were immunoprecipitated and resolved by SDS-PAGE and revealed by fluorography. B, apoC-III and control cells were labeled with [^{14}C]oleate (3 μCi/ml) in the presence of 0.4 mM OA and 20% FBS for 2 h. Cells were homogenized and microsomal membranes and luminal fractions were isolated as in A. membrane (M) and lumen (L) lipids were extracted, separated by TLC, and quantified by scintillation counting. Data are represented as a % of total lipid in all cellular fractions isolated. C, a Forest plot of findings from B, where the X axis represents the ratio of $(M/L)_{CIII}$ / $(M/L)_{neo}$. A value of 1 indicates no change in the distribution between membrane and lumen of lipid when the two cell lines are compared.

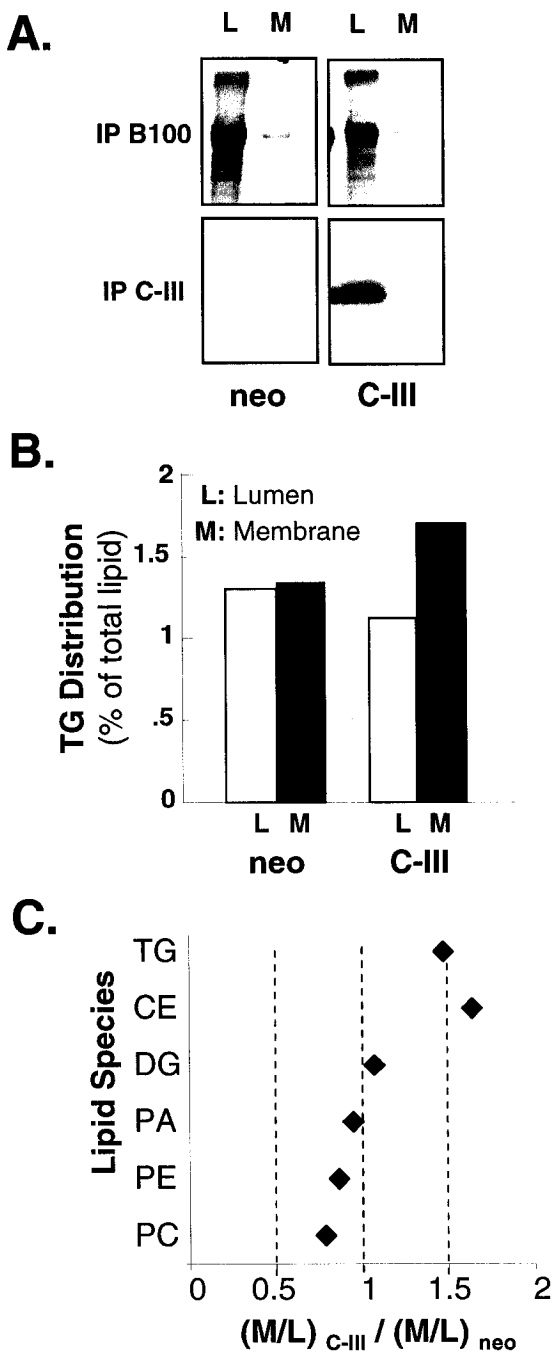
A.
L M L M
IP B100
IP C-III
neo C-III
B.
L: Lumen
M: Membrane
TG Distribution
(% of total lipid)
2
1.5
1
.5
0
L M L M
neo C-III
C.
Lipid Species
TG
CE
DG
PA
PE
PC
0 0.5 1 1.5 2
(M/L) C-III / (M/L) neo

A value grater than 1 represents a redistribution of lipid into the membrane in the C-III cells, while a value less than 1 represents a redistribution of lipid into the membrane of the control cells. The ^{14}C-phospholipids did not show any meaningful change in distribution while ^{14}C-TG and ^{14}C-CE were redistributed in the microsomal membrane in apoC-III expressing cells (Fig. 12C). This suggests that within the isolated microsomal membrane fraction the [^{14}C]oleate labeled neutral lipids are increased while the distribution of apoB protein and ^{14}C-PL remained unchanged.

Since MTP is an obligatory co-factor for LpB assembly and secretion I also explored a potential effect of apoC-III expression on the MTP activity. It has previously been shown by our laboratory that the activity of MTP is required for the accumulation of TG within the microsomal fraction of McA-RH7777 cells, which is requisite for TG rich VLDL assembly. Thus I investigated whether MTP activity was affected by apoC-III expression. Donor and acceptor lipid vesicles were prepared as described in [101] and cellular extracts were prepared by sonication as described previously by our laboratory [83]. I detected no difference in MTP activity in lysates from apoC-III expressing cells (data not shown).

Density Distribution of Secreted Lipoproteins

To determine the assembly and secretion of lipoproteins in response to apoC-III over expression, I employed metabolic labeling and rate floatation ultracentrifugation. This methodology allows the discrimination between large VLDL particles separating the S_f >100 ($VLDL_1$) from S_f 20-100 ($VLDL_2$) particles. Stable cell lines were metabolically labeled with [^{35}S]methionine/cysteine in the presence of 20% FBS and 0.4 mM OA. Medium from these cells were collected after 2 h and fractionated by rate floatation

Fig. 13. Rate floatation ultracentrifugation of apolipoprotein B-100 and ^{3}H-TG.

A, control cells were labeled with [^{35}S]methionine/cysteine (200 μCi/ml) for 2 h in the presence of 20% FBS and 0.4 mM OA. The medium was collected at the end of the labeling period and was fractionated by rate floatation ultracentrifugation. ApoB was isolated from each fraction by immunoprecipitation, resolved by SDS-PAGE and revealed by fluorography. B, apoC-III transfected stable cell lines were labeled as in A, the medium was collected and fractionated by rate floatation ultracentrifugation. ApoB was isolated from each fraction by immunoprecipitation, resolved by SDS-PAGE and revealed by fluorography. C, apoB-100 was excised from the gels in A (open bars, control) and B (filled bars, apoC-III) and was quantified by scintillation counting. Data are represented as the % of maximal apoB (lane 2) divided by the apoB-100 present in each lane. Representative data from triplicate independent experiments is shown D, stable cell lines expressing apoC-III (black) or control cells (white) were labeled with [^{3}H]glycerol (7 μCi/ml) in the presence of 0.4 mM OA and 20% FBS for 2 h. The labeling media was then removed and was fractionated by rate floatation ultracentrifugation. Lipids were extracted from each fraction as described in *Materials and Methods.* Secreted TG was resolved by TLC and quantified by scintillation counting. Data are represented as the secreted TG content of each fraction expressed as cpm/mg cell protein. Data is representative of triplicate experiments.

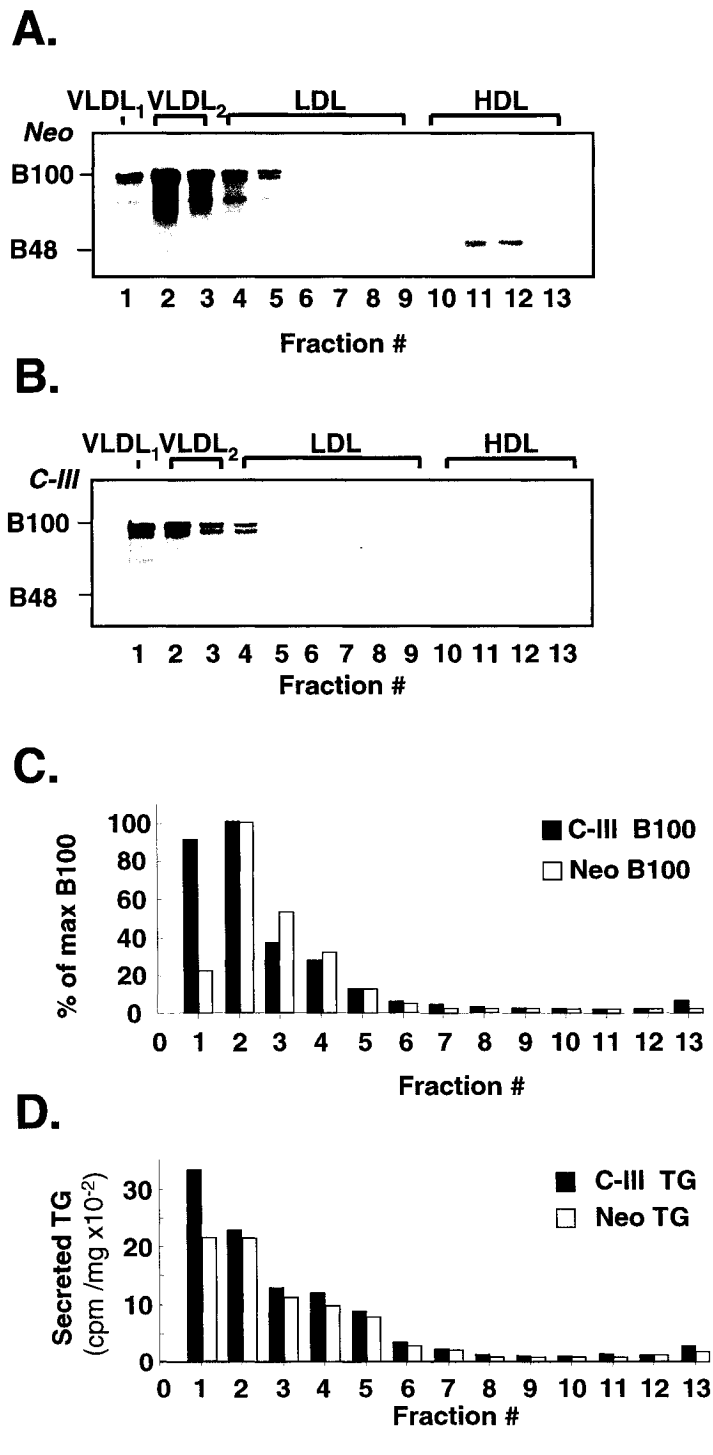
A.
VLDL1
VLDL2
LDL
HDL
Neo
B100
B48
1 2 3 4 5 6 7 8 9 10 11 12 13
Fraction #
B.
VLDL1
VLDL2
LDL
HDL
C-III
B100
B48
1 2 3 4 5 6 7 8 9 10 11 12 13
Fraction #
C.
% of max B100
100
80
60
40
20
0
C-III B100
Neo B100
0 1 2 3 4 5 6 7 8 9 10 11 12 13
Fraction #
D.
Secreted TG
(cpm /mg x10-2)
30
20
10
0
C-III TG
Neo TG
0 1 2 3 4 5 6 7 8 9 10 11 12 13
Fraction #

ultracentrifugation. I detected a difference in the apoB-100 distribution in response to apoC-III expression in the presence of OA (Fig. 13A vs. B). ApoB-100 in the $VLDL_1$ fraction is increased in response to apoC-III, however there is no difference in total secreted apoB (Fig. 11). This result indicates that apoC-III leads to an overproduction of TG rich $VLDL_1$ without increasing apoB secretion. The distribution of secreted apoB is represented in Figure 13C. This representation shows that the increased $VLDL_1$ detected in the media is produced at the expense of smaller particles. This may represent an enhancement of second step assembly by apoC-III where apoB-containing particles are promoted into the $VLDL_1$ density. When fractionation studies were performed in the absence of OA there was insignificant apoB-100 secretion in the buoyant densities and there was no difference between transfected and non-transfected cells in secreted apoB-100 (data not shown).

To determine if second step assembly was increased in the apoC-III expressing cells (in response to OA) the density distribution of lipid components of secreted lipoproteins were evaluated. Since a shift in the buoyant density of apoB-100 (Fig 13B) but no increase in apoB synthesis (Fig. 11A) was detected, ^{3}H-TG $VLDL_1$ was evaluated. This would determine whether larger but not more numerous LpB's were secreted. Stable cells expressing apoC-III were labeled with [^{3}H]glycerol in the presence of 0.4 mM OA and 20% FBS (Fig. 13D). Media from these cells were collected after 2 h and fractionated by rate floatation ultracentrifugation. Lipids were extracted from each fraction, dried under N_2 and resolved by two phase TLC before being scraped and quantified. Cells expressing apoC-III showed that in response to 0.4 mM oleate treatment there was a specific increase in $VLDL_1$ ^{3}H-TG (Fig. 13D). When the secreted ^{3}H-PC was

examined, there was no difference in the amount of ^{3}H-PC found in $VLDL_1$, there was however a significant increase in ^{3}H-PC found in the HDL density range in response to apoC-III expression (data not shown).

Apolipoprotein C-I and Apolipoprotein C-II Cell Lines

To investigate whether the effect of apoC-III expression on TG secretion was shared by other C apolipoproteins, I generated stable cell lines expressing apoC-I or C-II. These three proteins share a high level of structural homology with apoC-III. Conditioned medium was collected from stable cell lines, and apolipoproteins were analyzed by Western blot (Fig. 14A, inset). ApoC-I and apoC-II were detected using polyclonal antibodies (ABC) and there was no cross reactivity with respective antibodies. Stable McA-RH7777 cell lines expressing apoC-I or apoC-II were labeled with [^{3}H]glycerol for 2 h in the presence or absence of 0.4 mM OA and 20% FBS, medium and cellular samples were collected and lipids were extracted. Even without OA supplementation cell lines expressing apoC-I showed a significant increase in the secretion of ^{3}H-TG as compared to controls (**p <.0001, Fig. 14A). When cells were supplemented with 0.4 mM OA both the apoC-I and apoC-II cell lines secreted significantly more ^{3}H-TG than controls. In the case of the apoC-I transfected cells, there was a four fold increase in ^{3}H-TG secretion (*p<.00002, Fig. 14A). In the apoC-II cell line there was a two-fold increase (***p<.0004, Fig. 14A). When the intracellular levels of ^{3}H-TG were examined, only the apoC-I expressing cells demonstrated a significantly greater incorporation of [^{3}H]glycerol into cellular TG (****p<.003, Fig. 14B). Cells were labeled with [^{35}S]methionine/cysteine in the presence of 0.4 mM OA and 20% FBS to determine LpB particle size by rate floatation ultracentrifugation.

Fig. 14. ^{3}H-TG and ^{35}S-apoB secretion in apoC-I and apoC-II transfected cells.

A, stable cell lines expressing apoC-I, apoC-II and control cells were labeled with [^{3}H]glycerol (7 μCi/ml) in medium containing 20% FBS for 2 h in the presence (filled bars) or absence (open bars) of 0.4 mM OA. Medium samples were collected after 2 h and secreted lipids were extracted as described in *Materials and Methods,* secreted TG was resolved by TLC and quantified by scintillation counting (*p<.00002 +OA C-I vs. + OA control, ** p<.0002 –OA C-I vs. –OA control, ***p<.0004 +OA C-II vs. +OA control). Conditioned medium was collected from control, apoC-I and apoC-II cell lines, secreted proteins were subjected to SDS-PAGE then transferred to nitrocellulose and were revealed by chemiluminescence using either anti apoC-I or anti apoC-II antibodies (inset). B, cellular samples from A were collected in 1:1 methanol:water and lipids were extracted as described in *Materials and Methods.* Cellular ^{3}H-TG was resolved by TLC and quantified by scintillation counting (****p<.003 +OA C-I vs. +OA control). Data is representative of triplicate independent experiments and representative cell lines are shown C, stable cell lines expressing apoC-I or apoC-II were labeled with [^{35}S]methionine/cysteine (200 μCi/ml) for 2 h in the presence of 20% FBS and 0.4 mM OA. The medium was collected at the end of the labeling period and fractionated by rate floatation ultracentrifugation. ApoB was isolated from each fraction by immunoprecipitation, resolved by SDS-PAGE and revealed by fluorography. Each exposure was selected to show $VLDL_1$ and $VLDL_2$ and are not of equivalent exposure time. Findings are representative of duplicate independent experiments.

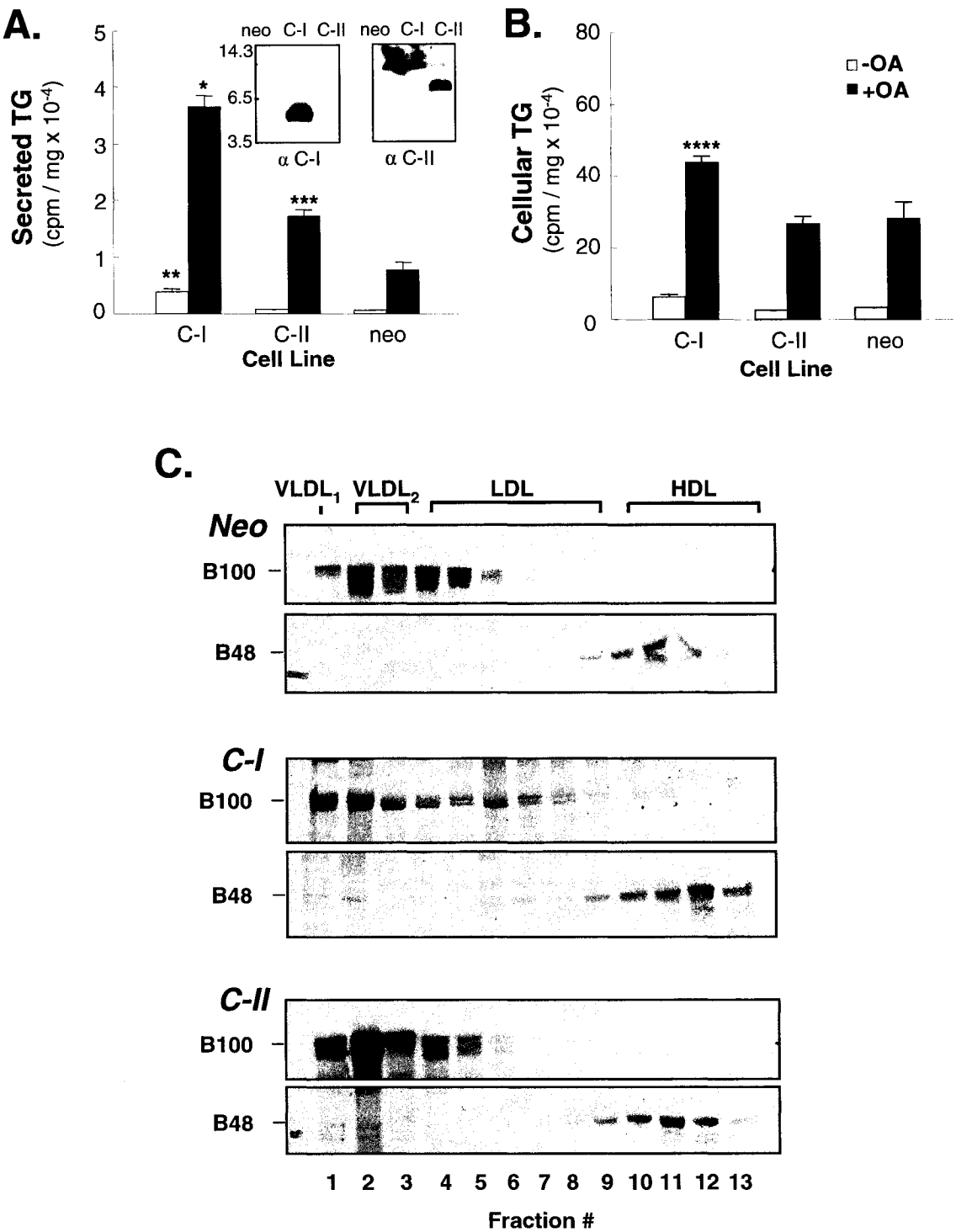
A.
Secreted TG
(cpm / mg x 10-4)
5
4
3
2
1
0
neo C-I C-II neo C-I C-II
14.3
6.5
3.5
α C-I
α C-II
*
**
***
C-I
C-II
neo
Cell Line
B.
Cellular TG
(cpm / mg x 10-4)
80
60
40
20
0
□-OA
■+OA
****
C-I
C-II
neo
Cell Line
C.
VLDL1
VLDL2
LDL
HDL
Neo
B100
B48
C-I
B100
B48
C-II
B100
B48
1 2 3 4 5 6 7 8 9 10 11 12 13
Fraction #

When apoB100 was immunoprecipitated from the fractions it revealed that both apoC-I and apoC-II (Fig. 14C) showed a shift in secreted apoB100 containing particles into a $VLDL_1$ density range. This is similar to what was detected in apoC-III expressing cells in Figure 13.

Discussion

Apolipoprotein C-III is known to be an independent risk factor for cardiovascular disease due to its hypertriglyceridemic association. Elevated apoC-III has also been found in patients with kidney dysfunction, type 2 diabetes and visceral obesity [5;107;108]. Recently apoC-III has also been associated with the hypertriglyceridemia seen in patients with metabolic syndrome [51]. In all of these situations the dysfunction of apoB containing lipoproteins is central to disease pathology. The postulated function for apoC-III in all these disorders has remained linked to the inhibitory role on LPL mediated LpB hydrolysis, or particle clearance [109]. It is clear that the lipid binding properties, and the ability to disrupt LPL are distinct. However since the observation by Sparrow that C terminal residues 41 and 79, disrupted LPL activity, further characterization has been limited [110]. Also since the activation domain of apoC-II had been localized to residues 55-78 the effects of the apoC's were taken to be well characterized [111] Experimental evidence to date supports a functional role for apoC-III in inhibition of LPL [112], and the disruption of particle uptake; we describe a new function for apoC-III in stimulating the intracellular assembly and secretion of TG-rich $VLDL_1$ particles, without increasing apoB-100 secretion.

I observed that the transient (Fig. 6) or stable transfection (Fig. 7) of human apoC-III in McA-RH7777 hepatoma cells when supplemented with 20% FBS and OA, leads to

a two-fold increase in TG secretion. In addition [^{3}H]glycerol or [^{14}C]oleate labeling both demonstrated a two-fold increase in the secretion of labeled TG but not PC (Fig. 10). This increase in TG secretion is reminiscent of the JCR:LA-cp rat (cp/cp) model, where the increase in TG rich VLDL is attributed to an increased rate of fatty acid synthesis. This animal lacks membrane-bound leptin receptors (ObR), and the autosomal recessive cp gene (cp/cp) leads to marked obesity due to functionally null mutations of the leptin receptor (Lepr) due to a T2349A transversion resulting in a Tyr763Stop nonsense mutation in the gene just before the transmembrane domain [113]. The resultant increase in hepatic TG has been proposed to drive increased TG rich VLDL secretion. The increase in TG secretion in response to OA was confirmed using a flag tagged construct, where two flag epitopes were added to the C-terminus, and also demonstrated a two-fold increase in ^{3}H-TG secretion with no detectable increase in ^{3}H-PC secretion in response to OA (Fig. 7C). This epitope insertion would not interfere with the putative fusogenic properties attributed to the tilted peptide motif within the N terminus of the peptide [28]. Both transient and stable cell lines demonstrated a dose dependent increase in secretion of ^{3}H-TG, only in the presence of OA (Fig. 6&7), reaching a maximum of two-fold in transient, stable, mixed cultures and flag tagged cell systems. This dose effect of apoC-III expression increasing TG secretion is reminiscent of the gene dose effect reducing circulating TG in apoC-III knockout mice. Also when Breslow [35] generated apoC-III over-expressing transgenic mice the plasma had a milky appearance similar to patients with severe hypertriglyceridemia even when fasting. It was also noted that hypertriglyceridemia caused by apoC-III was not accompanied by a concomitant rise in free cholesterol or circulating apoB-100 [36], as seen in other hyperlipidemic phenotypes.

I also detected an increase in cellular ^{14}C-TG in apoC-III expressing cells similar to the significant increase in cellular ^{3}H-TG (**p<.006) when cells were labeled with [^{3}H]glycerol in the presence of OA (Fig. 9B). ^{14}C-TG labeling under pulse chase conditions showed that apoC-III cells preferentially labeled TG over PC (Fig. 10). This is reminiscent of an enhanced PC to TG turnover which is one of the known mechanisms for TG production. In kinetic studies I found that the cellular levels of labeled TG increased dramatically in response to OA whereas the PC levels did not (Fig. 8), this may reflect a difference in the synthetic rate of ^{3}H-TG as compared to ^{3}H-PC. Thus the effect of apoC-III on TG secretion may be either mediated by increased TG synthesis and/or turnover. This dependence of apoC-III on OA supplementation is similar to the hyperinsulinemic state of cp/cp rats or patients with hyperinsulinemia where increased circulating FFA drives hepatic TG production and in turn may drive VLDL production.

When apoC-III expressing cells were metabolically labeled with [^{35}S]methionine/cysteine I detected no increase in the synthesis or secretion of apoB-100 (Fig. 11). This suggested that a similar number of lipoproteins were secreted but that increased ^{3}H-TG secretion may reflect an increase in VLDL size. To establish whether the apoC-III transfected cells were secreting more buoyant lipoproteins, medium was collected and subjected to rate floatation ultracentrifugation. This demonstrated that apoC-III expressing cells had more ^{35}S-apoB 100 floating in the $VLDL_1$ sub fraction (Fig. 13B) and that the increased ^{3}H-TG was only associated with the $VLDL_1$ sub fraction (Fig. 13D). This suggests that the recombinant expression of apoC-III in liver cells leads to a hyper-TG normo-B phenotype. This particular anomaly is detected in patients displaying FCHL [105]. To further confirm this observation I used stable cell lines

expressing apoC-I and apoC-II and found that both proteins also demonstrated increased ^{3}H-TG secretion in response to OA and increased apoB-100 in the $VLDL_1$ sub fraction (Fig. 14). This observation shows that accessory apolipoproteins may play a novel intracellular role in the assembly and secretion of TG rich VLDL particles. The lipid labeling studies also suggest that the mechanism may be mediated by an increase in cellular TG by either synthesis and/or turnover.

To further investigate the role of apoC structure sequence alignments were performed using the T-Coffee algorithm [114] on several exchangeable apolipoproteins (Fig. 15). This algorithm is particularly powerful in that it is capable of excluding large segments of sequence that do not align, as indicated by the blue triangles in Figure 15. (www.ch.embnet.org/software/TCoffee.html). I found as expected, apoC-III proteins from various species showed moderately high homology; this established a baseline for inter-comparison of apoC-I, II and III. When these three proteins were aligned, two central domains were common to all three proteins. This is similar to findings from 1974 where apoC-I [115] and later apoC-II [28;31] and apoC-III [116] were proposed to be structurally composed of two major domains. Despite the homology of the two central domains the termini of these proteins are clearly divergent, and may specify individual protein function. Since apoE transgenic animals showed increased LpB secretion [117], I used the T-Coffee algorithm to align apoC-III and apoE sequences. I was surprised by the contiguous homology between these two proteins, when certain segments present only in apoE were excluded (Fig. 15C blue triangles). Similar analysis using the Blossom algorithm in pair-wise protein Blast (NCBI) was not able to overcome these large segments excluded by the T-Coffee algorithm (Fig. 15C blue triangles below). Some

interesting regions of homology revealed by this analysis were: high homology in the signal peptide regions, some homology in the 5' end of the LDL-R binding region, the region of apoE that contains residue 158 (responsible for apoE isoform) and large regions of the C terminal domain of apoE that probably correspond to lipid binding regions. Since I have already shown that the introduction of apoA-I alone is insufficient to increase VLDL production [97], apoA-I and apoC-III were compared as a negative control. I found no homology over large segments of the protein and some intermediate homology in helical regions known to possess lipid binding properties [118]. Further investigation into the intracellular roles of these accessory molecules in the assembly of TG rich VLDL is now warranted. Of particular interest would be to define the domain structures that function as facilitators of TG-rich LP secretion. Recent data has already suggested that apolipoproteins such as apoA-V may play a role in attenuating LpB production [119].

Fig. 15. T-Coffee comparison of apolipoprotein C's.

A, multiple alignment of apoC-III primary amino acid sequences using the T-Coffee algorithm. Color scale indicates level of homology of individual residues and domains, (*) denotes identity (:) denotes conservative substitution, (.) denotes structural similarity. B, T-Coffee analysis of apoC-I, II and III, N and C terminal regions reveal low homology while two central domains show high >60% homology. C, comparison between human and murine apoC-III sequences, vs. an alignment of apoC-III human with human apoE. Note that with the exception of three regions, indicated by triangles, the sequences align well. These triangles represent residues looped out of the alignment of apoE and apoC-III. A portion of the LDL-R binding site (underlined) and apoE Arg 158 (underlined and italics) are indicated. Comparison between apoA-I and apoC-III is used as a negative control and illustrates that not all exchangeable apolipoproteins share high homology using this algorithm.

A.


AVERAGE
4 5 6 7

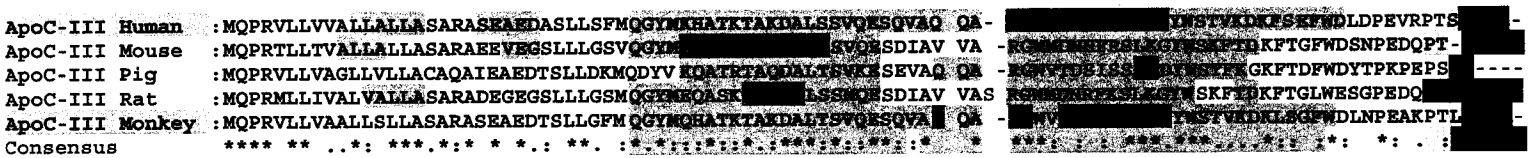
ApoC-III Human
ApoC-III Mouse
ApoC-III Pig
ApoC-III Rat
ApoC-III Monkey
Consensus

B.


ApoC-I
ApoC-II
ApoC-III
Consensus

C.

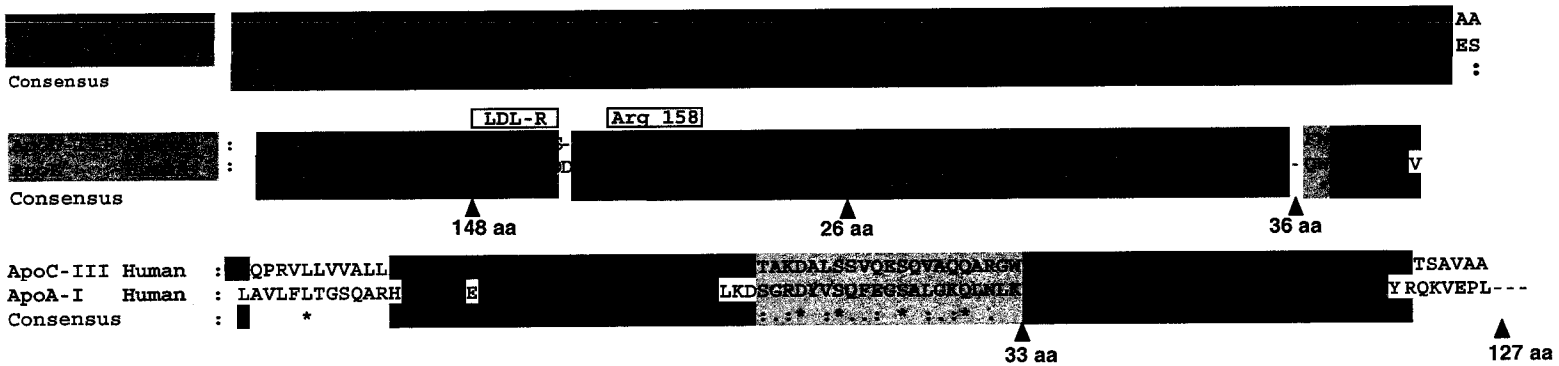
Consensus
LDL-R
Arg 158
Consensus
148 aa
26 aa
36 aa
ApoC-III Human
ApoA-I Human
Consensus
33 aa
127 aa

Chapter 4 Phosphatidate Phosphohydrolase (PAP)

Introduction

The assembly and secretion of TG-rich VLDL particles is dependant on the accessibility and production of necessary lipids. It is known that in the absence of MTP, LpB assembly and secretion is ablated [120;121]. However several other lipid modifying enzymes also appear to play a role in the assembly and secretion of VLDL particles such as PLD, $iPLA_2$, and PAP-1. These enzymes may provide critical substrates for the second step assembly of LpB, namely lipid substrates for TG-rich $VLDL_1$. To date our understanding of how lipids drive the assembly of lipoproteins is still incomplete, but candidate genes are now apparent.

The enzyme phosphatidate phosphohydrolase (PAP-1) (EC 3.1.3.4) catalyzes the hydrolysis of phosphatidate (PA) to yield *sn*-1,2-diacylglycerol and inorganic phosphate (Fig. 16A) [122]. This enzyme activity has been shown to respond to glucocorticoids such as cortisol and synthetic analogs like dexamethasone. Defects in this metabolic system are exemplified by Cushings syndrome where excessive fat depositions are associated with elevated circulating levels of cortisol [123]. In addition to the activation of PAP-1 activity, glucocorticoids also stimulate TG synthesis [124], promote VLDL secretion [125] and are capable of inducing fatty liver [126]. Further support for glucocorticoid regulation of PAP-1 was found in fatty acid or alcohol fed rats that, when stressed showed coincident up-regulation of PAP-1 activity and cortisol production [127]. In rats that underwent adrenalectomy no alcohol induced increase in PAP activity was evident, which suggests that the regulation of this effect is through a paracrine hormone [128]. Cortisol follows a diurnal pattern of release in rodents with an onset of secretion

Fig. 16. Glycerolipid synthesis and phosphatidate phosphohydrolase comparison. A, diagrammatic representation of some of the pathways for glycerol lipid synthesis. Arrowheads denote precursor-product relationships and double arrows indicate reactions that can occur in both directions. The enzyme responsible for each reaction is indicated. B, PAP isoforms are compared for their cellular distribution, temperature sensitivity, and requirement for cofactors.

A. ***Lipid Biosynthesis***

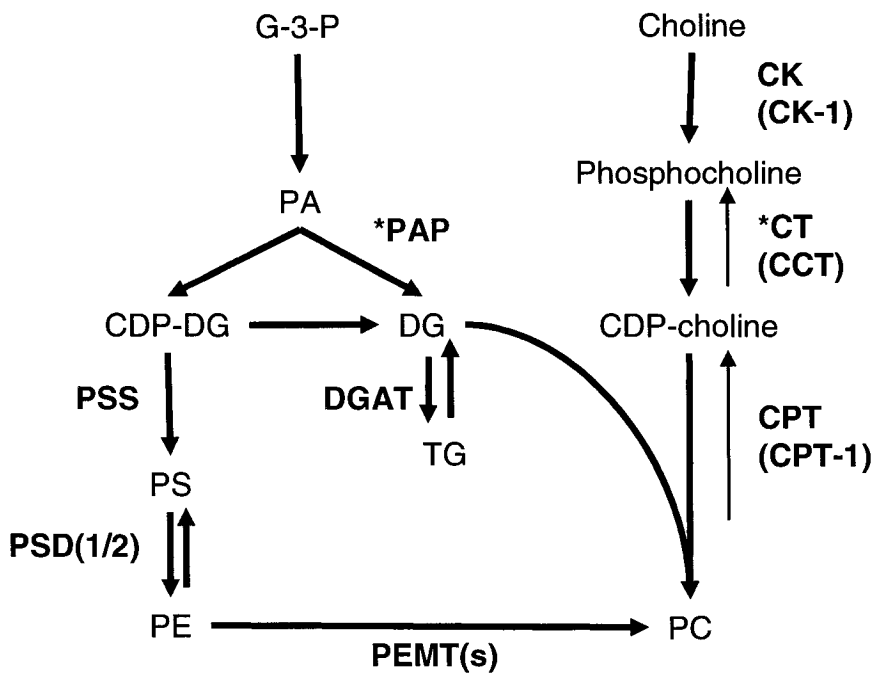

B.

PAP Isoforms

PAP-1	**PAP-2 (LPP)**
Localized to cytosol and translocates to ER in response to long chain FFA	**Localized to the Plasma Membrane**
Labile at temperatures >30 °C	**Temperature Stable to 55 °C**
Mg^{2+} Dependant	**Mg^{2+} Independent**
NEM Sensitive activity	**Insensitive to NEM**
Increase in activity in response to Dexamethasone (μM)	

at two hours before darkness. Studies of light conditioned rats showed that PAP-1 activity also followed a diurnal rhythm, with PAP-1 activity peaking shortly after cortisol levels [129].

Phosphatidic acid phosphohydrolase activity is in fact derived from at least two distinct enzymes described in Figure 16B. PAP-1 activity is located in the cytosol [130], and has been reported to translocate to the ER in response to glucocorticoid treatment [131]. This activity has an absolute requirement for Mg^{2+} [132] and is acutely sensitive to reagents such as *N*-ethyl-maleimide (NEM) [133]. Conversely PAP-2 or lipid phosphate phosphohydrolase (LPP) [133], is insensitive to NEM and is not inhibited by chelating agents such as EDTA or EGTA. PAP-2 isolated from liver was found to be highly glycosylated since when treated with n-glycanase the molecular weight changed from 50 to 28 KDa [134]. This enzyme has been cloned, and was found to contain six transmembrane domains which is in agreement with enzymology studies that have localized this activity to the plasma membrane [135]. PAP-2 is capable of acting as an ecto-enzyme (external) for growth factors that are involved in platelet signaling by responding to extra-cellular stimuli like lyso-PA or sphingosine-1-phosphate [134]. LPP's have broader substrate specificity than PAP-1, hydrolyzing lyso-PA, cerimide-1-phosphate and, sphingosine-1-phosphate, with an efficiency similar to PA [136]. The activity of LPP has been detected in all tissues studied, whereas PAP-1 has been found specifically in the liver, adipose tissue [137], bovine retina [138], pig and mouse brain [139;140], and also rat heart[141].

PAP-1 enzyme activity was first identified in plants by a Canadian biochemist Morris Kates in 1955 [142]. This activity was found to be associated with a 15,000 x g sedimented fraction from spinach leaf homogenate. When PC was used as a substrate he

noticed a lag between the production of choline and the detection of inorganic phosphate. Since then numerous researchers have attempted to purify this enzyme with great difficulty. In 1967 researchers achieved 16-fold purification [143], which was later improved by Hosaka's group to 20 fold in 1975 [144]. With modern chromatographic techniques Sturton in 1981 achieved 52-fold enrichment [145], but was later bested by Butterworth in 1984 who utilized Tween-20 to stabilize the activity and reached 416-fold enrichment [142]. Unfortunately these attempts have not provided sufficient materials to generate antibodies or other reagents that may allow the isolation of this enzyme.

There are several models that have been used to study the enzyme activity of PAP-1 including alcohol fed rat models [146], dexamethasone treated hepatocyte cultures [94] and partial purifications of rat liver homogenates [144]. With hepatocyte cultures researchers have shown twofold increases in VLDL and apoB secretion in response to 100 nM dexamethasone treatment [94]. However 50 nM insulin treatment was capable of antagonizing this effect on VLDL and apoB secretion [94]. Since efforts to identify PAP-1 have been unsuccessful I endeavored to use a novel methodology to isolate and clone PAP-1 (Fig. 17A). This investigation evaluated the utility of modern 2D-PAGE and differential display (DD-PCR) approaches. From the outset of this project it was realized that knowledge gained in this endeavor might be incremental, nevertheless I sought to employ modern techniques in isolating and identifying this enzyme. Since these methodologies were new to our laboratory, this project was an attempt to identify which approaches would be most utile and to propose a strategy to combine multiple approaches that in combination may lead to isolation of this enzyme.

Fig. 17. PAP-1 purification, cloning strategy and enzymatic assay.

A, flow chart diagramming the proposed steps to purify PAP-1 enzyme activity. Methods that involve the isolation of proteins are shown on top, while methods utilizing RNA are indicated at bottom. B, diagram of PAP-1 enzyme assay, illustrating cellular sample combined with Tris maleate buffer, [^{3}H]PA, Mg^{2+} and DTT, before allowing the reaction to proceed for 30 min at 37 °C. The reaction is stopped with olive oil and $CHCl_3$ before alumina is added. This sequesters unreacted PA and DG is removed in the chloroform phase. Samples are then allowed to dry before scintillation counting in a Wallac Scintillation device.

A.

Cloning Strategy

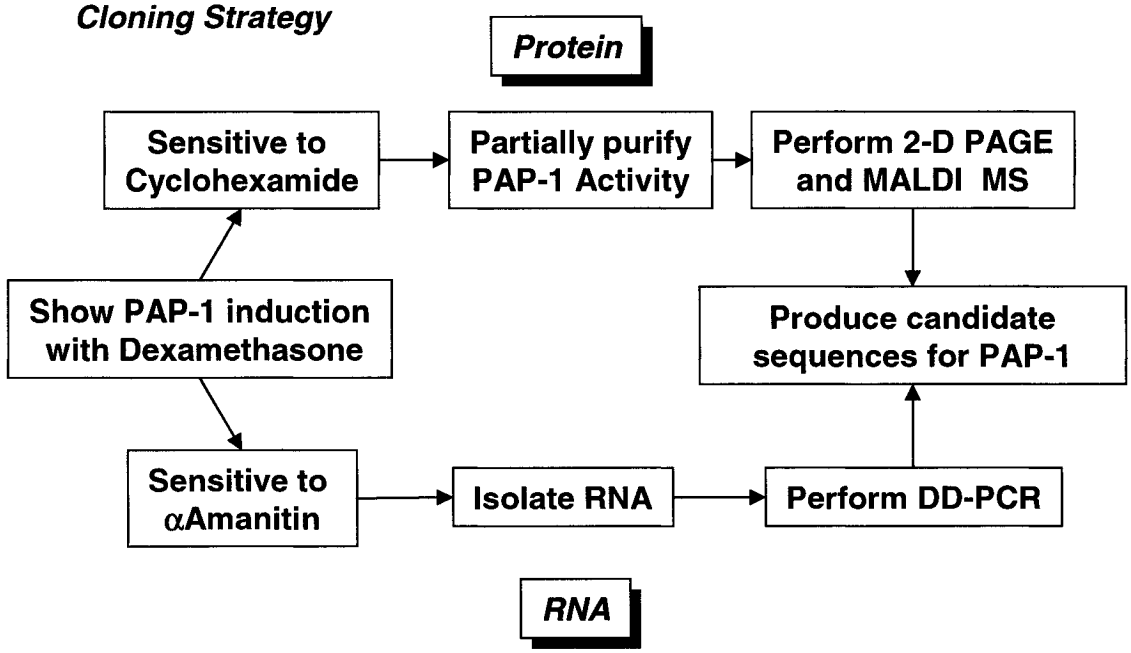

B.

PAP Assay

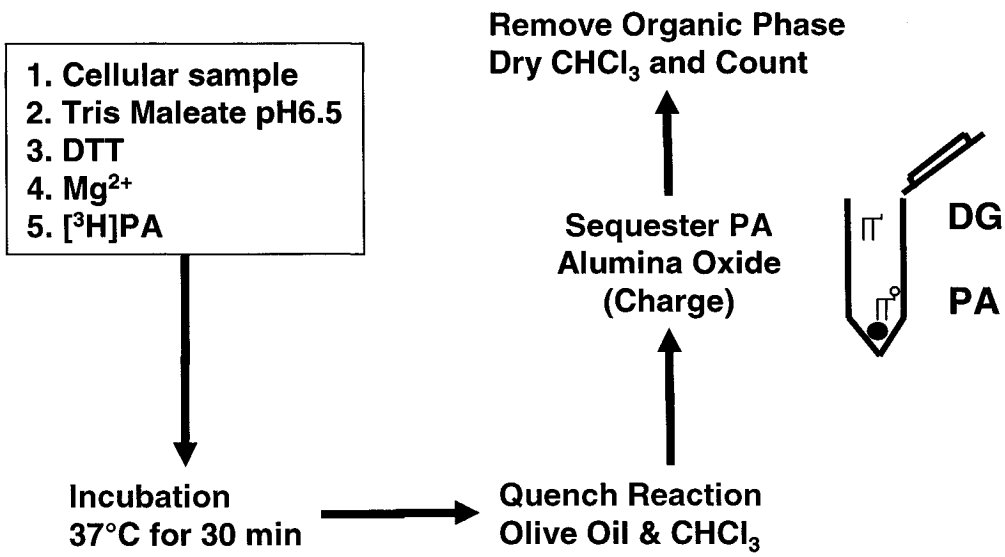

Our approach was two fold, first I sought to use primary hepatocyte cell cultures and alcohol fed rat liver models to assess mechanical means of purification. From this enrichment differentially expressed proteins (in response to dexamethasone or alcohol treatment) would be subjected to 2D-PAGE for identification by MALDI-TOF Mass Spectroscopy. The second half of our approach was to use dexamethasone induced hepatocyte cultures to produce RNA for dd-PCR. This method relies on the differential expression of PAP-1 mRNA in response to dexamethasone treatment. All up-regulated genes were reverse transcribed and PCR amplified with a library of degenerate primers (Table 3). By examining the expression profile, candidate genes could be isolated and sub-cloned. To identify the isolated fragments a bioinformatics strategy was developed and novel genes isolated by this methodology were characterized.

Determination of Enzymatic Activity

Before hepatocyte cultures were employed to isolate PAP-1 activity, the utility of the alcohol-fed rat liver model was evaluated. This model demonstrates an increase in PAP-1 activity, that could be compared to the cytosolic extracts of untreated livers. The methodology to quantify PAP-1 activity was based on the hydrolysis of [^{3}H]PA to [^{3}H]DG [147]. This method exploits the fact that when the inorganic phosphate is hydrolyzed from PA it will no longer be adsorbed to alumina oxide. The enzymatic activity can be monitored as the hydrolysis and generation of DG which was detected in the supernatant of an alumina oxide precipitation (Fig. 17B). Methodologies utilizing [^{32}P] labeled PA are also possible that directly measure inorganic phosphate release. Direct measurement of inorganic phosphate are routinely confounded by contaminating PLA activities [148]. Also by presenting the [^{3}H]PA in the presence of mixed micelles of

PC any nonspecific activities (i.e. PLA) can be minimized [147]. Any glycerol-3-phosphate produced in this reaction was removed by extracting the DG in chloroform before alumina adsorption of unreacted substrate [149]. In adipose tissue there is significant degradation of DG produced by PAP-1, therefore in this tissue a direct inorganic phosphate assay is required [150]. By assaying rat liver cytosol I was able to distinguish NEM sensitive and insensitive activities, which represent PAP-1 and PAP-2 respectively (Fig. 18A). By assaying several concentrations of cytosolic lysate, a linear increase in enzyme activity allowed me to calculate the specific activity from the slope (Fig. 18A). The amount of PAP-1 activity that I detected was 2.5 to 3 μmoles DG/mg/h, which was in agreement with levels found in the literature.

I determined whether PAP activity was amenable to salting out by using an ammonium sulfate precipitation. Using cytosol isolated from rat livers, I observed that PAP activity could be recovered by salt precipitation followed by extensive dialysis. The enzyme activity precipitated at a specific concentration of 30% ammonium sulfate (Fig. 18B). However this enrichment technique only yielded a 1.2 fold enrichment. I have also been able to develop conditions to effectively separate cytosolic proteins using a Bio-Rad 2D protein system. To determine the level of complexity in these cytosolic samples I performed 2D-PAGE using a pH gradient of 3-10 (Fig. 18C). Experiments have shown that to generate effective separation of proteins in the first (IEF) dimension, 50 μg/μl of protein was required (Fig. 18C). However the number of proteins resolved by this methodology was unsuitable for direct MALDI-TOF mass spectrometry analysis,

Fig. 18. Phosphatidate phosphohydrolase (PAP) activity in rat liver.

A, PAP-1 activity in rat liver cytosol was determined (2 M Tris maleate, 1 M DTT, 1 M Mg^{2+} pH 6.5). Duplicate sets of samples were assayed in the presence (filled squares) or absence of 0.4 mM NEM (open circles) to determine NEM sensitive (PAP-1) activity (the difference between –NEM and +NEM). The calculated activity was 2.5 μmoles DG/mg/h. B, rat liver was homogenized in 0.25 M sucrose buffer, 2 mM DTT with a glass Dounce homogenizer and cytosol was isolated. Proteins were precipitated with increasing concentrations of ammonium sulfate, at 4 °C. Samples were dialyzed against 4 l of PBS before total PAP activity (-NEM) was determined. C, rat liver cytosol was suspended 1:1 in IEF buffer (7 M urea, 2 M thiourea, 0.4% CHAPS, 0.1% DTT in ddH_2O) and adsorbed overnight into a pH 3-10 immobilized IPG strip. The strip was focused in a BioRad IPG apparatus as follows (step 1: 250V linear current for 30 min, step 2: 10,000V linear current for 2.5 h, step 3: 10,000 V rapid convex current to 40,000 Vhrs). The IEF strip was equilibrated, over-laid with agarose and resolved in the second dimension on a 10% SDS-PAGE gel and proteins were revealed by silver staining.

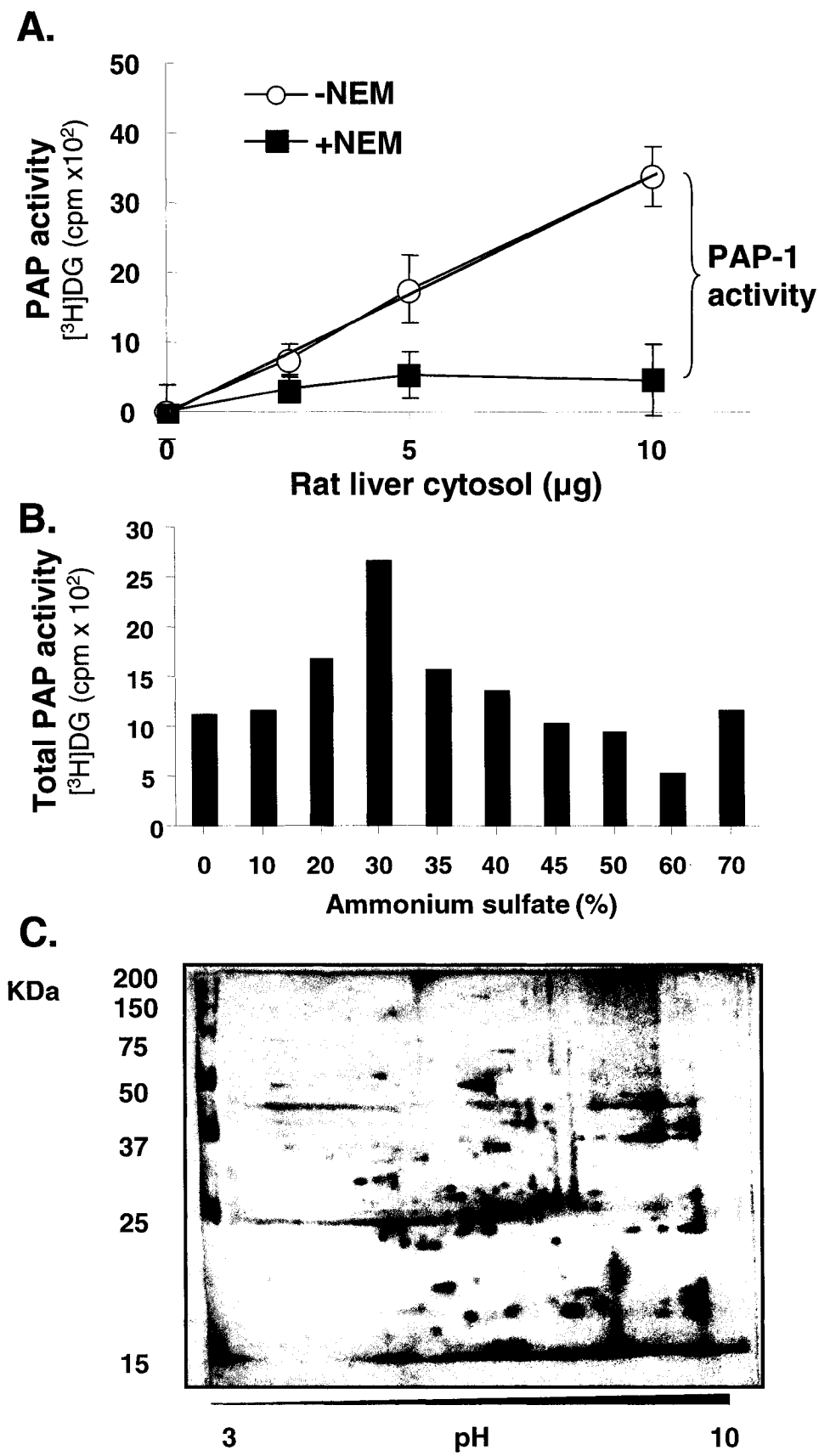
A.
50
40
30
20
10
0
-NEM
+NEM
PAP activity
[3H]DG (cpm x10²)
PAP-1
activity
0
5
10
Rat liver cytosol (µg)
B.
30
25
20
15
10
5
0
Total PAP activity
[3H]DG (cpm x 10²)
0
10
20
30
35
40
45
50
60
70
Ammonium sulfate (%)
C.
KDa
200
150
75
50
37
25
15
3
pH
10

(personal communication with Dr. Pierre Thibault at NRC laboratories). Since the number of proteins present in cytosolic lysate was too large I abandoned the direct comparison of alcohol fed rat liver cytosol as a way to differentially detect PAP-1 by 2D-PAGE analysis alone. Instead I evaluated dexamethasone induced differential display as a means of isolating PAP-1 mRNA.

Phosphatidate Phosphohydrolase Induction by Dexamethasone in Rat Hepatocytes

Using 75 g male Spauge Dawley rats I established primary hepatocyte cultures as described in *Materials and Methods*. These cells were cultured on fibronectin coated plastic ware in the presence of 20% FBS for 4 h, then cells were grown in serum deplete conditions for 16 h. Hepatocytes were then induced with 1 μM dexamethasone for 4 h and total cell lysates were assayed for PAP activity. Total PAP activity was markedly increased by dexamethasone treatment (Fig. 19B). To ensure that this increase of total activity reflected an increase in PAP-1, cell lysates were pre-incubated in the presence or absence of NEM for 30 min before the activity was measured. This revealed a eight fold increase in PAP-1 activity in response to dexamethasone treatment (Fig. 19C). In this experiment total lysates were used and there was also an increase in NEM insensitive enzyme activity. This may be due to an incomplete inactivation of PAP-1 by NEM because crude lysates were used, or alternatively it may reflect a *bona fide* increase in PAP-2 activity in response to dexamethasone treatment.

Fig. 19. Dexamethasone treatment of primary rat hepatocytes.

A, diagram of glucocorticoid analog dexamethasone (MW. 392.5). B, total cell lysate from primary rat hepatocytes was assayed for PAP activity when treated with (filled squares) or without 1 μM dexamethasone (open circles). C, primary rat hepatocytes were treated with 1 μM dexamethasone and total lysates were treated with (filled bars) or without (open bars) 0.4 mM NEM for 30 min before PAP activity was determined. Activity detected in the presence of NEM (filled bars) subtracted from total activity (open bars) represents PAP-1 activity.

A.

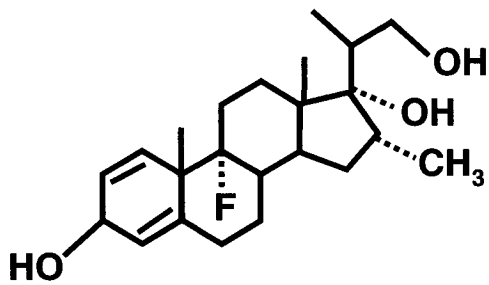

Dexamethasone

B.

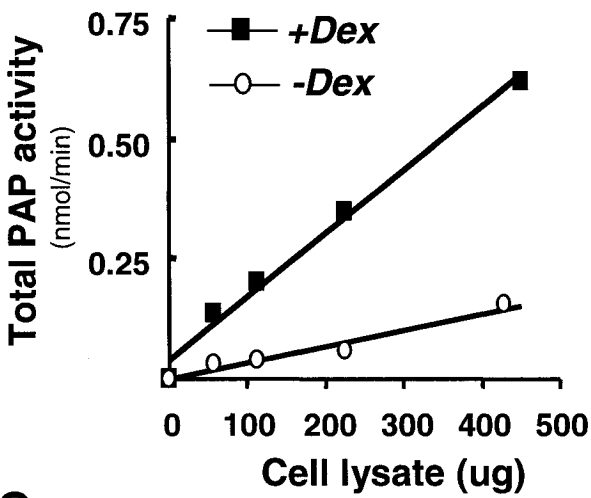

C.

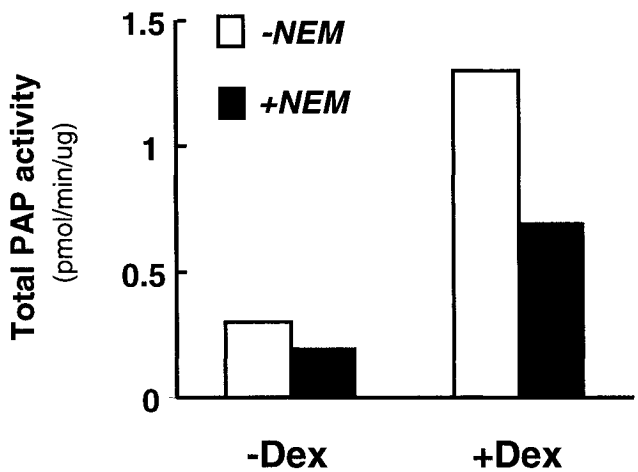

To ensure the treatment conditions used were maximizing the induction of PAP-1 activity, a dose curve experiment was performed with increasing concentrations of dexamethasone. From Figure 20A it is apparent that the concentration of 1 μM dexamethasone is yielding maximal induction of PAP-1 activity. It is also apparent that with higher concentrations of dexamethasone, there was an attenuation of PAP-1 enzyme induction (Fig. 20A). Also to ensure that the length of time that cells were treated with dexamethasone was sufficient, time course experiments were performed and showed that PAP-1 activity initially decreased as cells were cultured overnight in serum free medium (Fig. 20B). However maximal induction of PAP-1 activity was detected after 5 h of dexamethasone treatment and PAP-1 activity decreased after longer treatment periods (10 or 24 h). After establishing the conditions where an 8 fold induction of PAP-1 activity was detected I sought to determine whether the response to dexamethasone was at a transcriptional or translational level. To test this, primary rat hepatocytes were treated with dexamethasone or dexamethasone plus cyclohexamide or dexamethasone plus α-amanatin to inhibit protein synthesis or RNA synthesis, respectively. The induction of PAP-1 activity by dexamethasone treatment was inhibited with either cyclohexamide or α-amanatin (Fig. 20C). This suggests that the induction of PAP-1 in response to dexamethasone occurs at both transcriptional and translational levels.

Cell extracts were enriched by absorbing the PAP-1 activity to artificial membranes. Cytosolic isolates were combined with PC vesicles (80 nmol/mg) and 500 μM exogenous oleate. Artificial membranes were precipitated and the activity of PAP-1 was determined in the supernatant. I speculated that PAP-1 activity might translocate to

Fig. 20. Dexamethasone dose curve and time course.

A, to determine optimal dexamethasone dose for PAP-1 induction in primary rat hepatocytes, cells were cultured under serum depleted conditions for 16 h before increasing concentrations of dexamethasone were administered. Total cell lysates were collected 4 h after dexamethasone induction and PAP-1 activity was determined. B, to ensure the maximal induction of PAP activity, a time course was performed where samples were collected immediately after plating, 16 h after serum deprivation and after 5, 10 or 24 h of 1 μM dexamethasone treatment. Total PAP activity was determined. C, to determine whether PAP-1 activity induced by dexamethasone was sensitive to transcriptional or translational poisons, 1 μM dexamethasone induction was performed in the presence or absence of 1 nM α amanatin (αAM) or 50 μM cyclohexamide (cHex), or with no treatment (no Tx).

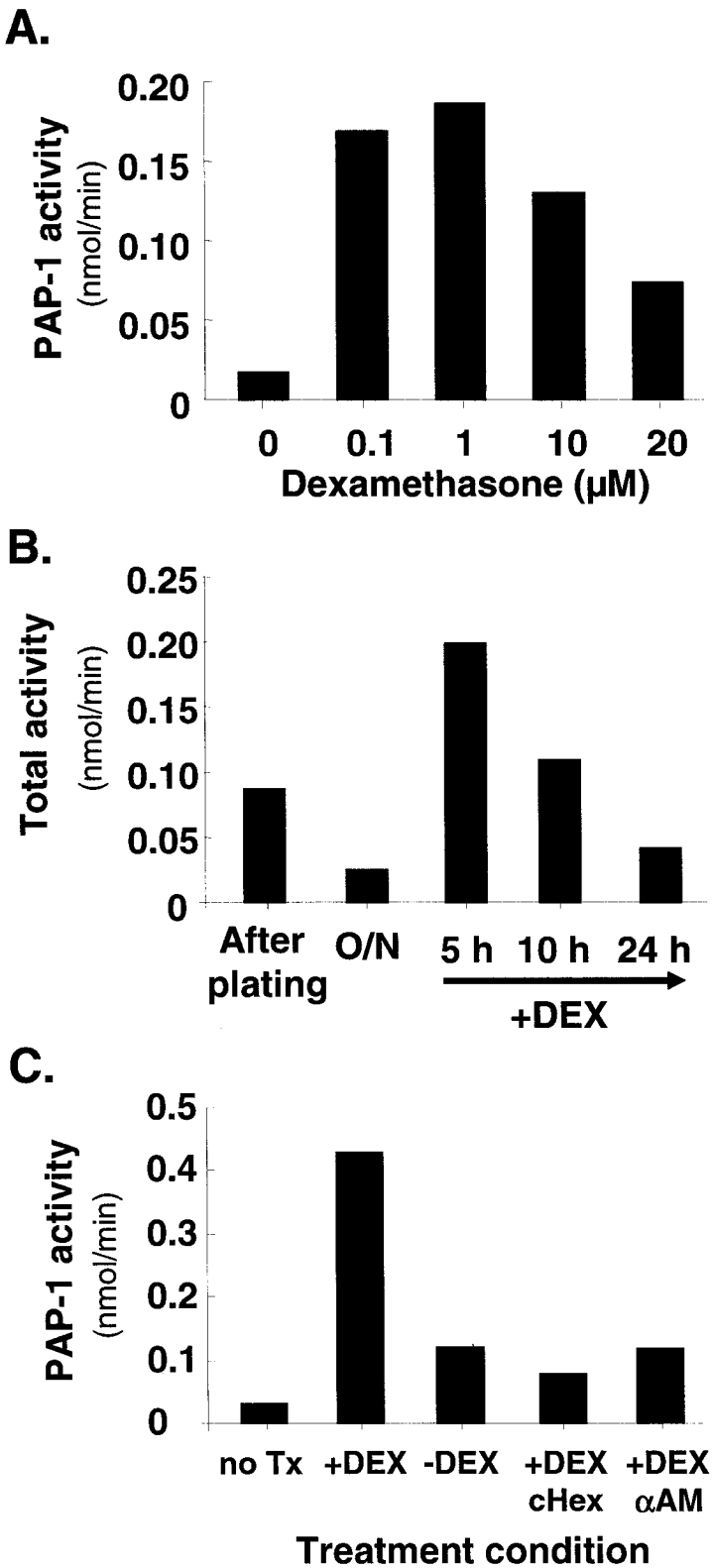
A.
PAP-1 activity
(nmol/min)
0.20
0.15
0.10
0.05
0
0
0.1
1
10
20
Dexamethasone (μM)
B.
Total activity
(nmol/min)
0.25
0.20
0.15
0.10
0.05
0
After plating
O/N
5 h
10 h
24 h
+DEX
C.
PAP-1 activity
(nmol/min)
0.5
0.4
0.3
0.2
0.1
0
no Tx
+DEX
-DEX
+DEX cHex
+DEX αAM
Treatment condition

the artificial membranes and after precipitation, a decrease in the cytosolic activity could be detected (Fig. 21A). When cytosolic extracts from dexamethasone treated cells were precipitated under these conditions a 50% decrease in the PAP-1 activity was detected in the supernatant (Fig. 21B). To test whether the translocation of PAP-1 could be induced before cell lysis, 0.5 mM OA was added to the culture medium before cell fractionation (Fig. 21C). Cells treated with OA before fractionation showed no increase in the PAP-1 detected in the cytosol (Fig. 21C). However if the dexamethasone induced lysates were treated with oleate after lysis but before membrane precipitation, a significant increase in PAP-1 was detected in precipitated membranes (Fig. 21D). To ensure that there was a specific OA effect I compared PAP-1 activity remaining in the cytosol using PC or PC +OA. I found OA treatment enhances precipitation of PAP-1 activity beyond that of PC alone (Fig. 21E).

An advantage of primary hepatocyte cell culture is that cells can be metabolically labeled with [^{35}S]methionine/cysteine identifying proteins synthesized during dexamethasone induction. Newly translated proteins were labeled to detect differentially expressed proteins in response to dexamethasone. This labeling was coupled to liposome precipitation as above and several unique proteins were detected in the liposome adsorbed precipitate that differed with dexamethasone induction. However, again because of the number of proteins present, this method alone would not be sufficient to directly identify candidate proteins (Fig. 21F).

Fig. 21. Liposome adsorption of phosphatidate phosphohydrolase (PAP) activity.

A, representation of cytosolic PAP adsorption to PC vesicles. After PAP was adsorbed in the presence of exogenously added 500 μM oleate (ex OA) vesicles were precipitated and PAP-1 activity was measured in the supernatant or pellet. B, cytosolic PAP activity was measured in primary rat hepatocytes induced for 4 h with 1 μM dexamethasone. Samples were then combined with PC liposomes (80 nmol/mg) precipitated, and the supernatant PAP-1 activity was determined. C, to determine if treatment of intact cells before homogenization would affect PAP-1 precipitation, 0.5 mM OA was added 1 h before cytosolic isolation and sample precipitation as before. Filled bars represent PAP-1 activity detected in the absence or presence of oleate supplemented medium (med OA). D, PAP-1 activity recovered in the pellet of PC liposomes, when 0.5 mM OA was added 1 h before cell lysis (med OA) or 500 μM OA was added immediately before precipitation of cell lysates (ex OA). E, to evaluate the increase in precipitation mediated by OA vs. PC alone, PAP-1 activity was determined by assaying the supernatant after precipitation (ex OA). F, dexamethasone induced and un-induced hepatocytes were labeled with [^{35}S]methionine/cysteine before cytosolic liposome in the presence of 500 μM OA immediately before precipitation of cell lysates. Pellets were re-solubilized and run on denaturing SDS PAGE and revealed by fluorography. Candidate proteins detected only in the +Dex precipitate are indicated by filled circles.

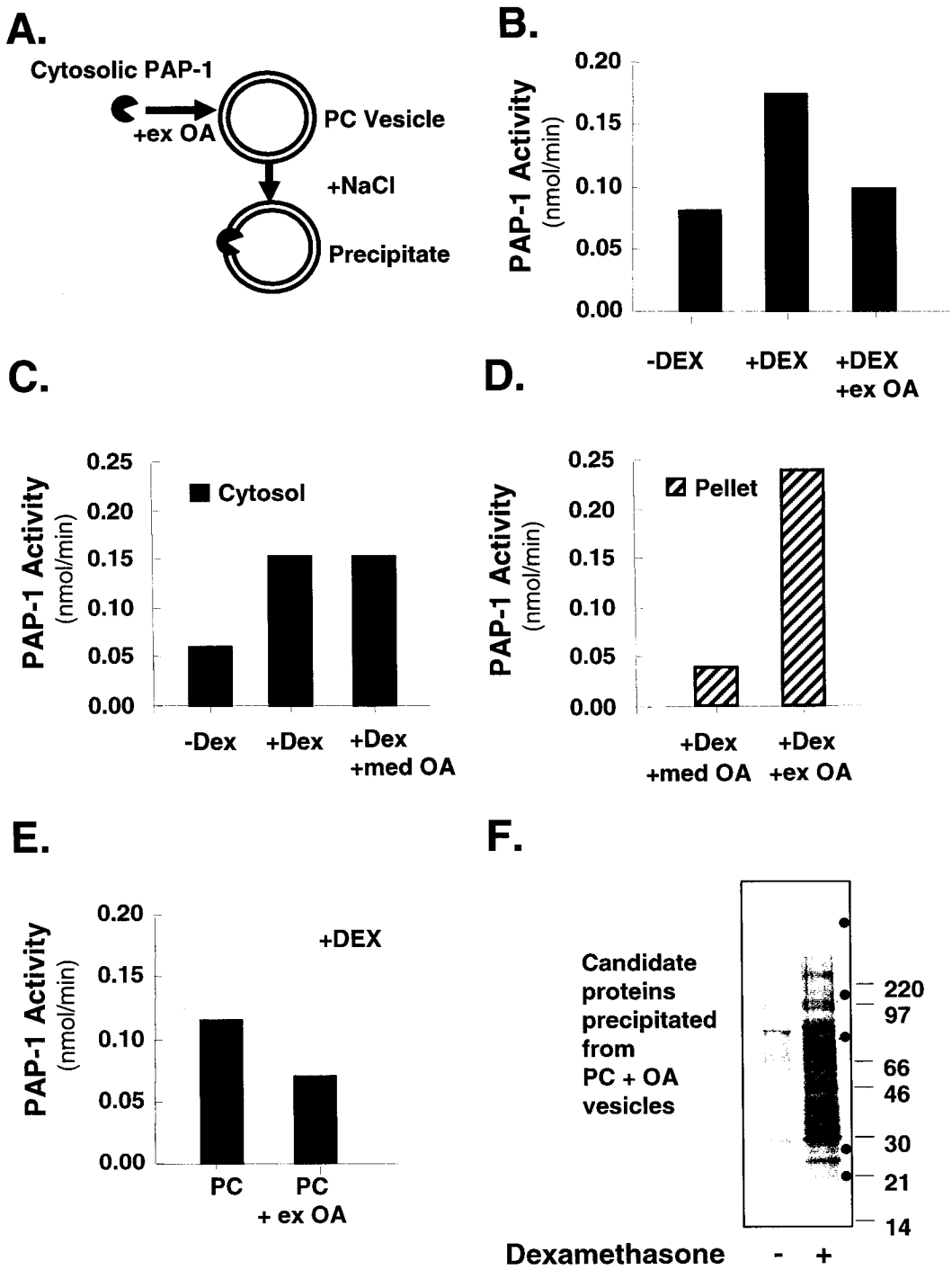
A.
Cytosolic PAP-1
+ex OA
PC Vesicle
+NaCl
Precipitate
B.
PAP-1 Activity
(nmol/min)
0.20
0.15
0.10
0.05
0.00
-DEX
+DEX
+DEX
+ex OA
C.
PAP-1 Activity
(nmol/min)
0.25
0.20
0.15
0.10
0.05
0.00
Cytosol
-Dex
+Dex
+Dex
+med OA
D.
PAP-1 Activity
(nmol/min)
0.25
0.20
0.15
0.10
0.05
0.00
Pellet
+Dex
+med OA
+Dex
+ex OA
E.
PAP-1 Activity
(nmol/min)
0.20
0.15
0.10
0.05
0.00
+DEX
PC
PC
+ ex OA
F.
Candidate
proteins
precipitated
from
PC + OA
vesicles
220
97
66
46
30
21
14
Dexamethasone
-
+

Partial Purification of Phosphatidate Phosphohydrolase (PAP-1) Protein

Since a more selective means of protein isolation was required, hydroxyapatite chromatography was used to enrich the PAP-1 enzyme activity. Cytosolic samples were prepared from dexamethasone treated primary rat hepatocytes by ball bearing homogenization. By batch adsorption, hydroxyapatite resin effectively removed PAP-1 activity from solution. Further the PAP-1 activity could not be removed by washing the resin with 70 mM potassium phosphate buffer (data not shown), whereas significant amounts of protein could be released from the resin. Dexamethasone treated rat hepatocyte cytosol was loaded onto a 3 ml column of hydroxyapatite that had been equilibrated with 10 mM DTT and 0.05% Tween-20. The column was washed with 10 ml of 70 mM potassium phosphate buffer (pH 7.4) and 1 ml fractions were collected. The column was then treated with 10 ml of 300 mM potassium phosphate buffer (pH 7.4) to elute proteins that were strongly bound to the resin. Fractions were assayed for PAP-1 activity and the majority of the activity eluted in the fourth fraction of the 300 mM potassium phosphate buffer wash. Eluates were also run on denaturing SDS-PAGE gels and silver stained to determine where the bulk of the proteins eluted (Fig. 22C). The 70 mM potassium phosphate buffer wash eluted many proteins loosely associated to the resin however, PAP-1 activity eluted with the bulk of the proteins in the 300 mM potassium phosphate buffer wash. This method led to a reproducible enrichment of enzyme activity by 24 fold.

Fig. 22. Hydroxyapatite chromatography of primary rat hepatocyte cytosol.

A, diagram of chromatography strategy for 3 ml of hydroxyapatite resin pre-equilibrated with 10 mM DTT and 0.05% Tween 20. After the addition of sample the column was washed with 10 ml of 70 mM KPO_4 and then 10 ml of 300 mM KPO_4. B, one ml fractions were collected and assayed for PAP-1 activity, the majority of the enzyme activity eluted in the first four fractions of the 300 mM KPO_4 wash and reproducibly led to a 24 fold enrichment in enzyme activity. C, fractions were run on a 10 % SDS-PAGE gel and eluted proteins were revealed by silver staining.

A.

Elution Reagents

10ml 10ml

B.

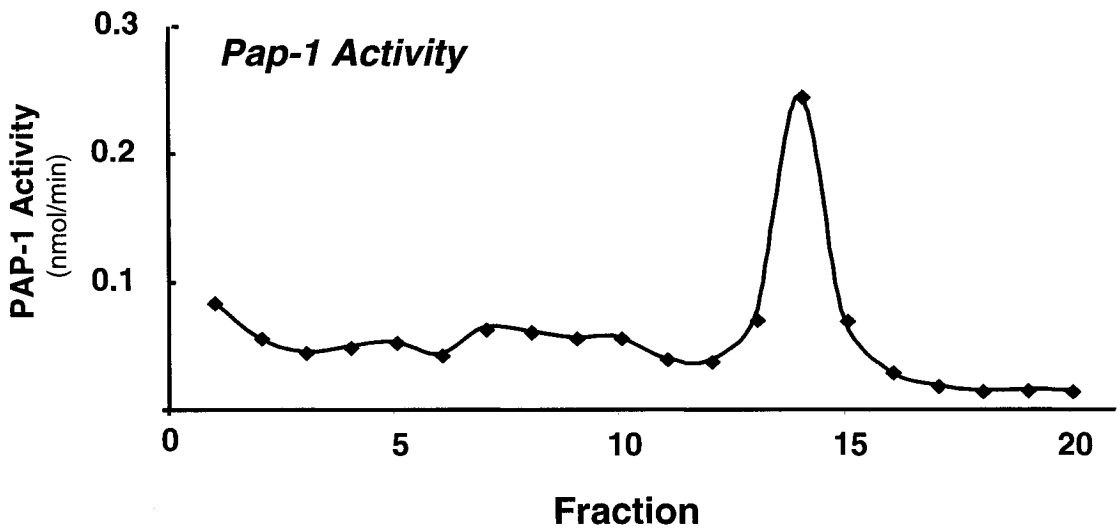

C. *Silver stain*

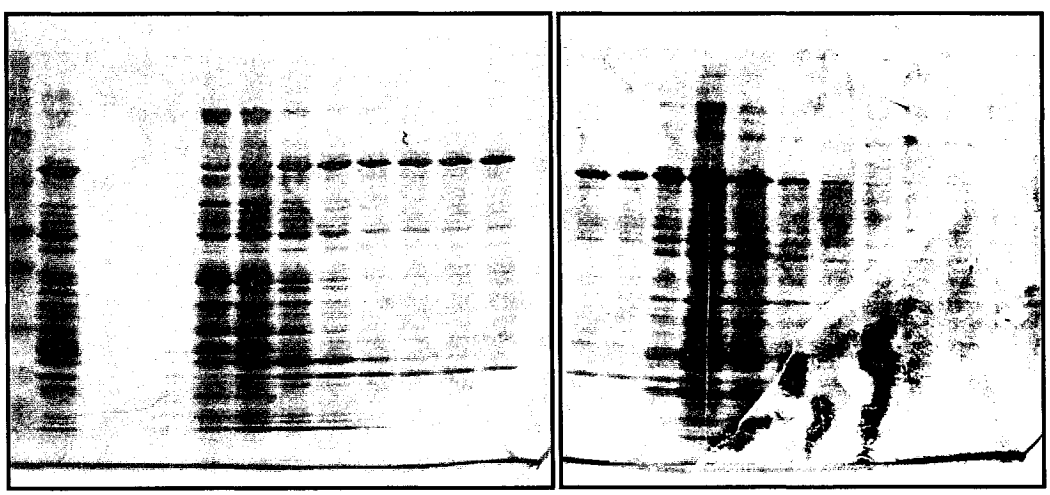

To identify proteins that were newly synthesized in response to dexamethasone, I radiolabelled the primary hepatocytes with [^{35}S]methionine/cysteine during PAP-1 induction with dexamethasone. The ^{35}S-labeled, dexamethasone induced protein did not interfere with our ^{3}H based determination of PAP-1 activity (data not shown). The ^{35}S-labeled cytosol was loaded onto the hydroxyapatite column, and was washed with 70 mM potassium phosphate buffer (pH 7.4). The column was then washed with 10 ml of 400 mM NaCl before eluting the PAP activity with 10 ml of 300 mM potassium phosphate buffer (pH 7.4) (Fig. 22A). The PAP-1 activity was no longer eluted with 300 mM potassium phosphate buffer, but there was a broad elution of PAP-1 activity in the 400 mM NaCl wash (Fig. 23B). When the fractions were run on denaturing SDS-PAGE gels and bands were revealed by fluorography, there was very little ^{35}S-labeled protein eluted in the salt wash (Fig. 23C). This observation may allow for a one step purification in which the bulk of the contaminating proteins can be removed. It is possible that the fractions eluted under the 400 mM NaCl condition may need to be pooled and concentrated for further analysis. However this approach shows the most promise for a one step enrichment before differential protein expression is compared.

Identification of Phosphatidate Phosphohydrolase by Differential Display PCR

In concert with the protein purification approach I also developed an alternate RNA based cloning strategy to identify PAP-1. If the increase in PAP-1 activity is due to an increase in gene transcription, PAP-1 might be detected using a differential display RNA screening approach. To do this, RNA was isolated from primary hepatocytes that were treated with and without dexamethasone. This RNA served as a template for

Fig. 23. Hydroxyapatite chromatography with salt elution.

A, diagram of chromatography strategy, 3 ml of hydroxyapatite resin was pre-equilibrated with 10 mM DTT and 0.05% Tween-20. Primary rat hepatocytes were labeled with [^{35}S]methionine/cysteine for 1 h and the cytosol was isolated as described in *Materials and Methods*. After the sample was added the column was washed with 10 ml of 70 mM KPO_4 and then 10 ml of 400 mM NaCl before, 10 ml of 300 mM KPO_4. B, one ml fractions were collected and assayed for PAP-1 activity, the majority of the enzyme activity eluted in a broad diffuse peak during the NaCl wash, and the enzyme elution peak was absent in the 300 mM KPO_4 wash. C, fractions were run on a 10% SDS-PAGE gel and proteins were revealed by fluorography.

A.

Elution Reagents

10ml 10ml 10ml

B.

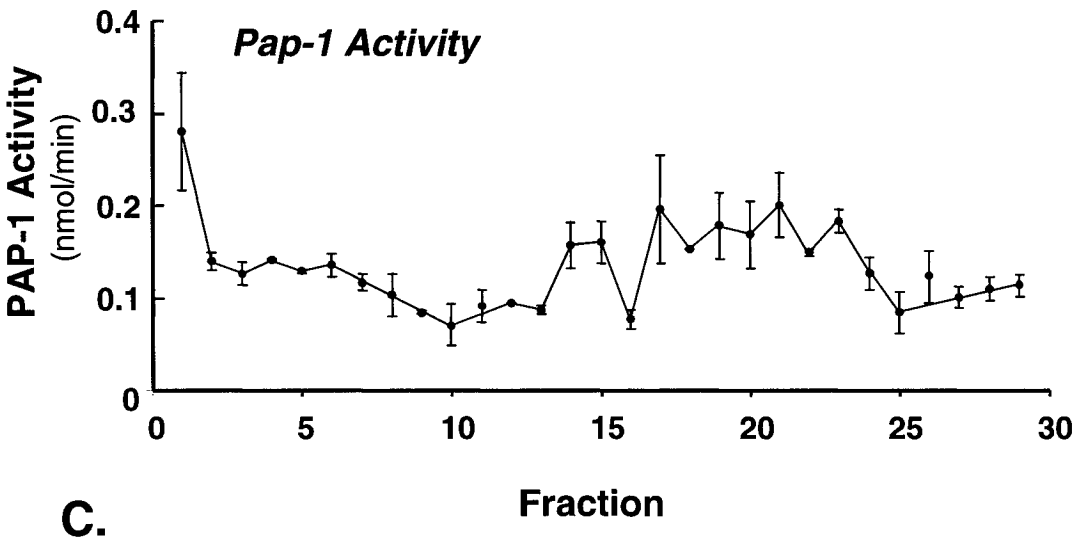

C.

^{35}S Cell lysate

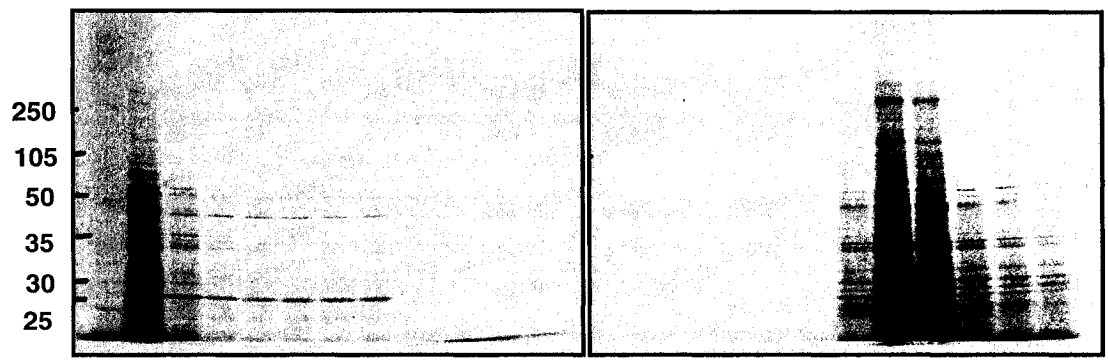

reverse transcription of total cellular RNA using three oligo dT primers that differed in their terminal 3' nucleotide. In this way cDNA templates were amplified from the cellular mRNA using 80 different degenerate 5' primers. These random primers generated PCR fragments from the entire complement of cellular RNA, since each 3' oligo dT primer was utilized with all 80 degenerate 5' primers, for a total of 240 PCR reactions. Each of these reactions was performed on samples taken from dexamethasone, insulin plus dexamethasone treated cells or cells that underwent no treatment. PCR reactions were performed in the presence of [^{33}P]dATP to label all reaction products. Candidate bands were identified as transcripts that were induced under the dexamethasone treated condition and not under insulin treated or basal conditions (Fig. 24A). Data was generated on all 240 sets of primers and 162 potential bands were identified. These candidate bands were individually excised and PCR amplified before being cloned into pGEM-T (Fig. 24B). The resulting clones were confirmed by excising the fragment and were sequenced bi-directionally to obtain the insert sequence.

Thirty five candidate sequences derived from the PCR cloning were subjected to BLAST searches, against the NCBI Pubmed NIH database (Bethesda MD). Searches were first conducted against the existing EST databases, in an attempt to extend the length of the unknown sequence (Fig. 24C). The average fragment size was 172 nucleotides, which was too short to search directly against the genomic databases. To extend the size of these sequences, I developed a "virtual sequence extension approach" (Fig. 24C). To do this, I first matched the sequence against an EST sequence using a standard blast search. EST's were considered "a match" when a region of greater than

Fig. 24. Differential display PCR cloning of dexamethasone induced hepatocytes.

A, primary rat hepatocytes were treated with 1 μM dexamethasone, 1 μM dexamethasone and 100 nm insulin or untreated (no Tx) for 4 h. Total RNA was extracted by Triazol method and reverse transcription reactions were performed. mRNA was then PCR amplified with degenerate primers obtained from Genehunter in the presence of 0.2 mCi $\alpha[^{32}P]$dATP. PCR samples were resolved on 6% denaturing acrylamide gels and bands were visualized by fluorography. Candidate bands were present in the dexamethasone treated condition. B, candidate bands were cut and PCR amplified before inserting into pGEM-T easy using a TA overhang strategy. Sequences were obtained bi-directionally from T7 and Sp6 promoter sites. C, the trimmed sequence was subjected to Blast searching on the NCBI database (Bethesda MD.) EST clones that matched with high homology (>95 %) were aligned using NCBI Pair wise Blast algorithms to ensure that the match corresponded to the 3' end of the sequence. The identified EST was then used to search the human genome for predicted gene sequences, and when positive hits occurred NCBI Pair wise Blast was used to align the 3' end of the predicted sequences.

A.

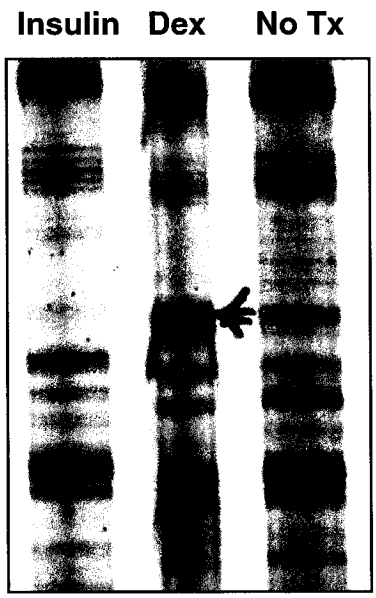
Insulin
Dex
No Tx

B.

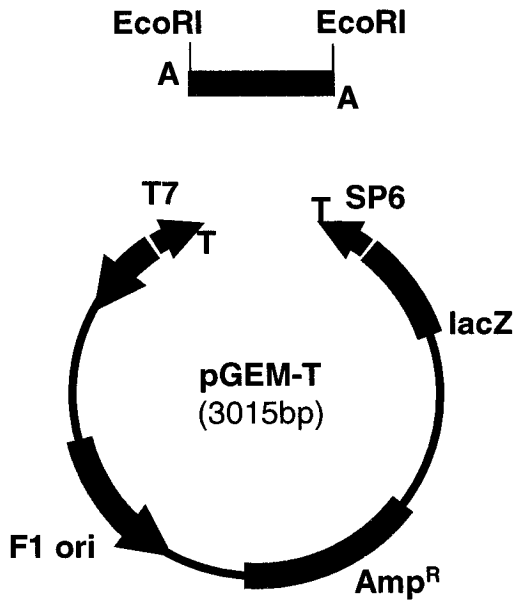
EcoRI
EcoRI
A
A
T7
T
SP6
T
lacZ
pGEM-T
(3015bp)
F1 ori
Amp^R

C.

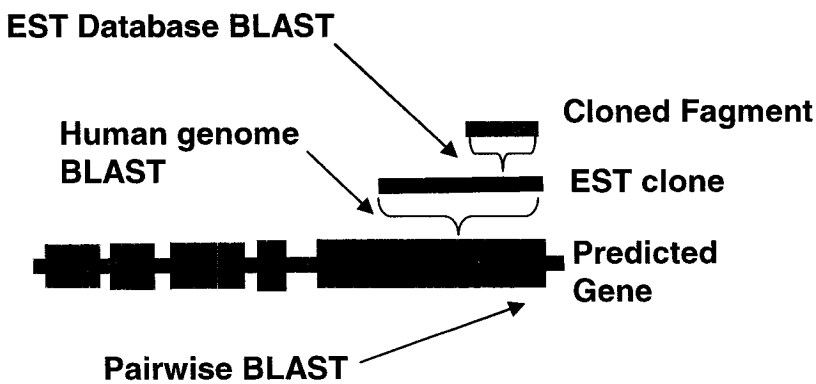
EST Database BLAST
Cloned Fagment
Human genome
BLAST
EST clone
Predicted
Gene
Pairwise BLAST

100 nucleotides matched at >95% identity. Typically the length of the clone was increased two to six-fold using this EST extension strategy. All four annotated EST databases were searched manually with each sequence (as shown in Fig. 25A). Tabulated examples of the results are shown in Figure 26A, where the effectiveness of various EST databases becomes apparent. These extended sequences were then used to search the human, mouse and yeast genomes directly. I developed an approach which is diagrammed in Figure 25B, where the largest match from our EST searches was used to query the genomic databases. Genes that have already been identified were typically recognized at this level. Using this strategy I identified several unknown open reading frames. One such human match was the computer predicted unknown clone FLJ13448. This predicted ORF from the human genome database was matched with a 97% identity over 230 nucleotides using the EST strategy detailed above. The cloned sequence and the EST were aligned using the Pairwise blast algorithm and both aligned with the 3' tail of the FLJ14448 candidate gene. This gene encodes a protein predicted to be 27 KDa with a pI of 9.6. One sequence of 256 nucleotides showed no homology to any sequences in the database. Other anomalous results included repeatedly identifying the same insert sequence with different primer combinations or fragments that were too short to yield EST hits. Representative data is presented in Figure 26.

Phosphatidate Phosphohydrolase Summary and Significance

To date the PAP-1 protein has eluded purification, a novel cloning approach is warranted. I considered two different approaches and evaluated them for their utility in developing a differential expression approach to cloning this recalcitrant enzyme. The first approach was to use conventional enzymology methods to perform a crude

Fig. 25. Bio-informatics strategy and flow chart.

A, flow chart representing the order of searches between unknown sequence and EST databases at NCBI PubMed. B, decision flow chart to illustrate how low homology hits or regions of homology were selected or rejected based on the results of NCBI Pair wise Blast alignment analysis.

A.

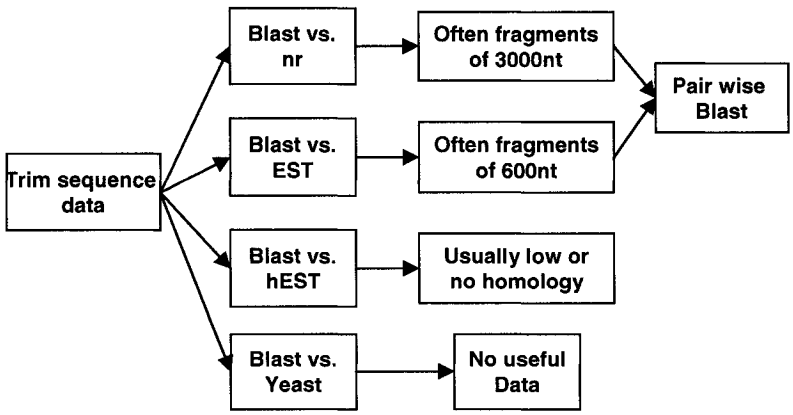
Trim sequence data
Blast vs. nr
Blast vs. EST
Blast vs. hEST
Blast vs. Yeast
Often fragments of 3000nt
Often fragments of 600nt
Usually low or no homology
No useful Data
Pair wise Blast

B.

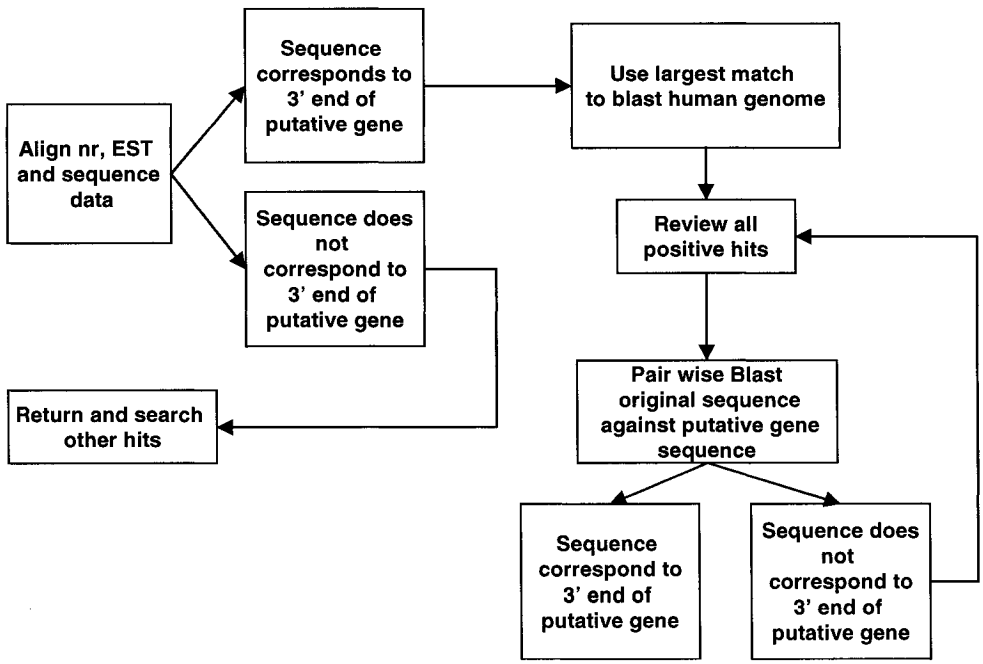
Align nr, EST and sequence data
Sequence corresponds to 3' end of putative gene
Sequence does not correspond to 3' end of putative gene
Return and search other hits
Use largest match to blast human genome
Review all positive hits
Pair wise Blast original sequence against putative gene sequence
Sequence correspond to 3' end of putative gene
Sequence does not correspond to 3' end of putative gene

Fig. 26. Informatics results.

A, tabulation of data obtained from informatics analysis of DD-PCR data. Individual sequences are described by their size in nucleotides, and the positive or negative hits obtained by Blast searching the sequence against the indicated EST databases. Where positive hits were obtained the accession number of the matching sequence is shown as well as its size and percent homology with the initial fragment. B, EST sequences were subjected to a Blast search against the human genome and predicted genes are listed. The accession number ascribed to known or predicted genes is indicated.

A.

Sequence	Fragment	Positive Blast hits					Largest Fragment		
	bp	nr	EST	mEST	yeast	hEST	accession	size	% homology
6A13-01	159	YES	YES	YES	NO	NO	AF147450	663	123/133
6A17-01	174	YES	YES	YES	NO	NO			137/150
6A17-02	304	YES	YES	YES	NO	NO	XM_131413	2977	249/274
6A17-03	313	YES	YES	YES	NO	NO	XM_131413	2977	249/274
6A17-04	285	YES	YES	YES	NO	NO	XM_123423	1859	
6A17-05	152	One	YES	YES	NO	NO	XM_148585	2043	
6A17-06	179	NO	YES	LOW	NO	NO	BQ204196	666	
							AC121664	142865	
6A20-01	293	NO	YES	Low	NO	NO	BQ194512	657	196/208
6A22-01	349	YES	YES	YES	NO	YES			
6A8-13	165	YES	YES	Low	NO	Low	S63167	2675	
6A8-23	144	YES	YES	Low	NO	Low	AF504920	1872	118/118
6A38-01	276	YES	YES	Low		NO	U31287	878	258/259
6A25-01	166	Low	YES	YES		Low			
6A31-01	170	Low	YES	YES		Low	BQ006440	762	130/141
6C17-01	152	Low	YES	YES	NO	NO	XM_148585	2043	117/131
6C17-04	256	NO	NO	NO	NO	NO			
6C17-05	123	YES	YES	YES	YES	Low	NM_009378	3636	92/98
6G18-01	135	YES	YES	YES	NO	Low	XM_009665	3045	94/101
6G20-01	253	YES	YES	YES	NO	YES	NM_013113	2528	182/182
6G21-01	233	YES	YES	YES		YES	M25160	8250	176/188
6G4-01	32								
6G4-06	32								
6G31-01	251	YES	YES	YES	NO	NO	XM_126832	5272	181/205

B.

Sequence	Chromosome	Accession	Gene
6A13-01			
6A17-01		AF326229	Translocon-associated protein alpha
6A17-02	9q31	LOC92089	similar to C2H2 zinc finger protein
6A17-03	9q31	LOC92089	similar to C2H2 zinc finger protein
6A17-04	10q24.5	BC001595	5'-nucleotidase, cytosolic II
6A17-05	3q21	AK027690	Unknown gene FLJ14784 DIRC2: disrupted in renal carcinoma 2
6A17-06			
		NM_005415	Solute carrier family 20 (Phosphate carrier)
6A20-01			
6A22-01			Na-/K+ ATPase
6A8-13	10q21		
6A8-23	Mitochondrial	AAM28878	mitochondrial ATPase synthase subunit 6 [Rattus norvegicus].
6A38-01			
6A25-01			
6A31-01	5q11.2	BQ006440	
6C17-01		XM_148585	Mus musculus similar to CG1358 gene product (LOC224132)
	3q21	AK027690	Unknown gene FLJ14784 DIRC2: disrupted in renal carcinoma 2
6C17-04			***No matches in any database
6C17-05	20p11.1	XM_009595	thrombomodulin (THBD)
6G18-01	20q12	AF134157	MAFB v-maf musculoaponeurotic fibrosarcoma oncogene homolog B (avian)
6G20-01	4p14-p12	AF067820	ATPase II type 8A; putative aminophospholipid transporter
6G21-01	1q23		
6G4-01			***Fragment is too short
6G4-06			***Fragment is too short
6G31-01	2p24.5	Hs2_4591	Lipin 1

mechanical purification and to propose how other strategies (such as precipitation or adsorption) may be combined to yield an enriched lysate suitable for differential protein expression profiling. I also evaluated the utility of a DD-PCR based cloning approach to identify this enzyme activity.

During the biochemical purification I observed a number of salient factors that should be considered for future cloning attempts. First, while the whole liver homogenates provide a material that shows detectable PAP-1 activity, this material requires significant enrichment before it can be utilized in more refined approaches . For example, without 30% $AmSO_4$ precipitation and a secondary washing step, this material did not separate from other proteins by hydroxyapetite chromatography. Despite several attempts to clean up this material I repeatedly observed that this lysate would yield diffuse elution peaks or simply would not absorb properly to the resin. This is probably due to the fact that the lysate contained far more contaminating proteins than samples obtained from cytosolic lysates of primary rat hepatocytes. Also cell culture lysates produced by ball bearing homogenization are highly uniform emulsions which perform well for chromatography, which is not the case for suspensions produced by Dounce homogenization from whole liver tissue.

The major advantage of using primary rat hepatocytes is that the PAP activity can be differentially induced and the cell proteins can be metabolically labeled with [^{35}S]methionine/cysteine. This approach not only produced lysates that were cleaner and more amenable to various purification steps but also produced fewer candidate proteins as identified by SDS-PAGE and autoradiography. However if such material was to be used for differential expression profiling by 2D-PAGE there are two critical points to be

considered. First, the cellular lysates, and by extension the hydroxyapatite purified samples, do not provide sufficient protein for resolution in the first (IEF) dimension of 2D-PAGE gels. I tried repeatedly under many different conditions but were unable to resolve protein lysates with less than 50 μg/ml. This very high concentration of protein was present in lysates obtained from rat liver and high resolution 2D-PAGE maps were generated from this material (Fig. 18C.). The best approach would probably be to couple these two methodologies; first isolating ^{35}S-labelled proteins from a hydroxyapatite column and then combining them with unlabelled lysates from whole rat livers to allow proper separation of the radio-labeled samples. The resulting 2-D PAGE gels could then be analyzed by fluorography and dexamethasone treated and untreated samples could be directly compared. The other key advantage of metabolically labeling differentially expressed proteins is that detection of ^{35}S-labelled proteins by SDS-PAGE is below the detection levels of most current MALDI TOF mass spectroscopy analysis (personal communication Dr. Pierre Thibault NRC). To provide sufficient sample to perform this analysis silver stained rat liver homogenates will probably have to be used. This may change as technologies develop but current detection limits were a consideration.

The most promising observation made by this work is that the elution of PAP-1 from hydroxyapatite chromatography yields a reproducible 24-fold enrichment of enzyme activity. In elution experiments where NaCl was used, not only did PAP-1 activity no longer elute from the resin with the bulk of proteins in 300 mM KPO_4 wash but there was a diffuse release of PAP-1 activity that eluted throughout the NaCl wash (Fig. 23B.). This suggests that specific PAP-1 elution may be possible without eluting other cytosolic proteins from the resin. There are a couple of considerations to be made

about this observation. Since the eluted activity of PAP-1 was diffuse across the NaCl wash, a more sophisticated chromatography technique will need to be employed to concentrate the sample, namely the use of NaCl gradients. It is possible that the use of a salt gradient alone may provide a less diffuse elution profile and a more concentrated PAP-1 sample. Also it would be important to evaluate approaches where the PAP-1 activity from these fractions could be pooled and concentrated. Since the elution may result in a very dilute sample, protein concentration techniques would undoubtedly need to be employed. Our observation that PAP-1 activity was adsorbed and precipitated on PC liposomes in the presence of OA may provide a novel technique whereby this diffuse activity could be concentrated.

In conclusion, this protein purification methodology is preferred for several reasons. The ability to track enzyme activity through the various purification steps ensures that the protein still remains and is active after any given purification step. Also the ability to metabolically label dexamethasone induced primary rat hepatocytes provides a clear and sensitive sample for any subsequent protein expression profiling. However the major weakness of this approach is that while cellular samples provide much cleaner and co-operative materials, there is likely not sufficient protein to be evaluated directly by mass spectroscopy. For this reason any hepatocyte protein purification approach will have to be combined with whole liver lysates to provide enough materials for analysis and identification of candidate proteins. It is reasonable to suspect that with future improvements in Mass Spectroscopy smaller samples will be resolved. However any approach that uses radio-labeled samples would not be favored

by mass spectroscopy operators since the sample would contaminate their apparatus (personal communication).

In concert with this protein purification approach, our dexamethasone induction experiments suggest that RNA may be a suitable template for a DD-PCR based cloning approach. Our intention was to determine whether the expression profiling approach by DD-PCR was feasible in that it lead to detectible differential increases in specific mRNAs in response to dexamethasone and insulin. Also I wanted to determine whether the number of candidate gene products was practical for a shotgun cloning approach. Finally I needed to determine whether informatics on these sequences could yield meaningful data that would suggest further experimentation was warranted. Of 162 target sequences identified by this approach the average size of these fragments was 172 nucleotides. Since these sequences were fairly short, a bioinformatics approach was adopted that used these fragments to probe the NCBI EST libraries for high fidelity matches. By setting a very high confidence limit for these small cloned fragments (>95% identity) surprisingly many corresponding EST's were identified. Despite the fact that the transcripts were produced from rat tissue high confidence hits were made within the non-repetitive EST database on human sequences (Fig. 24A). Similar results in the Yeast EST database were not obtained, and no hits were found with confidence limits >50%. This suggests that the nucleotide difference between yeast and mammalian transcripts is too dissimilar to attempt a direct comparison at this level. The EST matches (human or rat) of 500 nucleotides or greater were then used to perform BLAST searches of the human and mouse genomes. I found that at this level some EST sequences yielded multiple hits in the human genome on different chromosomes. These multiple hits

occurred in both known and unknown regions of the genome. With some EST's very high homology hits were made in regions of known or predicted genes (two examples are discussed above). When these hits were made, the unknown sequences were subjected to pair wise blast alignment against both the EST and the small cloned fragment to determine whether the sequences corresponded to the 3' terminus of the predicted gene. While this did occur in a few of the fragments studied, most were not resolved by this methodology. To confirm that predicted sequence is in fact expressed in response to dexamethasone treatment, differential expression profiling would have to be performed. This could be achieved by performing RT-PCR on dexamethasone treated RNA samples employing primers designed against the predicted EST sequences and unidentified gene sequences revealed by the BLAST searches. If this type of experiment were performed it would validate the primer extension strategy and the use of matching EST sequences as the templates for genome wide searching.

In conclusion, DD-PCR produced a feasible number of candidate genes for shotgun cloning. However the average fragment size was very short (< 200 NT) and larger inserts would increase confidence levels for further bioinformatics. Future experiments with this labor intensive methodology requires higher quality mRNA preparations. While it is possible that such a strategy could yield a hit on a gene in the human genome that corresponds to an unknown phosphatase, in the author's opinion this is unlikely. For this costly approach to be justified, further proofs should be required that the mRNA encoding PAP-1 was in fact present in these preparations. This could be achieved by reconstituting the activity through an in-vitro translation system. Perhaps this could be achieved through a shotgun expression approach where enzyme activity is

reconstituted from isolated or fractionated mRNA samples. Conversely perhaps a shotgun knock out strategy could be employed where iRNA fragments are developed against all sequences generated by differential cloning. These iRNA fragments could then be reintroduced *en masse* into PAP-1 expressing cells, and monitored for their ability to disrupt enzyme activity. Also the bioinformatics tools available did not lead to an unambiguous alignment between cloned fragments and known genes. This makes an unequivocal identification of genes by this approach not possible. Thus, future approaches must remain more closely linked to the detection of PAP-1 enzyme activity, or be focused on more unbiased identification of gene expression induced by dexamethasone treatment of primary hepatocytes. From the outset there are two important concessions about this strategy. Despite the fact that dexamethasone induced PAP-1 activity is abolished by treatment of the cells with α-amanatin and cyclohexamide, it does not mean that PAP-1 transcription and translation are required for the detected increase in activity. It is possible that a post translational modification leads to the dexamethasone mediated increase in PAP-1 activity. It is also possible that a co-factor, perhaps a kinase or phosphatase, is transcribed and translated in response to dexamethasone induction. If this is the case the levels PAP-1 mRNA would not change and therefore PAP-1 mRNA would be undetectable by this approach. To date I have not developed an effective control for this possibility and it is therefore an obvious limitation of our approach.

Chapter 5 Discussion

Cardiovascular disease remains the leading cause of death in North America. Many researchers had hoped that with the advent of the 'statin' family of drugs, major decreases in mortality would be achieved. Now 17 years after the introduction of these cholesterol reducing drugs the prevalence of this disease has not markedly decreased. In fact keeping patients on these drugs has proven to be a major obstacle in the treatment of CVD [151]. Conventional wisdom has taught that the key to reducing morbidity is to reduce a patient's LDL cholesterol (LDL-C) levels. However growing evidence suggests that in fact apoB levels and not LDL-C levels are a better predictor of clinical outcome [105]. This is due in part to the fact that measurement of apoB levels is an indicator of not only cholesterol rich LDL particles but also TG rich VLDL particles. Increasing evidence suggests that these TG rich VLDL particles are a significant risk factor for CVD. This is due in large part to the fact that the catabolism of these particles leads to the formation of small dense LDL particles. Some researchers are pressing for a quantification of small dense LDL to be included in the diagnostic criteria of FCHL [152]. To date the evaluation of hyperlipidemia has focused on effects mediated by or defects in the function of the key protein apoB.

Recombinant Expression of Apolipoprotein C's in McA-RH7777 Cells

Our work differs from the present thinking on hyperlipidemia, which focuses on aberrant apoB levels, this work described a hyper-TG normo-B phenotype. The major finding of this work is that the recombinant expression of human apoC-III in McA-RH7777 cells leads to a dose dependent increase in TG secretion (Fig. 7). Interestingly

this is not accompanied by an increase in apoB synthesis or secretion (Fig. 11). This increase in TG production was also only apparent when cells are supplemented with exogenous oleate (Fig. 6). This is similar to a metabolic state where elevated circulating FFA leads to an over production of LpB [153]. Overproduction of apoB may be brought on by insulin insensitivity or dietary state elevating the circulating FFA levels, this is detected clinically in some FCHL patients. In FCHL overproduction of LpB can manifest in two different forms [105]; some patients display elevated total apoB in the plasma, suggesting more particles in the circulation, while others produce large TG-rich particles. The first phenotype is commonly referred to as hyper-apoB, hyper-TG. In the second case there is an elevation of TG without an increase in circulating apoB levels. This is termed a hyper-TG normo-B phenotype. These two phenotypes were evaluated in the transfected McA-RH7777 cells by monitoring the synthesis and secretion of apoB by metabolic labeling. Since I detected no difference in the rates of synthesis and secretion of apoB between apoC-III transfected and control cells (Fig. 11), the phenotype detected in apoC-III transfected McA-RH7777 cells was hyper-TG normo-B.

There is growing evidence to support the observation that large TG rich VLDL particles are metabolized in the circulation to small dense LDL particles [154]. This is due in part to the actions of cholesterol ester transfer protein, which preferentially loads the core of these particles with FC [155]. This generates an LDL particle smaller in size but very cholesterol enriched [156]. Other researchers have proposed that small dense LDL particles become TG enriched [157]. These particles are very atherogenic, and because of their small size may be capable of penetrating the sub-endothelium and initiating or exacerbating plaque formation.

To examine the intracellular effects of apoC-III expression, fractionation experiments were performed which would determine the distribution of radio-labeled protein and lipid between the microsomal membrane and lumen (Fig. 12). It has been proposed that VLDL assembly requires the association of apoB with the membrane. Thus I evaluated the distribution of apoB between lumen and membrane and found no difference. I also evaluated the distribution of ^{14}C-labeled lipids and found that there was an increase in the membrane associated TG and CE in apoC-III expressing cells while the distribution of PC, PE and PA remained unchanged (Fig 12C). This suggests that apoC-III may allow the microsomal membrane to enlarge its neutral lipid content, while not affecting the association of apoB with the membrane.

Since apoC-III protein expression is capable of driving TG-rich VLDL assembly, under OA supplemented conditions, apoC-III may serve as a unique diagnostic marker for identification of hyper-TG normo-B FCHL patients. This may lead to an increased susceptibility in some patients of an overproduction of VLDL when circulating FFA is high. Or the over-expression of apoC-III may increase the intracellular stores of TG. For the clinician it is impractical to fractionate a patient's LpB to determine an accurate phenotype, but together analysis of total TG, total apoB and apoC may allow for more precise diagnostic criteria. Thus measurement of apoC levels may prove to be a marker of the presence of small dense LDL, even when profiling a patient's lipoproteins is impractical.

To progress farther, better assays for rapid determination and quantification of particle size and composition are required. Ideally this methodology would be applicable to not only the laboratory but also the clinical setting. A proposal for the separation of

lipoprotein fractions by FACS sorting is included in the *Future Directions* section. This work has also shown that the identification of constituent proteins required for VLDL assembly, particularly the second step assembly, remains unknown and their characterization may implicate the mechanism whereby final lipid loading and particle assembly occurs. In the case of the apoC proteins the presence of a tilted peptide motif, similar to that of HIV fusogenic peptides might lead us to speculate that the mechanism of apoC function is through a fusion event between the nascent lipoprotein particle and a TG engorged Golgi membrane [28]. Within apoC-III there is an asymmetrically distributed region of hydrophobic residues near the N terminus (6-20), that is reminiscent of the tilted peptides which are responsible for membrane fusion as exemplified by the HIV fusion peptide [158]. ApoC-III has been demonstrated to increase liposome fusion through this domain by *in vitro* fluorescence assays [159]. It is also possible that this domain assists in mobilizing TG for assembly into VLDL particles.

Phosphatidate Phosphohydrolase Experimentation

For many years purification of this enzyme has hinged on the use of plant or animal tissue [142]. The discovery by Brindley and colleagues that the alcohol fed rat liver could serve as a source of material for PAP-1 purification was clearly an advance in its time [127]. However work presented here clearly shows that this material is inferior to metabolically labeled cell lysates ([^{35}S]methionine/cysteine) or sub fractions obtained from cell culture sources. Furthermore, Brindley has also shown that dexamethasone will induce PAP-1 activity in rat hepatocytes. This thesis presents for the first time the use of material from metabolically labeled, dexamethasone treated isolated primary hepatocytes coupled to chromatographic purification methods. This approach is concluded to be the

most promising for the future purification of this enzyme, when compared to modern approaches (chromatography, 2-D or DD-PCR). Obviously the current work was limited by the lack of local chromatographic expertise, but the use of labeled material from cell culture has clearly been shown superior to whole tissue preparations. Hopefully future attempts at purification will use this seminal observation to markedly improve the sensitivity of any subsequent chromatographic approach. Metabolic labeling will reveal proteins undetectable by protein staining because of its increased sensitivity.

The experiments on PAP-1 in rat liver demonstrated an 8 fold increase in activity in response to dexamethasone. Our laboratory has previously demonstrated that the treatment of rat hepatocytes with dexamethasone leads to an increase in VLDL secretion[160]. Experimentation revealed that the most robust technique for purification of the PAP-1 activity was the use of hydroxyapatite chromatography. This method produced a reproducible enrichment of PAP-1 activity of 24-fold. Also when the sample was eluted with 400 mM NaCl, PAP-1 activity eluted in a broad diffuse peak, suggesting that refinement of this approach may yield even greater enzyme enrichment. PAP-1 was also shown to adsorb and precipitate on PC liposomes when exogenous oleate was added. This observation could be exploited to further concentrate chromatograpy eluate. Finally, if samples were prepared from metabolically labeled primary rat hepatocytes, the eluate could be recombined with cold material isolated from total rat liver to allow clean isoelectric focusing. Samples from dexamethasone induced and un-induced lysates prepared in this way could be compared by 2D PAGE and differentially expressed proteins could be excised for Mass Spectrometry.

Fig. 27. PAP-1 Identification strategy.

A, diagram of PAP-1 cloning using metabolic labeling (^{35}S-methionine/cystiene) in the presence or absence of dexamethasone (Dex). Samples would be partially purified and subjected to 2-D PAGE. Potential proteins would be identified by their presence in the dexamethasone induced 2-D autoradiogram (or increase in expression level). The candidate proteins would be excised and subjected to MALDI TOF MS. B, alternative differential expression approach using ^{14}N4-Arg (-Dex) or ^{15}N4Arg (+Dex) labeling conditions. Samples would be mixed (1:1) and partially purified using hydroxyapatite or other chromatographic methods. The sample would be digested with trypsin and subjected to LC-MS. Proteins unaffected by dexamethasone treatment would show no change in relative intensity, the +Dex peak would be shifted slightly to the right. In the case of proteins induced by dexamethasone the right shifted peak would increase in relative intensity in comparison to the -Dex (left peak). Samples showing an increase in relative intensity in response to dexamethasone treatment would be subjected to further analysis for peptide (and protein) identification. C, this approach could be expanded by performing a dexamethasone induction time course, where ^{12}C6^{14}N4-Arg, ^{13}C6^{14}N4-Arg, ^{13}C6^{14}N4-Arg, represent T=0, 5, 15 min respectively. After labeling samples would be mixed, partially purified by hydroxyapatite (and or other methods) then digested with trypsin and subjected to LC-MS. Proteins that follow the dexamethasone induction pattern of PAP-1 activity could then be identified.

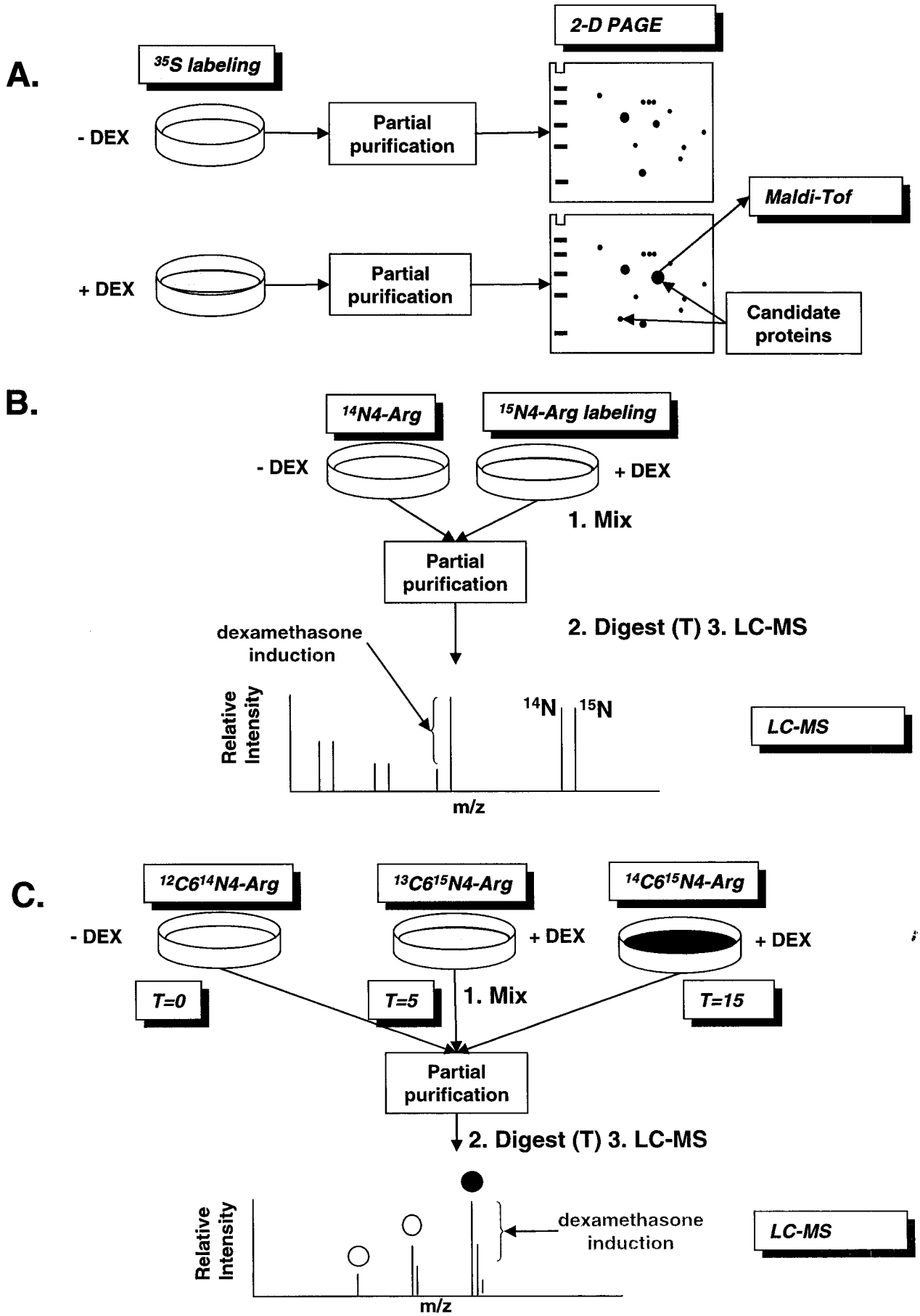
A.
35S labeling
- DEX
Partial purification
2-D PAGE
+ DEX
Partial purification
Maldi-Tof
Candidate proteins
B.
14N4-Arg
15N4-Arg labeling
- DEX
+ DEX
1. Mix
Partial purification
2. Digest (T) 3. LC-MS
dexamethasone induction
Relative Intensity
14N
15N
m/z
LC-MS
C.
12C614N4-Arg
13C615N4-Arg
14C615N4-Arg
- DEX
+ DEX
+ DEX
T=0
T=5
1. Mix
T=15
Partial purification
2. Digest (T) 3. LC-MS
Relative Intensity
dexamethasone induction
m/z
LC-MS

Metabolic labeling using ^{35}S-methonine/cystiene in the presence and absence of dexamethasone, and resolving partially purified proteins by 2-D PAGE for differential expression (Fig. 27 A), has a number of drawbacks that have been discussed above. A more promising approach using the metabolic labeling and fractionation approaches described here could be adapted for LC-MS (Liquid Chromatography-Mass Spectroscopy) [161]. Primary rat hepatocytes could be labeled with ^{14}N4-Arg[3] (-Dex) or ^{15}N4Arg (+Dex), then samples would be combined, homogenized by ball bearing homogenization and cytosolic extracts could be prepared. These extracts would then be partially purified using hydroxyapatite chromatography as discussed above, (with or without additional enrichment steps as in [161]) the combined enriched cell fractions would be dialyzed and digested with trypsin then subjected to LC-MS (Fig 27 B). Peptide peaks that show an increase between ^{14}N4-Arg labeled samples and ^{15}N4Arg labeled samples could then be sequenced as candidate peptides of PAP-1. Further refinement of this approach could be made by performing careful time course experiments first examining the induction of enzyme activity of PAP-1 in primary rat hepatocytes by dexamethasone. Once a precise time course of PAP-1 induction has been established metabolic labeling for LC-MS time course could then be employed. Time points corresponding to 0, 5, and 15 min in the presence of dexamethasone for example could be labeled with ^{12}C6^{14}N4-Arg, ^{13}C6^{14}N4-Arg, ^{13}C6^{14}N4-Arg respectively. Again samples would be combined, subjected to ball bearing homogenization and the cytosolic fraction would be isolated. This fraction would be further partially purified using hydroxyapatite purification (and or other methods) then would be dialyzed and digested with trypsin and subjected to LC-MS (Fig. 27C). Peptide fragments that match the enzymatic activity induction time course

[3] These reagents are available from Cambridge Isotope Laboratories

could then be sequenced as candidate peptides of PAP-1. This time course induction approach could be reversed using inhibitors of PAP-1 such as BEL or insulin, and again comparing the decrease in enzymatic activity profile to the profiles detected by LC-MS candidate peptides of PAP-1 could be identified by corresponding dose or time curves. Such inhibitors would need to be evaluated as in Figure 20 C. above to determine if they indeed inhibit at or before the translational level.

Other techniques such as DD-PCR were also evaluated for their utility in detecting differentially expressed proteins in the dexamethasone induced hepatocyte model. This approach yielded a reasonable number of fragments for shotgun cloning. However the size of the RNA fragments led to ambiguity in identifying the induced genes within the expression profile. To improve this approach longer RNA fragments would have to be prepared using more careful isolation methods. Also until one of these fragments is demonstrated to possess a PAP-1 activity the entire process may not be moving closer to the enzyme of interest.

There is much debate in the apoB field as to the importance or necessity of exogenous FFA for apoB containing lipoprotein secretion. Some researchers believe that nascent lipoprotein assembly can be achieved with pre-existing stores of TG and PL [162]. It is also unclear as to what if any the intracellular effect of OA may in fact be. Many researchers believe that oleate serves as a substrate for TG synthesis and is therefore necessary for TG rich particle formation [163]. Others have shown that it is PC turnover which is required for VLDL production and that the oleate somehow stimulates lipid turnover [164]. FFA has also been proposed to act as a signal for nuclear factors through the actions of liver fatty acid binding protein (LFABP) [165]. Interestingly one of the proposed

targets of oleate is the PPAR transcriptional factors which can influence the transcription of apoC-III [166]. Our work utilized apoC-III under the control of a constitutively active CMV promoter and I have shown that expression of apoC-III alone is not sufficient to increase TG secretion. Thus our work would seem to support the idea that there is another role for oleate in stimulating particle secretion. One other effect of FFA is to stimulate the intracellular translocation of enzymes to the surface of the ER. In this way some lipid synthetic enzymes are recruited to intracellular membranes. I found that PAP-1 may be capable of this sort of recruitment (Fig. 21), since *in vitro* assays detected a movement of enzyme activity onto artificial membranes [167]. If PAP-1 is important for TG synthesis it has been speculated that the recruitment and activation of this enzyme may be important for VLDL assembly [94;165].

The dependence of the transfected McA-RH7777 cells on OA is interesting in the context of the JCR:LA (cp/cp) corpulent rat [168]. This animal displays an overproduction of TG-rich VLDL which results from elevated circulating levels of FFA. In this case it has been postulated that the overproduction of VLDL is driven by TG availability [169]. This would fit with our data where cellular ^{3}H-TG levels are elevated (Fig. 9) and the rate of ^{3}H-TG production is also increased (Fig. 8A). Furthermore when ^{14}C-labelled OA was used I also detected an increase in cellular ^{14}C-TG that may reflect the driving force behind increased VLDL production. If oleate serves as an important substrate for PAP-1 production of TG then, this could explain why exogenous oleate is a requirement for the increased VLDL secretion. Thus substrate availability is a limiting factor in the production of LpB, a fact that has already been demonstrated for phospholipids [91].

To date only apoB and MTP have been shown to be obligatory constituents for VLDL assembly. This has been supported by studies in which the reintroduction of these two proteins into heterologous cell systems is sufficient to allow LpB particle formation and secretion [59]. An important caveat of this work is that large apoB truncates (>B48) secreted particles that reach only intermediate density. It would appear that these two proteins alone are capable of achieving first step assembly but not the second step. This is important since the particle buoyant density of LpB is a determinant of clinical outcomes. Thus an understanding of the additional factors required for second step assembly has now come of age. In determining the proteins required for second step assembly new targets for pharmaceutical intervention may become apparent. Since current statin therapy involves the disruption of endogenous cholesterol synthesis there is serious concern about the long term side effects of these drugs. By approaching auxiliary factors as a target, a more refined alteration of patient lipoprotein profile may be possible and such interventions might show improved patient compliance. Since VLDL production is sensitive to glucocorticoid treatment, the identification of novel protein factors may be possible by differential screening approaches. The preliminary work presented here suggests that PAP-1 activity is increased by this approach. It is also possible that other co-factors are produced during this activation which could be identified by DD-PCR methodologies. It is possible that other methodologies should be considered for the isolation of this activity.

Future Directions

While familial hyperlipidemia remains the most prevalent lipid disorder it is also present in up to 20% of all patients who perish from an acute coronary event [170].

Inaccurate diagnosis of FCHL patients has also plagued the attempts to establish genetic linkage, since total cholesterol levels and TG levels can vary greatly between sample collections [171]. Composition of lipoproteins is recognized to be a better determinant of CVD than conventional lipid measures [172]. Measurements of apoC-III levels in human plasma are not frequently made in a clinical setting. However apoB and apoA-I levels are readily and frequently monitored [172].

The establishment of conclusive linkage between apoC-III polymorphisms and CVD in women has been particularly affected by aberrant data [173]. It is possible that one of the reasons that the linkage between apoC and FCHL has been hampered is the interference of apoC levels in patients taking oral contraceptives. Since women who take oral contraception have an elevated circulating apoC-III level perhaps this drug interaction is masking apoC-III familial linkage in the female population [51]. Further when post menopausal women are evaluated the correlation between apoC gene polymorphisms and cardiovascular disease re-emerges [174]. Also noteworthy is that the effect on apoC-III levels seen in men in response to smoking and drinking is not evident in pre-menopausal women, again perhaps due to a masking effect of the drug [51]. It might be worthwhile to revisit these data and exclude patients that were taking oral contraceptives.

Since the distribution of LpB is now proving to be important in clinical treatment new methods for rapid determination of lipoprotein density are indicated. Conventional methods such as rate floatation ultracentrifugation are too costly and time consuming to use in clinical practice. Methods such as flow cytometry show great promise for the rapid separation and lipid profiling of patient samples. This technology can now separate

particles as small as 50 nM which could allow the sorting of individual lipoprotein particles. Particles may be classified based on size by simply determining the forward scatter (Fsc) as the particle passes the detector, and it is also possible that the side scatter (Ssc) or orthogonal scatter may provide meaningful data about individual particle composition [175]. Since these lipoprotein particles contain a single apoB molecule FACS sorting could employ currently available monoclonal antibodies to fluorescently detect individual lipoproteins. Further such an approach would allow the sorting of particles based on the presence of other surface accessory proteins (such as apoC-III) which are removed by current ultracentrifugation methods. Once sorted these particle fractions could be assayed directly for lipid components or be coupled to a tandem mass spec for unparalleled detail in patient lipid profiling. Since FACS technology is currently available in many diagnostic laboratories such a methodology could be rapidly implemented for improved physician diagnosis.

Statement of Collaboration

The figure showing secreted apolipoproteins in primary and McA-RH7777 cells was generated by Dr. Yao. The interest in apoC-III involvement in VLDL assembly has been a long term project in the Yao lab. ApoC-III mRNA isolation from transfected cells for Northern blotting was performed by Ph.D. student Jay Wang and summer student Shermin Rahimkhani. Kinetic data on apoC-III lipid secretion was produced by Jay Wang and Shermin Rahimkhani. Lipid secretion experiments from mixed culture experiments were performed by Mr. Shermin Rahimkhani. The phylogeny comparison was suggested by Dr. Hong-Yu Zhang, but the T-Coffee analysis presented in the paper was performed by the author. Some of the experiments where PAP-1 activity was determined in primary rat hepatocyte cells were performed on cells that were isolated by our technician Jenny Shan. RNA for DD-PCR on dexamethasone induced hepatocytes was prepared by Post Doctoral Fellow Dr. Khai Tran, and PCR reactions were performed by Ms. Jennifer Raven, a summer student in our laboratory. Alcohol fed rat livers were produced by Dr. David Brindley (University of Alberta). All other experiments described in this work were performed by the author.

Curriculum Vitae
Philip Harold Links

Distinctions and Awards:

1991 Invitation and interviewed for Moorehead Scholarship (This is the top entrance award offered by UNC $40,000 for combined leadership academics and athletics).
1992 Government of Saskatchewan Scholarship (Academics)
1993 Copp Family Scholarship Award University of Alberta ($2,500) This is the top entrance award offered by the University of Alberta for combined Athletics Academics and Community Leadership.
1993 Canada Scholar ($2,000) National Scholarship for Academics
1994 Summer Studentship, University of Alberta Heritage Medical Research Center
1994 Runner up, University of Alberta Medical Student Research Day, Oral Research Presentation
1995 Summer Studentship, University of Ottawa Heart Institute
1997 Medical Research Council of Canada Studentship ($19,000 /yr)
1998 Merk Frostt Award for Best Basic Research Presentation, University of Ottawa Heart Institute Research Day
1999 Best M.Sc. Student, University of Ottawa Department of Biochemistry poster presentation
1999 University of Ottawa Teaching award, Teaching Assistant of The Year
2000 Runner up Merk Frostt Award for Best Basic Research Presentation, University of Ottawa Heart Institute Research Day
2000 Runner up University of Ottawa Department of Biochemistry poster presentation
2000 Runner up University of Ottawa Department of Pathology research day
2001 Heart and Stroke / Canadian Institutes of Health Research national doctoral research award, national rank 57 / 409 ($26,000 /yr)
2001-2004 University of Ottawa excellence scholarship ($15,000 /yr)
2004 IUBMB/ASBMB Award for doctoral work presented at international annual meeting in Boston
2004 University of Ottawa post graduate travel award.

Teaching Positions:

1997-2001 Laboratory Instructor, University of Ottawa Department of Biochemistry

Society Memberships:

IUBMB/ASBMB	American Society for Biochemistry and Molecular Biology
ASCB	American Society for Cell Biology
RPSG	The Royal Philosophical Society of Glasgow
SAS	St. Andrew's Society Ottawa

Curriculum Vitae
Philip Harold Links

Refereed Papers:

Links, P.H., Yao, Z.. Expression of Apolipoprotein C-III in McA-RH7777 Cells Increases the Secretion of Triacylglycerol-rich VLDL. (2004 in Preparation)

Zhang, H., **Links, P.H**. Ngsee, J.K., Tran, K., Cui, Z., Ko, K.W.S., Yao,Z.: Localization of Low Density Lipoprotein Receptor-related Protein 1 to Caveolae in 3T3-L1 Adipocytes in Response to Insulin Treatment. (2003) *J. Biol. Chem.* **279**, 2221-2230.

Links, P.H., Zha, X., Marcel, Y.:Stable Expression of Human Caveolin-1 in McA-RH7777 Rat Hepatoma Cells Leads to Increased HDL Mediated Cholesterol Efflux and Increased Cholesterol Cycling (2003 in Preparation)

McLeod, R.S., Wang, Y., Wang, S., Rusinol, A., **Links, P.,** Yao, Z. Apolipoprotein B Sequence Requirements for Hepatic very low density lipoprotein assembly. (1996) *J. Biol. Chem.* **271**, 18445-18455.

Invited Oral Presentations:

Links, P.H., Yao, Z.: *Identification of protein factors involved in VLDL assembly* (2002) President of CIHR, Institute of Circulatory and Respiratory Health's (CIHR) Advisory Board Chateau Laurier, Ottawa Ont.

Refereed Poster Presentations:

Links, P.H., Yao, Z.. New insights into the hypertriglyceridemic effect of the over-expression of the C apolipoproteins. IUBMB/ASBMB Meeting Boston USA 15-20th June (2004).

Non- Refereed Articles:

Links, P.H., Zha, X., Marcel, Y.:Caveolin-1 Expression and its Role in Cholesterol Efflux in Rat Hepatoma Cells (1998) *Molecular Biology of the Cell* **9,** 97.

Oral Presentations (not exhaustive):

Links, P.H., Yao Z.:Cloning Phosphatidic Acid Phosphohydrolase. *Biochemistry Microbiology and Immunology Seminar Series University of Ottawa.* 15 January (2002).

Links, P.H., Zha, X, Marcel, Y.:Caveolin-1 expression increases HDL mediated cholesterol efflux by increasing cholesterol trafficking (2000) *Heart Institute Research Day.* **Runner up Merk Frosst Award for Best Basic Science presentation**

Links, P.H., Burgess, J., Yao, Z., Marcel, Y.:Caveolin Expression Increases Transcytosis (1998) *Heart Institute Research Day.* **Winner of Merk Frosst Award for Best Basic Science presentation**

Links, P., McLeod, R.S., Yao, Z.: Identification of a Degradation Sequence in Human ApoB. (1994) *University of Alberta Faculty of Medicine Research Day.* **Runner Up Best Oral Presentation**

Poster Presentations (not exhaustive):

Links, P.H., Zha, X., Marcel, Y.:*Caveolin-1 Expression and its Role in Cholesterol Efflux in Rat Hepatoma Cells.* Department of Pathology and Laboratory Medicine Research Day (1999). **Winner Best Poster Presentation**

Invited Symposia:

Science and Peace Opportunities in the Middle East Baroness Greenfield Director of the Royal Institution, Oxford. Invited by Sir Andrew Burns, British High Commissioner, 11 June (2003).

Heart & Stroke Salutes Research Excellence. Chimo Hotel Ottawa Canada, 9 May (2002)

Advances in Molecular and Cell Biology of Lipids and Lipoproteins Hosted by CIHR, Astra Zenica, Merk Frosst, GSK. National Gallery of Canada July 13-14 (2002).

Conference Attendance (not exhaustive):

The Canadian Lipoprotein Conference, Chateau Laurier Hotel, Ottawa Canada (1997)

The American Society for Cell Biology 41st Annual Meeting Dec 8-12 Washington convention center Washington DC (2001)

Trainees:

Miss Andrea McKenzie
Supervised as undergraduate, she went on to receive her M.Sc.

Miss Jennifer Raven
Supervised as a co-op student from Waterloo, currently pursuing a career in biomedical science.

Bibliography

1. Dallinga-Thie,G.M., M.Groenendijk, R.N.Blom, T.W.De Bruin, and E.De Kant. 2001. Genetic heterogeneity in the apolipoprotein C-III promoter and effects of insulin. *J.Lipid Res.* 42:1450-1456.

2. Sniderman,A., K.Williams, S.Haffner, and N.Sattar. 2004. Insights from apoB: from better diagnosis & therapy to the Medusa Hypothesis. *Atheroscler.Suppl* 5:19-24.

3. Campos,H., D.Perlov, C.Khoo, and F.M.Sacks. 2001. Distinct patterns of lipoproteins with apoB defined by presence of apoE or apoC-III in hypercholesterolemia and hypertriglyceridemia. *J.Lipid Res.* 42:1239-1249.

4. Yao,Z., K.Tran, and R.S.McLeod. 1997. Intracellular degradation of newly synthesized apolipoprotein B. *J.Lipid Res.* 38:1937-1953.

5. Chan,D.C., G.F.Watts, T.G.Redgrave, T.A.Mori, and P.H.Barrett. 2002. Apolipoprotein B-100 kinetics in visceral obesity: associations with plasma apolipoprotein C-III concentration. *Metabolism* 51:1041-1046.

6. Dallongeville,J., A.Meirhaeghe, D.Cottel, J.C.Fruchart, P.Amouyel, and N.Helbecque. 2001. Polymorphisms in the insulin response element of APOC-III gene promoter influence the correlation between insulin and triglycerides or triglyceride-rich lipoproteins in humans. *Int.J.Obes.Relat.Metab.Disord.* 25:1012-1017.

7. Katoh,N. and H.Nakagawa-Ueta. 2001. Concentrations of apolipoprotein C-III in healthy cows during the peripartum period and cows with milk fever. *J.Vet.Med.Sci.* 63:597-601.

8. Ardern,H.A., G.M.Benson, K.E.Suckling, M.J.Caslake, J.Shepherd, and C.J.Packard. 1999. Apolipoprotein B overproduction by the perfused liver of the St. Thomas' mixed hyperlipidemic (SMHL) rabbit. *J.Lipid Res.* 40:2234-2243.

9. de Roos,B., M.J.Caslake, H.A.Ardern, B.G.Martin, K.E.Suckling, and C.J.Packard. 2001. Insulin resistance in the St. Thomas' mixed hyperlipidaemic (SMHL) rabbit, a model for familial combined hyperlipidaemia. *Atherosclerosis* 156:249-254.

10. van Greevenbroek,M.M., V.M.Vermeulen, and T.W.De Bruin. 2004. Identification of novel molecular candidates for fatty liver in the hyperlipidemic mouse model, HcB19. *J.Lipid Res.* 45:1148-1154.

11. Eurlings,P.M., C.J.van der Kallen, J.M.Geurts, M.M.van Greevenbroek, and T.W.De Bruin. 2001. Genetic dissection of familial combined hyperlipidemia. *Mol.Genet.Metab.* 74:98-104.

12. Groenendijk,M., R.M.Cantor, T.W.De Bruin, and G.M.Dallinga-Thie. 2001. The apoAI-CIII-AIV gene cluster. *Atherosclerosis* 157:1-11.

13. Jansen,H., D.M.Waterworth, V.Nicaud, C.Ehnholm, and P.J.Talmud. 2001. Interaction of the common apolipoprotein C-III (APOC3 -482C > T) and hepatic lipase (LIPC -514C > T) promoter variants affects glucose tolerance in young

adults. European Atherosclerosis Research Study II (EARS-II). *Ann.Hum.Genet.* 65:237-243.

14. Chan,D.C., G.F.Watts, P.H.Barrett, J.C.Mamo, and T.G.Redgrave. 2002. Markers of triglyceride-rich lipoprotein remnant metabolism in visceral obesity. *Clin.Chem.* 48:278-283.

15. Pastier,D., J.M.Lacorte, J.Chambaz, P.Cardot, and A.Ribeiro. 2002. Two initiator-like elements are required for the combined activation of the human apolipoprotein C-III promoter by upstream stimulatory factor and hepatic nuclear factor-4. *J.Biol.Chem.* 277:15199-15206.

16. Katoh,N., S.Oikawa, T.Oohashi, Y.Takahashi, and F.Itoh. 2002. Decreases of apolipoprotein B-100 and A-I concentrations and induction of haptoglobin and serum amyloid A in nonfed calves. *J.Vet.Med.Sci.* 64:51-55.

17. Waterworth,D.M., J.Ribalta, V.Nicaud, J.Dallongeville, S.E.Humphries, and P.Talmud. 1999. ApoCIII gene variants modulate postprandial response to both glucose and fat tolerance tests. *Circulation* 99:1872-1877.

18. Schweitzer,M., D.Tessier, W.D.Vlahos, L.Leiter, J.P.Collet, M.J.McQueen, L.Harvey, and P.Alaupovic. 2002. A comparison of pravastatin and gemfibrozil in the treatment of dyslipoproteinemia in patients with non-insulin-dependent diabetes mellitus. *Atherosclerosis* 162:201-210.

19. Hertz,R., J.Bishara-Shieban, and J.Bar-Tana. 1995. Mode of action of peroxisome proliferators as hypolipidemic drugs. Suppression of apolipoprotein C-III. *J.Biol.Chem.* 270:13470-13475.

20. Guo,Q., P.R.Wang, D.P.Milot, M.C.Ippolito, M.Hernandez, C.A.Burton, S.D.Wright, and Y.Chao. 2001. Regulation of lipid metabolism and gene expression by fenofibrate in hamsters. *Biochim.Biophys.Acta* 1533:220-232.

21. Carlson,L.A. and D.Ballantyne. 1976. Changing relative proportions of apolipoproteins CII and CIII of very low density lipoproteins in hypertriglyceridaemia. *Atherosclerosis* 23:563-568.

22. Wang,C.S., W.J.McConathy, H.U.Kloer, and P.Alaupovic. 1985. Modulation of lipoprotein lipase activity by apolipoproteins. Effect of apolipoprotein C-III. *J.Clin.Invest* 75:384-390.

23. Jong,M.C., M.H.Hofker, and L.M.Havekes. 1999. Role of ApoCs in lipoprotein metabolism: functional differences between ApoC1, ApoC2, and ApoC3. *Arterioscler.Thromb.Vasc.Biol.* 19:472-484.

24. Brown,W.V. and M.L.Baginsky. 1972. Inhibition of lipoprotein lipase by an apoprotein of human very low density lipoprotein. *Biochem.Biophys.Res.Commun.* 46:375-382.

25. Ginsberg,H.N., N.A.Le, I.J.Goldberg, J.C.Gibson, A.Rubinstein, P.Wang-Iverson, R.Norum, and W.V.Brown. 1986. Apolipoprotein B metabolism in subjects with deficiency of apolipoproteins CIII and AI. Evidence that apolipoprotein CIII

inhibits catabolism of triglyceride-rich lipoproteins by lipoprotein lipase in vivo. *J.Clin.Invest.* 78:1287-1295.

26. Jackson,R.L., B.H.Chung, L.C.Smith, and O.D.Taunton. 1977. Physical, chemical and immunochemical characterization of a lipoprotein lipase activator protein from pig plasma very low density lipoproteins. *Biochim.Biophys.Acta* 490:385-394.

27. Kinnunen,P.K. and C.Ehnolm. 1976. Effect of serum and C-apoproteins from very low density lipoproteins on human postheparin plasma hepatic lipase. *FEBS Lett.* 65:354-357.

28. Lins,L., C.Flore, L.Chapelle, P.J.Talmud, A.Thomas, and R.Brasseur. 2002. Lipid-interacting properties of the N-terminal domain of human apolipoprotein C-III. *Protein Eng.* 15:513-520.

29. Brewer,H.B., Jr., R.Shulman, P.Herbert, R.Ronan, and K.Wehrly. 1974. The complete amino acid sequence of alanine apolipoprotein (apoC-3), and apolipoprotein from human plasma very low density lipoproteins. *J.Biol.Chem.* 249:4975-4984.

30. Roghani,A. and V.I.Zannis. 1988. Mutagenesis of the glycosylation site of human ApoCIII. O-linked glycosylation is not required for ApoCIII secretion and lipid binding. *J.Biol.Chem.* 263:17925-17932.

31. Segrest,J.P., M.K.Jones, H.De Loof, C.G.Brouillette, Y.V.Venkatachalapathi, and G.M.Anantharamaiah. 1992. The amphipathic helix in the exchangeable

apolipoproteins: a review of secondary structure and function. *J.Lipid Res.* 33:141-166.

32. Saito,H., S.Lund-Katz, and M.C.Phillips. 2004. Contributions of domain structure and lipid interaction to the functionality of exchangeable human apolipoproteins. *Prog.Lipid Res.* 43:350-380.

33. Jong,M.C., P.C.Rensen, V.E.Dahlmans, van der Boom H., T.J.van Berkel, and L.M.Havekes. 2001. Apolipoprotein C-III deficiency accelerates triglyceride hydrolysis by lipoprotein lipase in wild-type and apoE knockout mice. *J.Lipid Res.* 42:1578-1585.

34. Elam,M.B., H.G.Wilcox, L.M.Cagen, X.Deng, R.Raghow, P.Kumar, M.Heimberg, and J.C.Russell. 2001. Increased hepatic VLDL secretion, lipogenesis, and SREBP-1 expression in the corpulent JCR:LA-cp rat. *J.Lipid Res.* 42:2039-2048.

35. Sakurabayashi,I., Y.Saito, T.Kita, Y.Matsuzawa, and Y.Goto. 2001. Reference intervals for serum apolipoproteins A-I, A-II, B, C-II, C-III, and E in healthy Japanese determined with a commercial immunoturbidimetric assay and effects of sex, age, smoking, drinking, and Lp(a) level. *Clin.Chim.Acta* 312:87-95.

36. Aalto-Setala,K., E.A.Fisher, X.Chen, T.Chajek-Shaul, T.Hayek, R.Zechner, A.Walsh, R.Ramakrishnan, H.N.Ginsberg, and J.L.Breslow. 1992. Mechanism of hypertriglyceridemia in human apolipoprotein (apo) CIII transgenic mice. Diminished very low density lipoprotein fractional catabolic rate associated with increased apo CIII and reduced apo E on the particles. *J.Clin.Invest* 90:1889-1900.

37. Jong,M.C. and L.M.Havekes. 2000. Insights into apolipoprotein C metabolism from transgenic and gene-targeted mice. *Int.J.Tissue React.* 22:59-66.

38. de Silva,H.V., S.J.Lauer, J.Wang, W.S.Simonet, K.H.Weisgraber, R.W.Mahley, and J.M.Taylor. 1994. Overexpression of human apolipoprotein C-III in transgenic mice results in an accumulation of apolipoprotein B48 remnants that is corrected by excess apolipoprotein E. *J.Biol.Chem.* 269:2324-2335.

39. Ebara,T., R.Ramakrishnan, G.Steiner, and N.S.Shachter. 1997. Chylomicronemia due to apolipoprotein CIII overexpression in apolipoprotein E-null mice. Apolipoprotein CIII-induced hypertriglyceridemia is not mediated by effects on apolipoprotein E. *J.Clin.Invest.* 99:2672-2681.

40. Tomiyasu,K., B.W.Walsh, K.Ikewaki, H.Judge, and F.M.Sacks. 2001. Differential metabolism of human VLDL according to content of ApoE and ApoC-III. *Arterioscler.Thromb.Vasc.Biol.* 21:1494-1500.

41. Havel,R.J., V.G.Shore, B.Shore, and D.M.Bier. 1970. Role of specific glycopeptides of human serum lipoproteins in the activation of lipoprotein lipase. *Circ.Res.* 27:595-600.

42. Nestel,P.J. and N.H.Fidge. 1982. Apoprotein C metabolism in man. *Adv.Lipid Res.* 19:55-83.

43. Batal,R., M.Tremblay, P.H.Barrett, H.Jacques, A.Fredenrich, O.Mamer, J.Davignon, and J.S.Cohn. 2000. Plasma kinetics of apoC-III and apoE in normolipidemic and hypertriglyceridemic subjects. *J.Lipid Res.* 41:706-718.

44. Cohn,J.S., B.W.Patterson, K.D.Uffelman, J.Davignon, and G.Steiner. 2004. Rate of production of plasma and very-low-density lipoprotein (VLDL) apolipoprotein C-III is strongly related to the concentration and level of production of VLDL triglyceride in male subjects with different body weights and levels of insulin sensitivity. *J.Clin.Endocrinol.Metab.* 89:3949-3955.

45. Le,N.A., J.C.Gibson, and H.N.Ginsberg. 1988. Independent regulation of plasma apolipoprotein C-II and C-III concentrations in very low density and high density lipoproteins: implications for the regulation of the catabolism of these lipoproteins. *J.Lipid Res.* 29:669-677.

46. Wang,A.B., D.P.Liu, and C.C.Liang. 2003. Regulation of human apolipoprotein B gene expression at multiple levels. *Exp.Cell Res.* 290:1-12.

47. Chan,L. 1992. Apolipoprotein B, the major protein component of triglyceride-rich and low density lipoproteins. *J.Biol.Chem.* 267:25621-25624.

48. Ludwig,E.H., B.D.Blackhart, V.R.Pierotti, L.Caiati, C.Fortier, T.Knott, J.Scott, R.W.Mahley, B.Levy-Wilson, and B.J.McCarthy. 1987. DNA sequence of the human apolipoprotein B gene. *DNA* 6:363-372.

49. Milne,R., R.Theolis, Jr., R.Maurice, R.J.Pease, P.K.Weech, E.Rassart, J.C.Fruchart, J.Scott, and Y.L.Marcel. 1989. The use of monoclonal antibodies to localize the low density lipoprotein receptor-binding domain of apolipoprotein B. *J.Biol.Chem.* 264:19754-19760.

50. Innerarity,T.L., K.H.Weisgraber, K.S.Arnold, R.W.Mahley, R.M.Krauss, G.L.Vega, and S.M.Grundy. 1987. Familial defective apolipoprotein B-100: low density lipoproteins with abnormal receptor binding. *Proc.Natl.Acad.Sci.U.S.A.* 84:6919-6923.

51. Onat,A., G.Hergenc, V.Sansoy, M.Fobker, K.Ceyhan, S.Toprak, and G.Assmann. 2003. Apolipoprotein C-III, a strong discriminant of coronary risk in men and a determinant of the metabolic syndrome in both genders. *Atherosclerosis* 168:81-89.

52. Yamamoto,M., S.Y.Morita, M.Kumon, M.Kawabe, K.Nishitsuji, H.Saito, A.Vertut-Doi, M.Nakano, and T.Handa. 2003. Effects of plasma apolipoproteins on lipoprotein lipase-mediated lipolysis of small and large lipid emulsions. *Biochim.Biophys.Acta* 1632:31-39.

53. Segrest,J.P., M.K.Jones, V.K.Mishra, G.M.Anantharamaiah, and D.W.Garber. 1994. apoB-100 has a pentapartite structure composed of three amphipathic alpha-helical domains alternating with two amphipathic beta-strand domains. Detection by the computer program LOCATE. *Arterioscler.Thromb.* 14:1674-1685.

54. Tran,K., J.Boren, J.Macri, Y.Wang, R.McLeod, R.K.Avramoglu, K.Adeli, and Z.Yao. 1998. Functional analysis of disulfide linkages clustered within the amino terminus of human apolipoprotein B. *J.Biol.Chem.* 273:7244-7251.

55. Vukmirica,J., T.Nishimaki-Mogami, K.Tran, J.Shan, R.S.McLeod, J.Yuan, and Z.Yao. 2002. The N-linked oligosaccharides at the amino terminus of human apoB are important for the assembly and secretion of VLDL. *J.Lipid Res.* 43:1496-1507.

56. Segrest,J.P., M.K.Jones, H.De Loof, and N.Dashti. 2001. Structure of apolipoprotein B-100 in low density lipoproteins. *J.Lipid Res.* 42:1346-1367.

57. Dane-Stewart,C.A., G.F.Watts, P.H.Barrett, B.G.Stuckey, J.C.Mamo, I.J.Martins, and T.G.Redgrave. 2003. Chylomicron remnant metabolism studied with a new breath test in postmenopausal women with and without type 2 diabetes mellitus. *Clin.Endocrinol.(Oxf)* 58:415-420.

58. Hussain,M.M., J.Shi, and P.Dreizen. 2003. Microsomal triglyceride transfer protein and its role in apoB-lipoprotein assembly. *J.Lipid Res.* 44:22-32.

59. Wang,S., R.S.McLeod, D.A.Gordon, and Z.Yao. 1996. The microsomal triglyceride transfer protein facilitates assembly and secretion of apolipoprotein B-containing lipoproteins and decreases cotranslational degradation of apolipoprotein B in transfected COS-7 cells. *J.Biol.Chem.* 271:14124-14133.

60. Bakillah,A. and M.M.Hussain. 2001. Binding of microsomal triglyceride transfer protein to lipids results in increased affinity for apolipoprotein B: evidence for stable microsomal MTP-lipid complexes. *J.Biol.Chem.* 276:31466-31473.

61. Fisher,E.A. and H.N.Ginsberg. 2002. Complexity in the secretory pathway: the assembly and secretion of apolipoprotein B-containing lipoproteins. *J.Biol.Chem.* 277:17377-17380.

62. Du,X., J.D.Stoops, J.R.Mertz, C.M.Stanley, and J.L.Dixon. 1998. Identification of two regions in apolipoprotein B100 that are exposed on the cytosolic side of the endoplasmic reticulum membrane. *J.Cell Biol.* 141:585-599.

63. Asztalos,B.F., M.E.Brousseau, J.R.McNamara, K.V.Horvath, P.S.Roheim, and E.J.Schaefer. 2001. Subpopulations of high density lipoproteins in homozygous and heterozygous Tangier disease. *Atherosclerosis* 156:217-225.

64. Gusarova,V., A.J.Caplan, J.L.Brodsky, and E.A.Fisher. 2001. Apoprotein B degradation is promoted by the molecular chaperones hsp90 and hsp70. *J.Biol.Chem.* 276:24891-24900.

65. Huang,X.F. and G.S.Shelness. 1999. Efficient glycosylation site utilization by intracellular apolipoprotein B. Implications for proteasomal degradation. *J.Lipid Res.* 40:2212-2222.

66. Liang,S., X.Wu, E.A.Fisher, and H.N.Ginsberg. 2000. The amino-terminal domain of apolipoprotein B does not undergo retrograde translocation from the endoplasmic reticulum to the cytosol. Proteasomal degradation of nascent apolipoprotein B begins at the carboxyl terminus of the protein, while apolipoprotein B is still in its original translocon. *J.Biol.Chem.* 275:32003-32010.

67. Chuck,S.L. and V.R.Lingappa. 1992. Pause transfer: a topogenic sequence in apolipoprotein B mediates stopping and restarting of translocation. *Cell* 68:9-21.

68. Chuck,S.L., Z.Yao, B.D.Blackhart, B.J.McCarthy, and V.R.Lingappa. 1990. New variation on the translocation of proteins during early biogenesis of apolipoprotein B. *Nature* 346:382-385.

69. Liang,J., X.Wu, H.Jiang, M.Zhou, H.Yang, P.Angkeow, L.S.Huang, S.L.Sturley, and H.Ginsberg. 1998. Translocation efficiency, susceptibility to proteasomal

degradation, and lipid responsiveness of apolipoprotein B are determined by the presence of beta sheet domains. *J.Biol.Chem.* 273:35216-35221.

70. Morrisett,J.D., G.Abdel-Fattah, and B.D.Kahan. 2003. Sirolimus changes lipid concentrations and lipoprotein metabolism in kidney transplant recipients. *Transplant.Proc.* 35:S143-S150.

71. Benhizia,F., H.N.Ginsberg, S.E.Humphries, and P.J.Talmud. 2001. Variation in the human ApoB signal peptide modulates ApoB17 translocation. *Biochem.Biophys.Res.Commun.* 283:149-157.

72. Sturley,S.L., P.J.Talmud, R.Brasseur, M.R.Culbertson, S.E.Humphries, and A.D.Attie. 1994. Human apolipoprotein B signal sequence variants confer a secretion-defective phenotype when expressed in yeast. *J.Biol.Chem.* 269:21670-21675.

73. Morrisett,J.D., G.Abdel-Fattah, R.Hoogeveen, E.Mitchell, C.M.Ballantyne, H.J.Pownall, A.R.Opekun, J.S.Jaffe, S.Oppermann, and B.D.Kahan. 2002. Effects of sirolimus on plasma lipids, lipoprotein levels, and fatty acid metabolism in renal transplant patients. *J.Lipid Res.* 43:1170-1180.

74. Tran,K., G.Thorne-Tjomsland, C.J.DeLong, Z.Cui, J.Shan, L.Burton, J.C.Jamieson, and Z.Yao. 2002. Intracellular assembly of very low density lipoproteins containing apolipoprotein B100 in rat hepatoma McA-RH7777 cells. *J.Biol.Chem.* 277:31187-31200.

75. Alexander,C.A., R.L.Hamilton, and R.J.Havel. 1976. Subcellular localization of B apoprotein of plasma lipoproteins in rat liver. *J.Cell Biol.* 69:241-263.

76. Yamaguchi,J., M.V.Gamble, D.Conlon, J.S.Liang, and H.N.Ginsberg. 2003. The conversion of apoB100 low density lipoprotein/high density lipoprotein particles to apoB100 very low density lipoproteins in response to oleic acid occurs in the endoplasmic reticulum and not in the Golgi in McA RH7777 cells. *J.Biol.Chem.* 278:42643-42651.

77. Gueguen,S., B.Herbeth, P.Pirollet, F.Paille, G.Siest, and S.Visvikis. 2002. Changes in serum apolipoprotein and lipoprotein profile after alcohol withdrawal: effect of apolipoprotein E polymorphism. *Alcohol Clin.Exp.Res.* 26:501-508.

78. Sauvaget,D., V.Chauffeton, D.Citadelle, F.P.Chatelet, C.Cywiner-Golenzer, J.Chambaz, M.Pincon-Raymond, P.Cardot, J.Le Beyec, and A.Ribeiro. 2002. Restriction of apolipoprotein A-IV gene expression to the intestine villus depends on a hormone-responsive element and parallels differential expression of the hepatic nuclear factor 4alpha and gamma isoforms. *J.Biol.Chem.* 277:34540-34548.

79. Kris-Etherton,P.M., W.S.Harris, and L.J.Appel. 2003. Fish consumption, fish oil, omega-3 fatty acids, and cardiovascular disease. *Arterioscler.Thromb.Vasc.Biol.* 23:e20-e30.

80. Krauss,R.M. 2004. Hold the antioxidants and improve plasma lipids? *J.Clin.Invest* 113:1253-1255.

81. Stillemark,P., J.Boren, M.Andersson, T.Larsson, S.Rustaeus, K.A.Karlsson, and S.O.Olofsson. 2000. The assembly and secretion of apolipoprotein B-48-containing very low density lipoproteins in McA-RH7777 cells. *J.Biol.Chem.* 275:10506-10513.

82. Swift,L.L., K.Valyi-Nagy, C.Rowland, and C.Harris. 2001. Assembly of very low density lipoproteins in mouse liver: evidence of heterogeneity of particle density in the Golgi apparatus. *J.Lipid Res.* 42:218-224.

83. Wang,Y., K.Tran, and Z.Yao. 1999. The activity of microsomal triglyceride transfer protein is essential for accumulation of triglyceride within microsomes in McA-RH7777 cells. A unified model for the assembly of very low density lipoproteins. *J.Biol.Chem.* 274:27793-27800.

84. Pelletier,L., E.Jokitalo, and G.Warren. 2000. The effect of Golgi depletion on exocytic transport. *Nat.Cell Biol.* 2:840-846.

85. Ktistakis,N.T., H.A.Brown, P.C.Sternweis, and M.G.Roth. 1995. Phospholipase D is present on Golgi-enriched membranes and its activation by ADP ribosylation factor is sensitive to brefeldin A. *Proc.Natl.Acad.Sci.U.S.A* 92:4952-4956.

86. Wieland,F. and C.Harter. 1999. Mechanisms of vesicle formation: insights from the COP system. *Curr.Opin.Cell Biol.* 11:440-446.

87. Asp,L., C.Claesson, J.Boren, and S.O.Olofsson. 2000. ADP-ribosylation factor 1 and its activation of phospholipase D are important for the assembly of very low density lipoproteins. *J.Biol.Chem.* 275:26285-26292.

88. Hammond,S.M., J.M.Jenco, S.Nakashima, K.Cadwallader, Q.Gu, S.Cook, Y.Nozawa, G.D.Prestwich, M.A.Frohman, and A.J.Morris. 1997. Characterization of two alternately spliced forms of phospholipase D1. Activation of the purified enzymes by phosphatidylinositol 4,5-bisphosphate, ADP-ribosylation factor, and Rho family monomeric GTP-binding proteins and protein kinase C-alpha. *J.Biol.Chem.* 272:3860-3868.

89. Wiggins,D. and G.F.Gibbons. 1996. Origin of hepatic very-low-density lipoprotein triacylglycerol: the contribution of cellular phospholipid. *Biochem.J.* 320:673-679.

90. Tran,K., Y.Wang, C.J.DeLong, Z.Cui, and Z.Yao. 2000. The assembly of very low density lipoproteins in rat hepatoma McA-RH7777 cells is inhibited by phospholipase A2 antagonists. *J.Biol.Chem.* 275:25023-25030.

91. Yao,Z.M. and D.E.Vance. 1988. The active synthesis of phosphatidylcholine is required for very low density lipoprotein secretion from rat hepatocytes. *J.Biol.Chem.* 263:2998-3004.

92. Shachter,N.S. 2001. Apolipoproteins C-I and C-III as important modulators of lipoprotein metabolism. *Curr.Opin.Lipidol.* 12:297-304.

93. Olin-Lewis,K., R.M.Krauss, M.La Belle, P.J.Blanche, P.H.Barrett, T.N.Wight, and A.Chait. 2002. ApoC-III content of apoB-containing lipoproteins is associated with binding to the vascular proteoglycan biglycan. *J.Lipid Res.* 43:1969-1977.

94. Martin-Sanz,P., J.E.Vance, and D.N.Brindley. 1990. Stimulation of apolipoprotein secretion in very-low-density and high-density lipoproteins from cultured rat hepatocytes by dexamethasone. *Biochem.J.* 271:575-583.

95. Olivieri,O., C.Stranieri, A.Bassi, B.Zaia, D.Girelli, F.Pizzolo, E.Trabetti, S.Cheng, M.A.Grow, P.F.Pignatti, and R.Corrocher. 2002. ApoC-III gene polymorphisms and risk of coronary artery disease. *J.Lipid Res.* 43:1450-1457.

96. Martin-Sanz,P., J.E.Vance, and D.N.Brindley. 1990. Stimulation of apolipoprotein secretion in very-low-density and high-density lipoproteins from cultured rat hepatocytes by dexamethasone. *Biochem.J.* 271:575-583.

97. McLeod,R.S., Y.Wang, S.Wang, A.Rusinol, P.Links, and Z.Yao. 1996. Apolipoprotein B sequence requirements for hepatic very low density lipoprotein assembly. Evidence that hydrophobic sequences within apolipoprotein B48 mediate lipid recruitment. *J.Biol.Chem.* 271:18445-18455.

98. Macala,L.J., R.K.Yu, and S.Ando. 1983. Analysis of brain lipids by high performance thin-layer chromatography and densitometry. *J.Lipid Res.* 24:1243-1250.

99. Ruiz,J.I. and B.Ochoa. 1997. Quantification in the subnanomolar range of phospholipids and neutral lipids by monodimensional thin-layer chromatography and image analysis. *J.Lipid Res.* 38:1482-1489.

100. Bradford,M.M. 1976. A rapid and sensitive method for the quantitation of microgram quantities of protein utilizing the principle of protein-dye binding. *Anal.Biochem.* 72:248-254.

101. Wetterau,J.R., L.P.Aggerbeck, M.E.Bouma, C.Eisenberg, A.Munck, M.Hermier, J.Schmitz, G.Gay, D.J.Rader, and R.E.Gregg. 1992. Absence of microsomal triglyceride transfer protein in individuals with abetalipoproteinemia. *Science* 258:999-1001.

102. Altomonte,J., L.Cong, S.Harbaran, A.Richter, J.Xu, M.Meseck, and H.H.Dong. 2004. Foxo1 mediates insulin action on apoC-III and triglyceride metabolism. *J.Clin.Invest.* 114:1493-1503.

103. Ito,Y., N.Azrolan, A.O'Connell, A.Walsh, and J.L.Breslow. 1990. Hypertriglyceridemia as a result of human apo CIII gene expression in transgenic mice. *Science* 249:790-793.

104. Milne,R.W. and Y.L.Marcel. 1982. Monoclonal antibodies against human low density lipoprotein. Stoichiometric binding studies using Fab fragments. *FEBS Lett.* 146:97-100.

105. Sniderman,A.D. 2002. How, when, and why to use apolipoprotein B in clinical practice. *Am.J.Cardiol.* 90:48i-54i.

106. Hebbachi,A.M. and G.F.Gibbons. 2001. Microsomal membrane-associated apoB is the direct precursor of secreted VLDL in primary cultures of rat hepatocytes. *J.Lipid Res.* 42:1609-1617.

107. Atger,V., P.Beyne, K.Frommherz, J.B.Roullet, and T.Drueke. 1989. Presence of Apo B48, and relative Apo CII deficiency and Apo CIII enrichment in uremic very-low density lipoproteins. *Ann.Biol.Clin.(Paris)* 47:497-501.

108. Lee,S.J., H.Campos, L.A.Moye, and F.M.Sacks. 2003. LDL containing apolipoprotein CIII is an independent risk factor for coronary events in diabetic patients. *Arterioscler.Thromb.Vasc.Biol.* 23:853-858.

109. Liu,H., P.J.Talmud, L.Lins, R.Brasseur, G.Olivecrona, F.Peelman, J.Vandekerckhove, M.Rosseneu, and C.Labeur. 2000. Characterization of recombinant wild type and site-directed mutations of apolipoprotein C-III: lipid binding, displacement of ApoE, and inhibition of lipoprotein lipase. *Biochemistry* 39:9201-9212.

110. Sparrow,J.T., H.J.Pownall, F.J.Hsu, L.D.Blumenthal, A.R.Culwell, and A.M.Gotto. 1977. Lipid binding by fragments of apolipoprotein C-III-1 obtained by thrombin cleavage. *Biochemistry* 16:5427-5431.

111. Kinnunen,P.K., R.L.Jackson, L.C.Smith, A.M.Gotto, Jr., and J.T.Sparrow. 1977. Activation of lipoprotein lipase by native and synthetic fragments of human plasma apolipoprotein C-II. *Proc.Natl.Acad.Sci.U.S.A* 74:4848-4851.

112. Ginsberg,H.N., N.A.Le, I.J.Goldberg, J.C.Gibson, A.Rubinstein, P.Wang-Iverson, R.Norum, and W.V.Brown. 1986. Apolipoprotein B metabolism in subjects with deficiency of apolipoproteins CIII and AI. Evidence that apolipoprotein CIII

inhibits catabolism of triglyceride-rich lipoproteins by lipoprotein lipase in vivo. *J.Clin.Invest.* 78:1287-1295.

113. Wu-Peng,X.S., S.C.Chua, Jr., N.Okada, S.M.Liu, M.Nicolson, and R.L.Leibel. 1997. Phenotype of the obese Koletsky (f) rat due to Tyr763Stop mutation in the extracellular domain of the leptin receptor (Lepr): evidence for deficient plasma-to-CSF transport of leptin in both the Zucker and Koletsky obese rat. *Diabetes* 46:513-518.

114. Notredame,C., D.G.Higgins, and J.Heringa. 2000. T-Coffee: A novel method for fast and accurate multiple sequence alignment. *J.Mol.Biol.* 302:205-217.

115. Jackson,R.L., J.D.Morrisett, J.T.Sparrow, J.P.Segrest, H.J.Pownall, L.C.Smith, H.F.Hoff, and A.M.Gotto, Jr. 1974. The interaction of apolipoprotein-serine with phosphatidylcholine. *J.Biol.Chem.* 249:5314-5320.

116. Li,W.H., M.Tanimura, C.C.Luo, S.Datta, and L.Chan. 1988. The apolipoprotein multigene family: biosynthesis, structure, structure-function relationships, and evolution. *J.Lipid Res.* 29:245-271.

117. Huang,Y., X.Q.Liu, S.C.Rall, Jr., J.M.Taylor, A.von Eckardstein, G.Assmann, and R.W.Mahley. 1998. Overexpression and accumulation of apolipoprotein E as a cause of hypertriglyceridemia. *J.Biol.Chem.* 273:26388-26393.

118. Rogers,D.P., L.M.Roberts, J.Lebowitz, G.Datta, G.M.Anantharamaiah, J.A.Engler, and C.G.Brouillette. 1998. The lipid-free structure of apolipoprotein A-I: effects of amino-terminal deletions. *Biochemistry* 37:11714-11725.

119. Schaap,F.G., P.C.Rensen, P.J.Voshol, C.Vrins, H.N.van der Vliet, R.A.Chamuleau, L.M.Havekes, A.K.Groen, and K.W.van Dijk. 2004. ApoAV reduces plasma triglycerides by inhibiting very low density lipoprotein-triglyceride (VLDL-TG) production and stimulating lipoprotein lipase-mediated VLDL-TG hydrolysis. *J.Biol.Chem.* 279:27941-27947.

120. Hui,T.Y., L.M.Olivier, S.Kang, and R.A.Davis. 2002. Microsomal triglyceride transfer protein is essential for hepatic secretion of apoB-100 and apoB-48 but not triglyceride. *J.Lipid Res.* 43:785-793.

121. Fleming,J.F., G.M.Spitsen, T.Y.Hui, L.Olivier, E.Z.Du, M.Raabe, and R.A.Davis. 1999. Chinese hamster ovary cells require the coexpression of microsomal triglyceride transfer protein and cholesterol 7alpha-hydroxylase for the assembly and secretion of apolipoprotein B-containing lipoproteins. *J.Biol.Chem.* 274:9509-9514.

122. Kocsis,M.G. and R.J.Weselake. 1996. Phosphatidate phosphatases of mammals, yeast, and higher plants. *Lipids* 31:785-802.

123. Bray,G.A. and D.A.York. 1979. Hypothalamic and genetic obesity in experimental animals: an autonomic and endocrine hypothesis. *Physiol. Rev.* 59:719-809.

124. Glenny,H.P. and D.N.Brindley. 1978. The effects of cortisol, corticotropin and thyroxine on the synthesis of glycerolipids and on the phosphatidate phosphohydrolase activity in rat liver. *Biochem.J.* 176:777-784.

125. Mangiapane,E.H. and D.N.Brindley. 1986. Effects of dexamethasone and insulin on the synthesis of triacylglycerols and phosphatidylcholine and the secretion of very-low-density lipoproteins and lysophosphatidylcholine by monolayer cultures of rat hepatocytes. *Biochem.J.* 233:151-160.

126. Hill,R.B., Jr. and W.A.Droke. 1963. Production of fatty liver in the rat by cortisone. *Proc.Soc.Exp.Biol.Med.* 114:766-769.

127. Brindley,D.N., B.S.McCann, R.Niaura, C.M.Stoney, and E.C.Suarez. 1993. Stress and lipoprotein metabolism: modulators and mechanisms. *Metabolism* 42:3-15.

128. Brindley,D.N., J.Cooling, S.L.Burditt, P.H.Pritchard, S.Pawson, and R.G.Sturton. 1979. The involvement of glucocorticoids in regulating the activity of phosphatidate phosphohydrolase and the synthesis of triacylglycerols in the liver. Effects of feeding rats with glucose, sorbitol, fructose, glycerol and ethanol. *Biochem.J.* 180:195-199.

129. Knox,A.M., R.G.Sturton, J.Cooling, and D.N.Brindley. 1979. Control of hepatic triacylglycerol synthesis. Diurnal variations in hepatic phosphatidate phosphohydrolase activity and in the concentrations of circulating insulin and corticosterone in rats. *Biochem.J.* 180:441-443.

130. Jamal,Z., A.Martin, A.Gomez-Munoz, and D.N.Brindley. 1991. Plasma membrane fractions from rat liver contain a phosphatidate phosphohydrolase distinct from that in the endoplasmic reticulum and cytosol. *J.Biol.Chem.* 266:2988-2996.

131. Gomez-Munoz,A., E.H.Hamza, and D.N.Brindley. 1992. Effects of sphingosine, albumin and unsaturated fatty acids on the activation and translocation of phosphatidate phosphohydrolases in rat hepatocytes. *Biochim.Biophys.Acta* 1127:49-56.

132. Roberts,R., V.A.Sciorra, and A.J.Morris. 1998. Human type 2 phosphatidic acid phosphohydrolases. Substrate specificity of the type 2a, 2b, and 2c enzymes and cell surface activity of the 2a isoform. *J.Biol.Chem.* 273:22059-22067.

133. Brindley,D.N. and D.W.Waggoner. 1998. Mammalian lipid phosphate phosphohydrolases. *J.Biol.Chem.* 273:24281-24284.

134. Waggoner,D.W., A.Martin, J.Dewald, A.Gomez-Munoz, and D.N.Brindley. 1995. Purification and characterization of novel plasma membrane phosphatidate phosphohydrolase from rat liver. *J.Biol.Chem.* 270:19422-19429.

135. Kai,M., I.Wada, S.Imai, F.Sakane, and H.Kanoh. 1996. Identification and cDNA cloning of 35-kDa phosphatidic acid phosphatase (type 2) bound to plasma membranes. Polymerase chain reaction amplification of mouse H2O2-inducible hic53 clone yielded the cDNA encoding phosphatidic acid phosphatase. *J.Biol.Chem.* 271:18931-18938.

136. Waggoner,D.W., A.Gomez-Munoz, J.Dewald, and D.N.Brindley. 1996. Phosphatidate phosphohydrolase catalyzes the hydrolysis of ceramide 1-phosphate, lysophosphatidate, and sphingosine 1-phosphate. *J.Biol.Chem.* 271:16506-16509.

137. al Shurbaji,A. and L.Berglund. 1989. Rat adipose tissue phosphatidic acid phosphatase: lack of effect of nucleotides on cytosolic enzyme activity. *Acta Chem.Scand.* 43:680-683.

138. Pasquare,S.J. and N.M.Giusto. 1993. Differential properties of phosphatidate phosphohydrolase and diacylglyceride lipase activities in retinal subcellular fractions and rod outer segments. *Comp.Biochem.Physiol B* 104:141-148.

139. Jamdar,S.C. and H.J.Fallon. 1973. Glycerolipid synthesis in rat adipose tissue. II. Properties and distribution of phosphatidate phosphatase. *J.Lipid Res.* 14:517-524.

140. Ng,T.B. and P.P.Tam. 1986. Changes of acid and alkaline phosphatase activities in the developing mouse brain. *Biol.Neonate* 50:107-113.

141. Schoonderwoerd,K., S.Broekhoven-Schokker, W.C.Hulsmann, and H.Stam. 1990. Properties of phosphatidate phosphohydrolase and diacylglycerol acyltransferase activities in the isolated rat heart. Effect of glucagon, ischaemia and diabetes. *Biochem.J.* 268:487-492.

142. Kates,M. 1955. Hydrolysis of lecithin by plant plastid enzymes. *Can.J.Med.Sci.* 33:575-589.

143. Sedgwick,B. and G.Hubscher. 1967. Metabolism of phospholipids. X. Partial purification and properties of a soluble phosphatidate phosphohydrolase from rat liver. *Biochim.Biophys.Acta* 144:397-408.

144. Hosaka,K., S.Yamashita, and S.Numa. 1975. Partial purification, properties, and subcellulsr distribution of rat liver phosphatidate phosphatase. *J.Biochem.(Tokyo)* 77:501-509.

145. Sturton,R.G., S.C.Butterwith, S.L.Burditt, and D.N.Brindley. 1981. Effects of starvation, corticotropin injection and ethanol feeding on the activity and amount of phosphatidate phosphohydrolase in rat liver. *FEBS Lett.* 126:297-300.

146. Sturton,R.G., P.H.Pritchard, L.Y.Han, and D.N.Brindley. 1978. The involvement of phosphatidate phosphohydrolase and phospholipase A activities in the control of hepatic glycerolipid synthesis. Effects of acute feeding with glucose, fructose, sorbitol, glycerol and ethanol. *Biochem.J.* 174:667-670.

147. Sturton,R.G. and D.N.Brindley. 1978. Problems encountered in measuring the activity of phosphatidate phosphohydrolase. *Biochem.J.* 171:263-266.

148. Brindley,D.N., M.Bowley, S.Burditt, H.Pritchard, K.A.Lloyd-Davies, and P.Boucrot. 1976. The effects of administering N-(2-benzoyloxyethyl) norfenfluramine to rats on the hepatic synthesis of glycerolipids. *J.Pharm.Pharmacol.* 28:676-682.

149. Martin,A., P.Hales, and D.N.Brindley. 1987. A rapid assay for measuring the activity and the Mg2+ and Ca2+ requirements of phosphatidate phosphohydrolase in cytosolic and microsomal fractions of rat liver. *Biochem.J.* 245:347-355.

150. Lawson,N., A.D.Pollard, R.J.Jennings, M.I.Gurr, and D.N.Brindley. 1981. The activities of lipoprotein lipase and of enzymes involved in triacylglycerol synthesis

in rat adipose tissue. Effects of starvation, dietary modification and of corticotropin injection. *Biochem.J.* 200:285-294.

151. 2002. Third Report of the National Cholesterol Education Program (NCEP) Expert Panel on Detection, Evaluation, and Treatment of High Blood Cholesterol in Adults (Adult Treatment Panel III) final report. *Circulation* 106:3143-3421.

152. Veerkamp,M.J., J.de Graaf, S.J.Bredie, J.C.Hendriks, P.N.Demacker, and A.F.Stalenhoef. 2002. Diagnosis of familial combined hyperlipidemia based on lipid phenotype expression in 32 families: results of a 5-year follow-up study. *Arterioscler.Thromb.Vasc.Biol.* 22:274-282.

153. Lewis,G.F., K.D.Uffelman, L.W.Szeto, B.Weller, and G.Steiner. 1995. Interaction between free fatty acids and insulin in the acute control of very low density lipoprotein production in humans. *J.Clin.Invest.* 95:158-166.

154. Veniant,M.M., S.Withycombe, and S.G.Young. 2001. Lipoprotein size and atherosclerosis susceptibility in Apoe(-/-) and Ldlr(-/-) mice. *Arterioscler.Thromb.Vasc.Biol.* 21:1567-1570.

155. Chung,B.H., J.P.Segrest, and F.Franklin. 1998. In vitro production of beta-very low density lipoproteins and small, dense low density lipoproteins in mildly hypertriglyceridemic plasma: role of activities of lecithin:cholester acyltransferase, cholesterylester transfer proteins and lipoprotein lipase. *Atherosclerosis* 141:209-225.

156. Barter,P.J., H.B.Brewer, Jr., M.J.Chapman, C.H.Hennekens, D.J.Rader, and A.R.Tall. 2003. Cholesteryl ester transfer protein: a novel target for raising HDL and inhibiting atherosclerosis. *Arterioscler.Thromb.Vasc.Biol.* 23:160-167.

157. Veniant,M.M., M.A.Sullivan, S.K.Kim, P.Ambroziak, A.Chu, M.D.Wilson, M.K.Hellerstein, L.L.Rudel, R.L.Walzem, and S.G.Young. 2000. Defining the atherogenicity of large and small lipoproteins containing apolipoprotein B100. *J.Clin.Invest.* 106:1501-1510.

158. Liu,H., P.J.Talmud, L.Lins, R.Brasseur, G.Olivecrona, F.Peelman, J.Vandekerckhove, M.Rosseneu, and C.Labeur. 2000. Characterization of recombinant wild type and site-directed mutations of apolipoprotein C-III: lipid binding, displacement of ApoE, and inhibition of lipoprotein lipase. *Biochemistry* 39:9201-9212.

159. Lins,L., C.Flore, L.Chapelle, P.J.Talmud, A.Thomas, and R.Brasseur. 2002. Lipid-interacting properties of the N-terminal domain of human apolipoprotein C-III. *Protein Eng.* 15:513-520.

160. Wang,C.N., R.S.McLeod, Z.Yao, and D.N.Brindley. 1995. Effects of dexamethasone on the synthesis, degradation, and secretion of apolipoprotein B in cultured rat hepatocytes. *Arterioscler.Thromb.Vasc.Biol.* 15:1481-1491.

161. Blagoev,B., S.E.Ong, I.Kratchmarova, and M.Mann. 2004. Temporal analysis of phosphotyrosine-dependent signaling networks by quantitative proteomics. *Nat.Biotechnol.* 22:1139-1145.

162. Luchoomun,J. and M.M.Hussain. 1999. Assembly and secretion of chylomicrons by differentiated Caco-2 cells. Nascent triglycerides and preformed phospholipids are preferentially used for lipoprotein assembly. *J.Biol.Chem.* 274:19565-19572.

163. Zhang,Y.L., A.Hernandez-Ono, C.Ko, K.Yasunaga, L.S.Huang, and H.N.Ginsberg. 2004. Regulation of hepatic apolipoprotein B-lipoprotein assembly and secretion by the availability of fatty acids. I. Differential response to the delivery of fatty acids via albumin or remnant-like emulsion particles. *J.Biol.Chem.* 279:19362-19374.

164. Higgins,J.A. and J.K.Fieldsend. 1987. Phosphatidylcholine synthesis for incorporation into membranes or for secretion as plasma lipoproteins by Golgi membranes of rat liver. *J.Lipid Res.* 28:268-278.

165. Linden,D., K.Lindberg, J.Oscarsson, C.Claesson, L.Asp, L.Li, M.Gustafsson, J.Boren, and S.O.Olofsson. 2002. Influence of peroxisome proliferator-activated receptor alpha agonists on the intracellular turnover and secretion of apolipoprotein (Apo) B-100 and ApoB-48. *J.Biol.Chem.* 277:23044-23053.

166. Staels,B., J.Dallongeville, J.Auwerx, K.Schoonjans, E.Leitersdorf, and J.C.Fruchart. 1998. Mechanism of action of fibrates on lipid and lipoprotein metabolism. *Circulation* 98:2088-2093.

167. Cascales,C., E.H.Mangiapane, and D.N.Brindley. 1984. Oleic acid promotes the activation and translocation of phosphatidate phosphohydrolase from the cytosol to particulate fractions of isolated rat hepatocytes. *Biochem.J.* 219:911-916.

168. Vance,J.E. and J.C.Russell. 1990. Hypersecretion of VLDL, but not HDL, by hepatocytes from the JCR:LA-corpulent rat. *J.Lipid Res.* 31:1491-1501.

169. Kowal,R.C., J.Herz, K.H.Weisgraber, R.W.Mahley, M.S.Brown, and J.L.Goldstein. 1990. Opposing effects of apolipoproteins E and C on lipoprotein binding to low density lipoprotein receptor-related protein. *J.Biol.Chem.* 265:10771-10779.

170. de Graaf,J., M.J.Veerkamp, and A.F.Stalenhoef. 2002. Metabolic pathogenesis of familial combined hyperlipidaemia with emphasis on insulin resistance, adipose tissue metabolism and free fatty acids. *J.R.Soc.Med.* 95 Suppl 42:46-53.

171. de Graaf,J. and A.F.Stalenhoef. 1998. Defects of lipoprotein metabolism in familial combined hyperlipidaemia. *Curr.Opin.Lipidol.* 9:189-196.

172. Tilly,P., C.Sass, M.Vincent-Viry, D.Aguillon, G.Siest, and S.Visvikis. 2003. Biological and genetic determinants of serum apoC-III concentration: reference limits from the Stanislas Cohort. *J.Lipid Res.* 44:430-436.

173. Pallaud,C., R.Gueguen, C.Sass, M.Grow, S.Cheng, G.Siest, and S.Visvikis. 2001. Genetic influences on lipid metabolism trait variability within the Stanislas Cohort. *J.Lipid Res.* 42:1879-1890.

174. Dallongeville,J., A.Meirhaeghe, D.Cottel, J.C.Fruchart, P.Amouyel, and N.Helbecque. 2000. Gender related association between genetic variations of APOC-III gene and lipid and lipoprotein variables in northern France. *Atherosclerosis* 150:149-157.

175. Herzenberg,L.A. and S.C.De Rosa. 2000. Monoclonal antibodies and the FACS: complementary tools for immunobiology and medicine. *Immunol.Today* 21:383-390.

176. Balsinde,J. and E.A.Dennis. 1996. Bromoenol lactone inhibits magnesium-dependent phosphatidate phosphohydrolase and blocks triacylglycerol biosynthesis in mouse P388D1 macrophages. *J.Biol.Chem.* 271:31937-31941.

177. Fuentes,L., R.Perez, M.L.Nieto, J.Balsinde, and M.A.Balboa. 2003. Bromoenol lactone promotes cell death by a mechanism involving phosphatidate phosphohydrolase-1 rather than calcium-independent phospholipase A2. *J.Biol.Chem.* 278:44683-44690.